Shielding Effectiveness Investigations Using a Reverberation Chamber

by

Nancy A. Omollo

Thesis presented in partial fulfilment of the requirements for the degree Master of Engineering (Research) in the Faculty of Engineering at Stellenbosch University

Department of Electrical and Electronic Engineering,
University of Stellenbosch,
Private Bag X1, Matieland 7602, South Africa

Supervisor: Dr. P. G. Wiid

April 2019

Declaration

I have read and understand the Stellenbosch University Policy on Plagiarism and the definitions of plagiarism and self-plagiarism contained in the Policy [Plagiarism: The use of the ideas or material of others without acknowledgement, or the re-use of one's own previously evaluated or published material without acknowledgement or indication thereof (self-plagiarism or textrecycling)].

I also understand that direct translations are plagiarism, unless accompanied by an appropriate acknowledgement of the source. I also know that verbatim copy that has not been explicitly indicated as such, is plagiarism.

I know that plagiarism is a punishable offence and may be referred to the University's Central Disciplinary Committee (CDC) who has the authority to expel me for such an offence.

I know that plagiarism is harmful for the academic environment and that it has a negative impact on any profession.

Accordingly all quotations and contributions from any source whatsoever (including the internet) have been cited fully (acknowledged); further, all verbatim copies have been expressly indicated as such (e.g. through quotation marks) and the sources are cited fully.

I declare that, except where a source has been cited, the work contained in this assignment is my own work and that I have not previously (in its entirety or in part) submitted it for grading in this module/assignment or another module/assignment.

	April 2019
Signature	Date
Nancy Omollo	

Abstract

Electromagnetic interference (EMI) is one of the most common problems encountered in radio astronomy observatories. Interaction of electromagnetic (EM) waves from different sources may result in device malfunction due to misinterpretation of the transferred data or information loss. Most equipment and facilities at a radio astronomy observatory are sensitive to this interference. It is therefore important to find a solution to protect these sensitive instruments from damage that may result due to EMI.

Many steps have been taken to provide these solutions, including radio frequency campaigns, careful design of electronic systems, radio frequency propagation investigations and shielding. In the latter case, there have been several materials that have been used in shielding at different levels. However, most of the commonly used materials are costly.

This project characterizes alternative affordable commercial materials that can be used for shielding. Characterization of these materials is done using a reverberation chamber and specific to the nested reverberation chamber technique for repeatability purposes. The measurements are done in frequency domain (FD) and validated using time domain (TD) methods. The two sets of measurements are carried out in two different reverberation chambers with different physical dimensions and characteristics. The TD measurement is investigated for measurement time speed-up. Measurement in TD is done using the real time analyser (RTA), which is a high dynamic range instrument with a measurement bandwidth of up to 3 GHz.

A few of the investigated materials showed effective shielding. The absorbing sheet material and the radiant barrier roofing material showed shielding values of at least 30dB and above. These cheaper materials are therefore recommended for use at the Square Kilometre Array (SKA) buildings for additional shielding.

Uittreksel

Elektromagnetiese inmenging (EMI) is een van die hoofprobleme wat sterrekundiges en ingenieurs in die radio-sterrekunde-observatoria ondervind. Interaksie van elektromagnetiese (EM) golwe uit verskillende bronne kan apparaatfout, datavervorming of dataverlies veroorsaak. Die meeste toerusting en fasiliteite by 'n radio-sterrekunde-observatorium is sensitief vir hierdie inmenging. Dit is dus belangrik om 'n oplossing te vind om hierdie sensitiewe instrumente te beskerm teen skade wat mag voortspruit uit EMI.

Daar is baie stappe gedoen om hierdie oplossings te voorsien, insluitend radiofrekwensie veldtogte, versigtige ontwerp van elektroniese stelsels, ondersoek van radiofrekwensievoortplanting en afskerming. In laasgenoemde geval was daar verskeie materiale wat op verskillende vlakke in afskerming gebruik is. Die meeste van die algemeen gebruikte materiale is egter duur.

Hierdie projek kyk na die karakterisering van alternatiewe bekostigbare kommersiële materiaal wat vir afskerming gebruik kan word. Karakterisering van hierdie materiale word gedoen met behulp van 'n weerkaats-kamer en spesifiek vir die geneste weerkaats-kamer tegniek vir herhaalbaarheid doeleindes. Die metings word in frekwensiedomein (FD) gedoen en valideer met behulp van tyddomein (TD) metodes. Die twee stelle metings word uitgevoer in twee verskillende weerkaats-kamer met verskillende fisiese dimensies en eienskappe. Die TD-meting word ondersoek vir metingstyd versnelling. Meting in TD word gedoen met behulp van die Real Time Analyzer (RTA), wat 'n hoë dinamiese bereik instrument met 'n meting bandwydte van tot 3 GHz is.

'n Paar van die materiale wat ondersoek is, het effektiewe afskerming getoon. Die absorberende plaatmateriaal en die stralingsdempende dakmateriaal het skermwaardes van minstens 30 dB en hoër vertoon. Hierdie materiaal kan aanbeveel word by SKA geboue vir bykomende afskerming teen lae koste.

Acknowledgements

I would like to express my sincere appreciation to Dr. Gideon Wiid for his supervision, guidance, support and encouragement throughout the study. Thank you Daktari.

I am grateful to Anneke Beste, Wessel Croukamp, Dr TJ Phiri and Dr Joely Andriambeloson for their assistance with different measurements and nested chamber construction. I also appreciate the love, support and assistance of all the E212 EMRIN members.

I also owe a debt of gratitude to my family for their endless love, support and encouragement throughout my life, and most especially during this period that this work was done.

I would also like to thank SKA SA (SARAO), for providing me with funding for this work.

Above all, I thank the almighty God for his grace and mercies. He has kept me in good health and has been my provision. I also thank Him for His love that I have experienced through different people that I've had the opportunity to meet and work with during this masters program.

Contents

List of Figures

List of Tables

Nomenclature

Acronyms

CM	Common mode
dB	Decibel
DUT	Device under test
DM	Differential mode
DR	Dynamic Range
EUT	Equipment under test
EM	Electromagnetics
EMC	Electromagnetic compatibility
EME	Electromagnetic environment
EMI	Electromagnetic Interference
FD	Frequency Domain
GHz	Gigahertz
GPIB	General Purpose Interface Bus
KAPB	Karoo Array Processing Building
KAT	Karoo Array Telescope
kHz	Kilohertz
LPDA	Log Periodic Dipole Array
MUT	Material Under Test
NRC	Nested reverberation chamber
PC	Personal Computer
PDF	Probability density function
PDP	Power delay profile
RATTY	Real Time Transient Analyser
RC	Reverberation chamber
RF	Radio frequency
RFI	Radio frequency interference
SARAO	South Africa Radio Astronomy Observatory
RTA	Real Time Analyser
SKA SA	Square Kilometre Array South Africa
SE	Shielding effectiveness
SKA	Square kilometer array
TD	Time Domain
TEM	Transverse Electromagnetic
VNA	Vector network analyser

Chapter 1

INTRODUCTION

1.1 The Square Kilometre Array (SKA)

The Square Kilometre Array (SKA) will be the largest, most sensitive radio telescope ever to be constructed. It is constructed in two countries, South Africa (SA) and Australia [1,2]. South Africa will host the mid-frequency telescopes whereas Australia will host the low frequency telescopes. The SKA organisation was established as a non-profit company to centralise the leadership of the project. Its key objective is to conduct a transformational science that will be able to redefine our understanding of space. Its headquarters is at Jodrell Bank Observatory, UK.

Of the phase built in South Africa, the SKA SA has taken a major step towards the entire project, by building two project demonstrators. The first was called the Karoo Array Telescope Seven (KAT-7) comprising of 7 dishes, followed by a premier cm-wavelength radio astronomy facility, the MeerKAT, which would later be integrated into the first phase of the mid-frequency SKA. The MeerKAT is made up of 64 Gregorian-offset sub reflector and reflector dishes [3] . It will be the most sensitive telescope in the southern hemisphere until when the entire SKA project will be realised. The SKA1-mid phase site has been proclaimed a radio-quite zone. The telescopes and hence the project is an ambitious step towards finding answers to some mysteries around: big bang; the violent lives of galaxies; birth and death of stars; as well how dark energy is accelerating the expansion of the universe; among other fundamental issues.

Figure 1.1: The 64-antenna MeerKAT radio telescope, in the Karoo, will be incorporated into Phase 1 of the SKA-MID telescope. Photo credit: SARAO.

Due to its sensitivity, the instrument is very susceptible to radio frequency interference

(RFI) and/or electromagnetic interference (EMI). EMI is defined as a disturbance that affects an electrical circuit causing temporary or permanent disruption of its functionality. Therefore, having a radio quiet environment for the best performance of the instrument is vital. However, as much as the construction site for the SKA has been proclaimed quiet, the quietness is not fully guaranteed for effective operation of the instruments. Due to this, a range of measures are required to ensure that the environment is conducive to the best performance of the radio telescope.

One of the measures taken in ensuring an electromagnetic compatible environment for the best operation of the instrument is shielding. Shielding can be done at different stages for better compatibility of the entire system. For instance, the karoo array processing building (KAPB) needs to be shielded to prevent interference from noisy equipment within the processor building may be prevented to reach the sensitive radio telescope receivers.

1.2 Radio Astronomy and Interference

Radio Astronomy is the study of celestial objects that emit radio waves. Through radio astronomy, different astronomical phenomena can be studied. This would include the observation of galaxies, stars and other interesting phenomena from the sky, through sky imaging, using radio telescopes. [4].

Radio astronomical data collection has been affected by man-made and natural sources of EMI, which potentially may be of great effect when the SKA is finally up and running. This may ultimately hinder the achievement of goals of the entire project. Therefore, it would be of great interest to understand the potential limitation that interference might pose to the SKA-enabled science and how it can be mitigated.

Man-made EMI can be categorised as either internal or external. Internal EMI is as a result of interference from within the system itself and can be managed through careful system design. External EMI on the other hand is as a result of interference from external environment to the system. These interferences cannot be mitigated through careful system design. Different methods of mitigation is thus used to protect the system, especially when these interferences appear in the RFI bandwidth of the electromagnetic spectrum. Radio telescopes collect/observe data within this bandwidth, and as much as some frequency bands are reserved for these astronomical observations by international agreement on electromagnetic spectrum, science requirements encourage observations beyond these bands. Therefore, extra measures aside from system design must be taken into consideration in order to properly mitigate external EMI [5].

One of the major impacts of EMI is that it's costly. In radio astronomy observation for instance, EMI affects the efficiency of the telescopes and hence results in corrupted data.

This reduces the productivity of the entire system. This data corruption due to EMI jamming may result in increased cost in post processing the data. This is because more labour may be needed to work on the editing of the data manually, in order to remove the effects of EMI. This process, besides being costly is very tedious and tiresome since wider frequency bands are considered. Therefore, proper shielding is of great importance to ensure that the emissions from within the processor building at the core site of SKA does not reach and affect the telescopes functionality and corrupt the data being collected.

The SKA has achieved good shielding of its building. This has involved selecting very effective materials to shield doors and windows and different openings in the Karoo Array Procesor Building (KAPB). They have also built a berm one side of the KAPB, to enhance shielding of the interference. The radio frequency materials used for shielding in the building, however, are quite expensive [2].

1.3 Project Objective

To shield the subsystems and the entire building, the shielding effectiveness of material samples has to be evaluated to identify which materials are suited in shielding at the different levels. These have been done using several methods. The main aim of the thesis is;

- To investigate the shielding effectiveness of cost effective shielding materials in a reverberation chamber. SKA uses costly materials for shielding purposes. It is thus of great importance to study, investigate, measure and quantify the shielding effectiveness of cost-effective commercial materials that can be used as alternative shielding materials by the SKA.
- To develop a measurement set-up that can be used to conduct such measurements with a good level of repeatability.
- TTo carry of the materials shielding effectiveness measurements, both in frequency domain and time domain methodologies. The TD measurements are investigated for validation and measurement time speed-up.

1.4 Thesis Outline

The second chapter of this thesis gives a literature review of the subject, a substantial theory on electromagnetic interference and compatibility as well as the description to shielding effectiveness. The different methods of measurements are then narrowed down to the measurement method used in the thesis, that is, the reverberation chamber. It

describes the reverberation chamber and gives a brief description of several methods of measurements in a reverberation chamber.

The third chapter explains measurement methodologies both in frequency domain and time domain, a full description of the measurement set-up and the technique used for measurements, and the nested reverberation chamber technique. It provides a wider explanation and understanding of the different parts that form the entire set-up and how these different parts work together to achieve the desired functionality and results.

The fourth chapter provides and discusses results of the measurements done both in frequency domain and time domain. It also discusses the relationship of those results with previous similar work as well as the available manufacturer data. The validity of these results from the comparisons done with these previous data as well as the results comparisons as obtained from the two reverberation chambers used in this study, are also provided in this chapter.

The final chapter of this thesis summarises the entire work done, achieved objectives, the drawbacks and challenges encountered during the measurement process as well as recommendations and suggestions for future work along the same line of measurement.

Chapter 2

LITERATURE REVIEW

This chapter provides details on a survey done on the available literature pertaining to shielding effectiveness investigations in reverberation chambers. Theory on electromagnetic compatibility (EMC) and electromagnetic interference (EMI) is also explained. Alternative methods for measuring the shielding effectiveness of materials and the standards observed in such measurements are provided as well.

2.1 Introduction

The increasing complexity and increased use of electronic devices and/or systems have resulted in increased electromagnetic interference. EMI consists of many unwanted radiated signals which can affect the performance of devices and/or systems in a given electromagnetic environment, by causing them to malfunction or otherwise degrade their performance. But since these devices and/or systems need to perform up to standard in the real world and in the environment where they are intended to work, there is need to create an electromagnetically compatible environment around each system in order to achieve its intended functionality. Electromagnetic compatibility addresses the problem of electromagnetic interference, and can be achieved through different methods discussed later in this chapter.

2.2 Electromagnetic Interference

Electromagnetic interference is the process by which unwanted and disruptive electromagnetic energy is transmitted from one device or system to another through radiated or conducted paths. The transmission of the unwanted electromagnetic energy can also take place through both of the two mechanisms [6].

EMI can prevent the efficient use of radio frequency spectrum and distort data collected from observation within the electromagnetic spectrum coverage, which is received as noise by the susceptible devices. Interference can thus be defined as an undesirable effect of noise.

Any electrical device which has changing voltages and currents within its circuits can be a source of noise. This is because of the presence of electrical signals in the circuit

other than the desired signals, due to these changing voltages and currents. In this aspect, noise can thus be defined as any electrical signal present in a circuit other than the desired signal. In a given environment,there are several sources of noise. These sources can be grouped into the following three categories:

- **Intrinsic noise sources** - sources that result due to changes in the physical quantities of the system.
- **Man-made noise sources** - sources that emerge from man made electrical and electronic devices computer, phones, radio transmitters, radars etc.
- **Natural sources** -Noise caused by natural occurrences, such as lightning and sunspots.

Electromagnetic noise causes electromagnetic interference. Suppression of this noise in the transmission path requires an understanding of the equipment and systems present in the particular electromagnetic environments. In order to have a better understanding of the mechanism of noise interference, the following section focuses on the electromagnetic compatibility in an electromagnetic environment (EME).

2.3 Electromagnetic Compatibility (EMC)

Electromagnetic Compatibility (EMC) is defined as the ability of equipment or systems to function satisfactorily in their electromagnetic environment without introducing intolerable electromagnetic disturbances to any other equipment or systems in that environment [7, 8] (according to IEC definition).

EMI is of great concern for the SKA project. Therefore, there is an attempt to ensure that proper EMC techniques are followed in order to achieve electromagnetic compatibility within the environment the instruments are operating. This would ensure that the performance of the instruments at the SKA sites are not degraded due to EMI. When different equipment and systems are operating in proximity to one another, or in the same environment, they are prone to affect the functionality of one another due to the radiated emissions that they produce. On the other hand, according to design and different clock rates of different sub-systems in a system, a system may as well interfere with itself. Therefore, electromagnetic compatibility may be described as the ability of an equipment or a system to function satisfactorily in its electromagnetic environment without interfering with itself or other equipment and/or systems in that environment. [9]

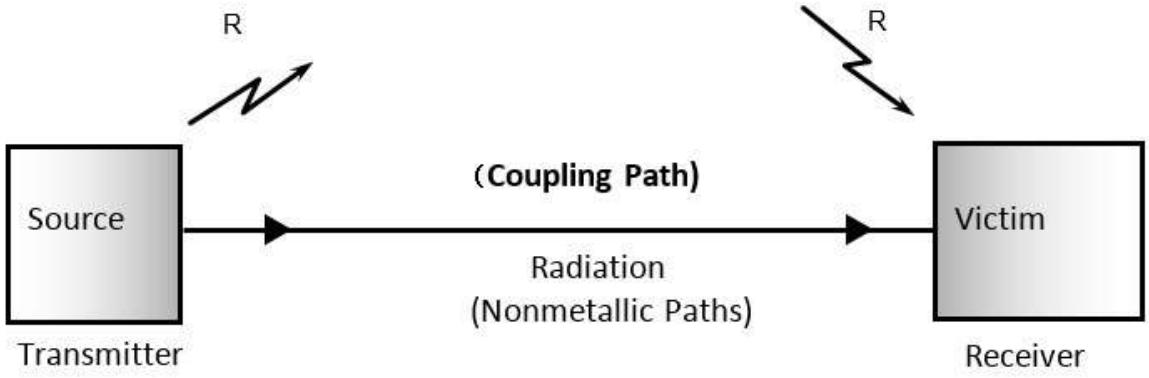

Figure 2.1: Elements of electromagnetic compatibility, and their relationship in an electromagnetic environment with regard to radiated coupling.

2.3.1 Composition of Electromagnetic Compatibility

For an electromagnetic interference problem to exist in any electromagnetic environment there must be a noise/interference source, a victim and a path for the energy to be transferred from the source to the victim [10]. This is represented in the figure 2.1. for the case of radiated coupling.

In this context, the victim is any circuit, device or system where the electromagnetic interference problem occurs, that is, the equipment or system whose performance is degraded or caused to malfunction. Since it is not possible to eliminate any of these three basic elements of EMC, any effective electromagnetic interference control method/technique therefore addresses the interference problem in all the three elements, for achieving electromagnetic compatibility. The control methods focus on design such that the radiated and/or emitted interference is attenuated to magnitude levels adequate to be discriminated by the victim. For an effective EME with good EMC, emissions should be suppressed at the source, the coupling path made as inefficient as possible and the receptors/victims made less susceptible. In some cases, there is little or nothing that can be done on either the source or the victim. Therefore, of the three elements, the control techniques majorly lie in the coupling path.

2.3.2 Coupling Mechanism

Electromagnetic noise/disturbance may be transferred from a source to a victim by some mechanism. This mechanism of transfer of an interfering signal from the source to the victim is referred to as coupling. To understand the various ways of coupling between

systems, it is necessary to define a few terms. There are the two main mechanisms by which electromagnetic noise couples to a victim circuit, conduction and radiation [10].

Conducted Interference

Conducted emissions are unwanted transient signals and other disturbances that couples to other structures through circuit wiring or through portions of the system that are conductive, causing interferences in the functionality of those systems/structures [10]. The power source and the load are connected via wire, which forms the coupling path. Stray currents and voltages that exist in these connecting wires result into stray capacitances and inductance. They are divided into two:

- **Common mode interference (CM)**: In this case the interfering signal appears between two conductors and the ground. The two conductors could be two input terminals of a system or a circuit. The ground is the reference point. Both the interfering signal and the system signal flow in the same direction.
- **Differential mode (DM)**: In this case, the interfering signal flow in the opposite direction as the system signal in the conductor and appears at the input terminal of a circuit. This is shown in figure 2.2. These transient signals are generally measured with voltage and current measurements on the cables.

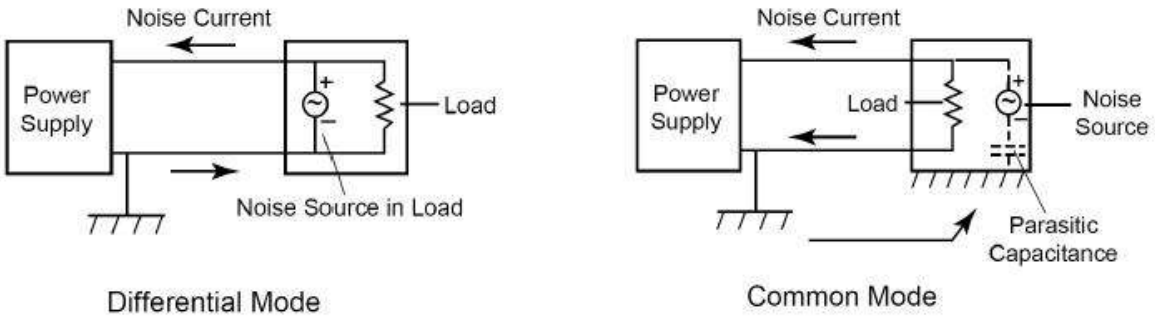

Figure 2.2: Illustartion of signal flows in a common mode and differential mode circuits.

The CM and DM currents in a circuit can induce radiated emission in the same system. Due to these stray currents, parts of the circuit of a system may start to act as antennas which consequently transmit high frequency oscillations, especially in high frequency circuits. At any point where an imbalance in the circuit occurs, radiated EMI is generated through stray impedances and the radiation problem may worsen. The breakpoint between conducted emissions and radiated emissions is 30 MHz. Therefore, for frequencies above 30 MHz, radiated emissions are defined.

Radiated Interference

Radiated interference consists of field-to-cable coupling, cable-to-cable coupling, and common-

mode impedance coupling. In the radio frequency band, radiation is the common and dominant mechanism of EMI/RFI propagation [11]. Radiating emitters can be categorised into two main groups:

- Intentional emitters: these are devices that emit unwanted emissions which may be in the form of harmonics and are directly associated with the function of the equipment that is emitting.
- Unintentional emitters: these are devices which generate emissions as a by-product of the main function of the equipment and/or device. They include computers and mobile phones among other devices.

Coupling may occur through one mechanism or both. Coupling through a combination of mechanisms may result when, for instance, noise or interference, is conducted from an emitter to a point of radiation at the source antenna, then radiated through antenna receptor and re-conducted to the victim device. To mitigate interference that reach the victim device through multiple mechanisms is quite challenging. This is because eliminating one path may not entirely do away with the interference.

Radiated interference targets victims that operate in the high frequency bands of the electromagnetic spectrum. In the scope of this work, the coupling mechanism that is addressed is one that is radiated and thus forms a significant part of the electromagnetic spectrum.

The Electromagnetic Spectrum
The electromagnetic spectrum is the entire range of all type of electromagnetic radiation extending from gamma rays to radio waves [12]. Figure 2.3 shows the spectrum. Generally, EMI problems are caused by electromagnetic energy at any frequency in the spectrum. RFI on the other hand is caused by frequency that occur within the radio frequency band.

The electromagnetic spectrum is shown from the longest wavelengths and lowest frequencies to the shortest wavelengths and highest frequencies. The radiation with lower energy photons and conversely longest wavelengths are the major causes of Electromagnetic interference, and these are the radio waves. Designation to these frequency bands are given in table 2.1, where we mainly consider the high frequency band,very high frequency band and the ultra high frequency band.

2.3.3 Classification of EMI

EMI can be classified by its position of occurrence in the electromagnetic environment (EME). EMI can be either narrowband or broadband interference. These terms refer to the

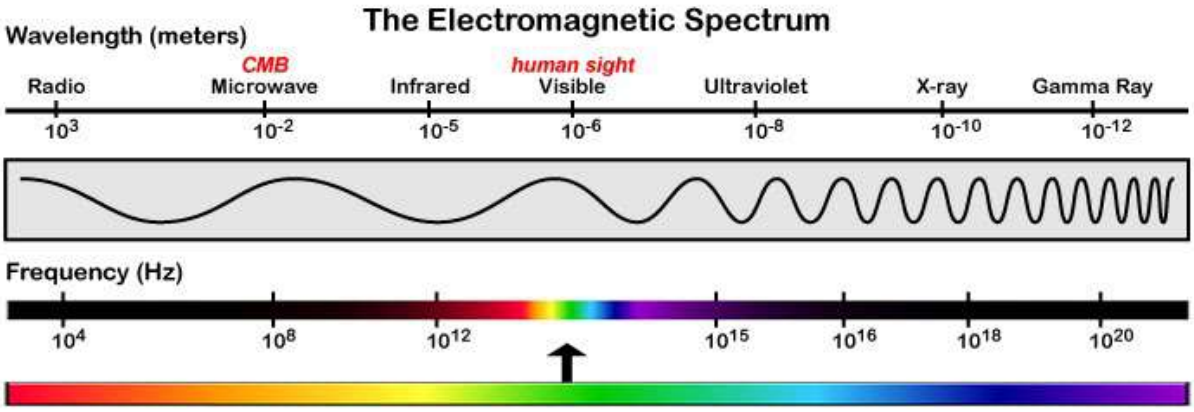

Figure 2.3: The electromagnetic spectrum demonstrating the relation between wavelength and corresponding frequency; from lowest frequency/longest wavelength to highest frequency/shortest wavelength. (Credit: NASA's Imagine the Universe)

Frequency	**Designation**	**Abbreviation**
3 - 30Hz	Extremely low frequenc	ELF
30 - 300Hz	Super low frequency	SLF
300 - 3000Hz	Ultra low frequency	ULF
3 - 30kHz	Very low frequency	VLF
30 - 300kHz	Low frequency	LF
300 - 3MHz	Medium frequency	MF
3 - 30MHz	High frequency	HF
30 - 300MHz	Very high frequency	VHF
300 - 3GHz	Ultra high frequency	UHF
3 - 30GHz	Super high frequency	SHF
30 - 300GHz	Extremely high frequency	EHF
300 - 3000GHz	Tremendously high frequency	THF

Table 2.1: Radio-frequency spectrum broken down into different frequency bands [12]

frequency spectrum that the interference covers. This section discusses the classification of the EMI according to the position of the elements of EMC [10, 12].

Inter-System EMI

When the source of interference and the victim are in separate systems, the interference situation is considered as inter-system EMI. Examples include: personal computer interfering with the operation of a television, or a radar a flying drone interferes with the operation of an airplane.

Intra-system EMI

Unlike the inter-system interference, an intra-system EMI occurs when all the three elements of EMC are in the same system. That is, the source, the victim and thus the coupling path, all exist in the same system. This means that more than one coupling mechanism exist in such environment. For example, a system may emit interference that gets conducted by another system in that same environment. Part of a circuit or a system may act as an antenna and pick up emissions from an adjacent system and similarly radiate that interference into that same environment. This could get picked up and a train of intra-system EMI created.

Regions of Electromagnetic Interference

Having identified radiated emissions as the major type of interference that needs mitigation in the scope of this work, it is important to understand their sources. The source of interference determines the kind of measures that need to be taken to mitigate the given interference. The regions can be categorized as near-field or far-field [8], depending on the space surrounding it, as described below and depicted in figure 2.4.

Far-field Region

This is the region that exists far away from the source, usually at a distance r larger than $\frac{\lambda}{2\pi}$, [8], see equation 2.1, where λ is the wavelength of the source. This region is also referred to as the radiation field. In this region, the field properties are determined by the characteristics of the medium through which the field propagate.

$$r > \frac{\lambda}{2\pi} \tag{2.1}$$

Near-field Region

This is the region that is close to the EMI emitting source, mostly at distances less than $\frac{\lambda}{2\pi}$, [8], see equation 2.2, and is also referred to as the induction field. For this region, characteristic of the field source determines the properties of the field.

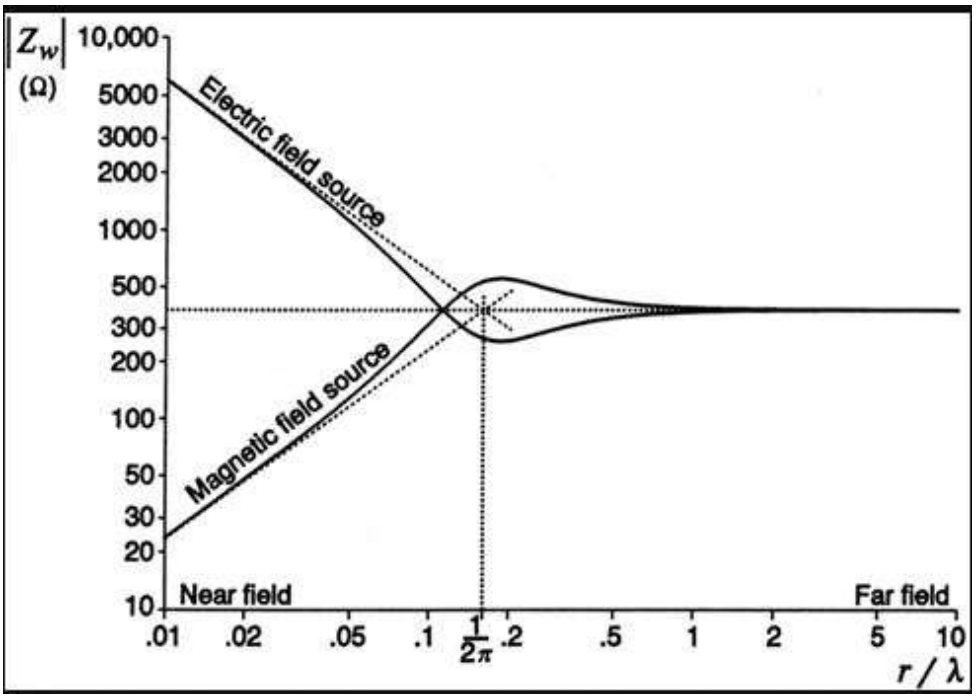

Figure 2.4: Representation of the EMI field, the near and far-field regions [8].

$$r < \frac{\lambda}{2\pi} \tag{2.2}$$

Measurements of radiated emissions must not be done near the source, because they may not be accurate since the field structure is complex when the source is near. Thus electric (E) and magnetic (H) fields will not decay with distance at the same rate. When the field is far, the field structure becomes simpler and the two fields, E and H decays with distance at the same rate, as illustrated in figure 2.4. Therefore, the source of interference for this study is in the Far-field. These sources, due to their large distances from the victim can be considered as electromagnetic plane waves.

Electromagnetic Waves

The basic component of EMI is an electromagnetic wave. A transverse electromagnetic wave is a wave that consists of an electric field (E) and a magnetic field (H), which are perpendicular to each other and to the direction of the wave propagation [13], as represented in figure 2.5. For a shield to be effective, we must block both the electric and magnetic fields in any combinations they may appear.

According to [13], the ratio of the electric field, E to the magnetic field, H is called wave the impedance, Z_w and is given by equation 2.3.

$$Z_w = \frac{E}{H} \tag{2.3}$$

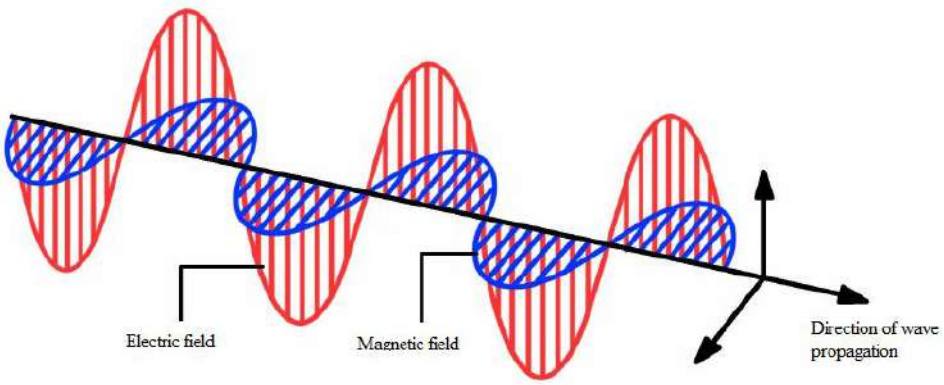

Figure 2.5: Representation of a plane wave, where the electric field and magnetic field are perpendicular to each other and to the direction of wave propagation [13].

The wave impedance of free space is referred to as the intrinsic impedance of free space [13, 14], and is equal to 377 Ω, according to equation 2.4.

$$\eta_0 = \frac{E}{H} = 377\ \Omega \tag{2.4}$$

Equation 2.3 can also be expressed in terms of the permittivity ϵ_0 and permeability μ_0 of free space as shown in equation 2.5 below.

$$\eta_0 = \sqrt{\frac{\mu_0}{\epsilon_0}} \tag{2.5}$$

EM waves, like light, travel in free space with a velocity of 3.00×10^8 m/s . Therefore, referring to the relationship between the speed of light, frequency and wavelength, which is the measured speed of light (c), frequency (f) and wavelength (λ) , EM wave speed in free space is given equation (2.6);

$$c = \lambda f \tag{2.6}$$

where c is speed of light, f is frequency and λ is wavelength.

The field characteristics of the electric field and magnetic field, E and H, depend upon their relative distance from the sources generating the waves. The nature of the source is also a factor in determining the characteristic of those respective fields. This implies that, for every type of interference, there is a wave impedance associated with it. In the Far-field region, any source of interference radiated is considered to be an electromagnetic plane wave, and therefore, the wave impedance of any interference from this region is the characteristic impedance of free space.

In the near-field however, the wave impedance is determined by the source characteristics and the distance from the source to where the field is observed, as shown in figure 2.4. If the source has high current and low voltage, then the wave impedance is less than the characteristic impedance of free space, and the near-field is said to be predominantly magnetic. Otherwise, the near-field is predominantly electric.

2.4 Electromagnetic Interference Mitigation

An electromagnetic environment may be made compatible by reducing the susceptibility of equipment, which are the victims, by reducing EMI from the sources or by introducing attenuation in all EMI coupling paths between sources and susceptible equipment. Either one of these measures will ensure that the victim and the source can exist in the same environment without interfering with each other. Since the source of electromagnetic interference cannot be easily controlled, the compatibility is majorly achieved by acting on the coupling path.

EMI suppression techniques are the methods employed between the source and the victims to suppress or attenuate the EM energy and prevent it from interfering with the victim circuit or system. Several techniques have been used including shielding, grounding and filtering.

While grounding and filtering are primarily used for protecting victim circuits and systems from near-field interference, shielding is used extensively in Far-field interference mitigations. It is the primary means of EMI mitigation.

2.4.1 EMI Shielding

A shield is a conductive barrier that prevents time-varying electromagnetic fields/energy from coupling to or radiating from an electronic circuit or a system. EMI shields are used to partially or completely obstruct any interference from reaching the victim which could be a system or a circuit. Shields can be used at different levels and differently. One way could be the construction of enclosures which can be used to house and envelop electronic circuits, such as integrated electronic boards and printed circuit board. They can also be used to make shielded rooms and even for shielding buildings. Therefore, shields prevent external energy from interfering with sensitive circuits, prevent noisy circuits and devices from interfering with neighbouring devices and provide self compatibility, that is, prevent a device from interfering with itself.

The performance of a shield is determined by several factors:

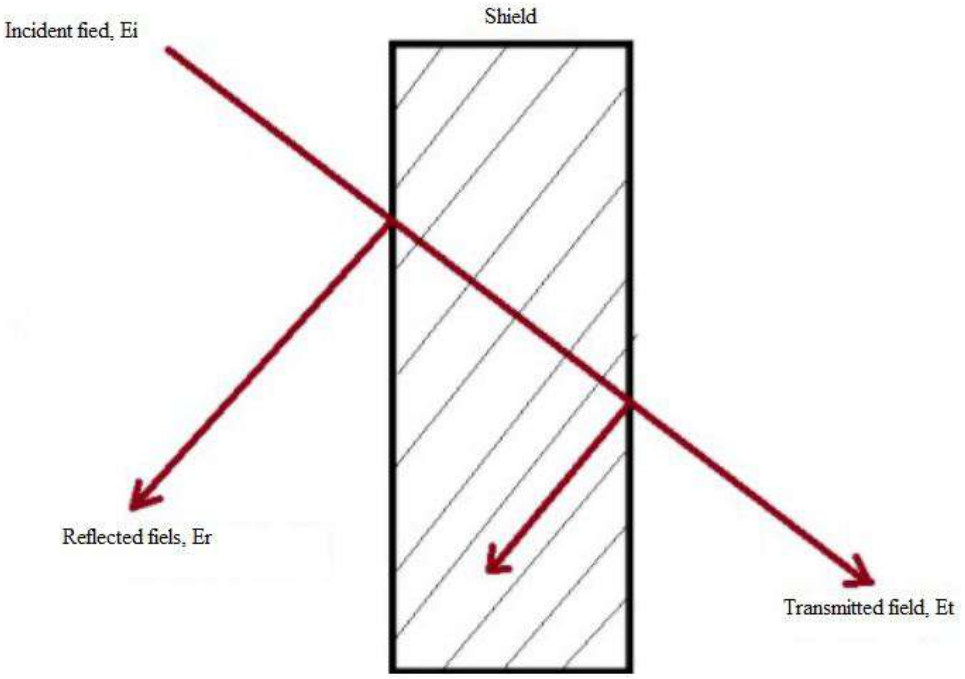

Figure 2.6: Representation of shielding phenomena for plane waves through a metal barrier.

- Conductivity of the material, σ, its ability to conduct an electric current.
- Permeability of the material, μ, that is, the measure of its ability to support the formation of magnetic field within itself.
- Material thickness.
- Frequency, f, of the impinging interference signal.

These factors mostly play a role when the effectiveness of the shield is to be computed numerically. In measurements however, one need not necessarily know all of these factors in order to evaluate the effectiveness of a shield.

2.4.2 Shielding Effectiveness

Shielding effectiveness is the ratio of the magnitude of the electric or magnetic field that is incident on the barrier to the magnitude of the electric or magnetic field that is transmitted through the barrier [8, 15–17]. When an electromagnetic wave passes through a shield, figure 2.6, absorption and reflection take place. The remaining energy that is neither reflected or absorbed is transmitted through the shield.

Thus, shielding effectiveness (SE) of a barrier or material is the term used to quantify its shielding performance either for an electric or magnetic field expressed in dB as given in equations 2.7 and 2.8, and in terms of power as given in equation 2.9.

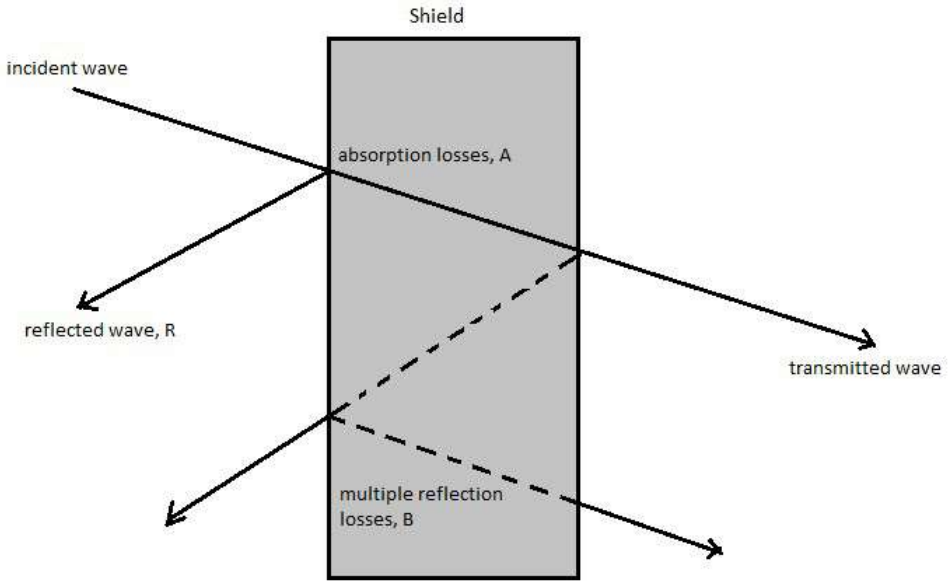

Figure 2.7: Diagramatic representation of losses due to a shield.

$$SE(dB) = 20log_{10}(\frac{E_t}{E_i}) \tag{2.7}$$

$$SE(dB) = 20log_{10}(\frac{H_t}{H_i}) \tag{2.8}$$

$$SE(dB) = 10log_{10}(\frac{P_t}{P_i}) \tag{2.9}$$

where E and H are electric and magnetic fields and the subscripts t and i refer to the transmitted and incident waves. E is measured in V/m and H in A/m. SE is a function of frequency since E and H are frequency dependent.

Representation of Shielding Mechanism for Plane Waves

When an electromagnetic wave is incident to a shield some of its energy is reflected at the first surface of the shield, some is absorbed by the shield, and some is transmitted through the shield. Within the shield multiple reflections also occur, before the wave finally exits the shield at a reduced magnitude [8]. The attenuation of an electromagnetic wave can therefore be said to occur by three mechanisms, according to the above description as shown in figure 2.7.

Based on that description given by [8], there are three mechanisms that compose the computation of SE of a material, the absorption losses denoted as A, reflection losses at the boundaries denoted as R, and multiple reflections losses within the shield denoted as

B [8]. The first effect is reflection at the left surface of the barrier. The portion of the incident field that is reflected is given by the reflection coefficient for that surface. The rest of the wave that travels into the shield strikes the inner walls of the shield and is reflected multiple times. The remaining portion of the wave thus emerges the shield as transmitted wave, at a much reduced magnitude due to the attenuations as a result of reflection, absorption and multiple reflections.

Therefore, the shielding effectiveness given in equations 2.7-2.9 can be broken into the product of three terms each representing one of the phenomena of reflection loss (R), absorption loss (A), and multiple reflections (B) [8, 10] . In decibels these factors add to give the total shielding effectiveness (SE dB) of the shield as in equation 2.10. Each term of A, R and B can be calculated according to equations 2.11-2.13.

$$SE(dB) = R(dB) + A(dB) + B(dB) \tag{2.10}$$

The reflection losses and absorption losses are responsible for a major part of shielding [8]. However, multiple reflections within the shield also contribute to the general shielding effectiveness of a shield. Material samples for the shielding effectiveness investigations will be chosen based on cost, weight, good mechanical properties and commercial availability.

$$R = 168.14 + 20log\sqrt{\frac{\sigma}{f\mu_r}} \tag{2.11}$$

$$A = 20loge^{\frac{t}{\delta}} \tag{2.12}$$

$$B = 20log(1 - e^{\frac{-2t}{\delta}}) \tag{2.13}$$

where,
t, is material thickness (m)
μ_r, is material permeability relative to air
σ_r, is material conductivity relative to air
f, is frequency (Hz)

2.5 Shielding Effectiveness Determination

Evaluation and determination of SE of materials is very valuable. SE of a material can either be determined through numerical modelling or through measurements. However, numerical methods for SE determination are very difficult and time consuming due to complexity of different materials and many factors that need to be considered.

In the numerical analysis and computation of material's SE, one needs to know the properties of the shield as discussed above, the conductivity of the material and the permeability among others. For many materials, this information is not available rendering this method of shielding effectiveness determination often infeasible. For this reason, measurements are often preferred in recent years for the determination of SE of materials.

2.5.1 EMI shielding Effectiveness Measurement Techniques

International and governmental bodies have put in place several standards to be observed for compliance in regard to electromagnetic emissions, immunity, and shielding effectiveness testing procedures. Testing for compliance with these international standards has led to the development of various test facilities, methods and techniques for electromagnetic compatibility [18–21]. Given below, are some of the methods commonly used in EMC measurements;

- Transverse electromagnetic cells
- Anechoic and semi-anechoic chambers
- Reverberation chambers
- Free space method
- Open area test sites
- Shielded room method

Transverse Electromagnetic (TEM) Cell

The transverse electromagnetic (TEM) cell provides a uni-polarized, propagating plane wave. The electromagnetic environment (EME) is calculable, highly uniform within its working volume and has a field amplitude uncertainty low enough to be used for probe calibration [20, 22]. To provide a robust test, the equipment under test (EUT) must be rotated through multiple, three-dimensional orientations with respect to the plane wave.

TEM cells can be used for both immunity and emissions tests. The working volume is frequency dependent.

Anechoic Chamber

An anechoic chamber is a room or an electromagnetic measurement environment that emulates free space. It is made of radio frequency absorbing materials aligned on its entire inner surface area. The absorbing materials absorbs electromagnetic energy that is propagated away from the device under test (DUT) or antenna under test (AUT), thus eliminating any boundaries and formation of standing waves [19].

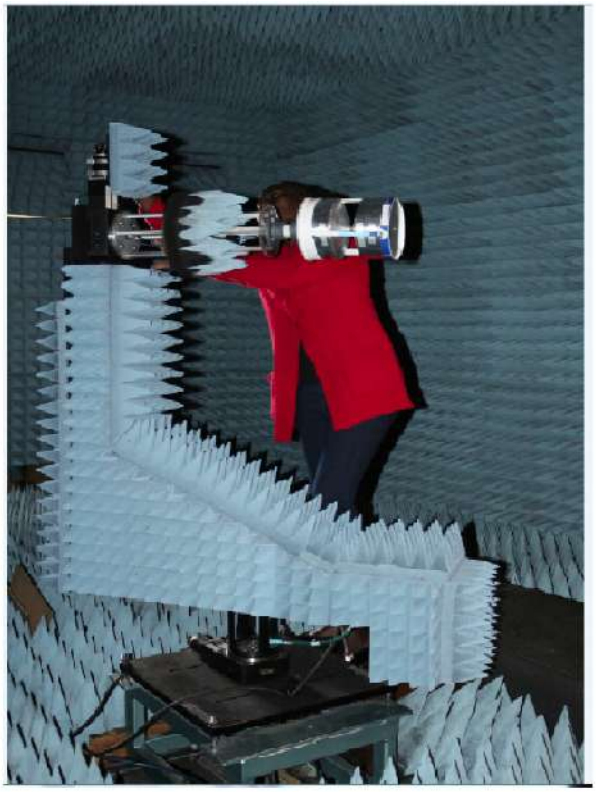

Figure 2.8: Photograph of an anechoic chamber at Stellenbosch University. The antenna under test is elevated on a pedestal for proper orientation during measurement

An anechoic chamber (AC) is used for different types of antenna measurements as well as EMI and EMC measurements. Some of them are only a reflection free room, while others besides being a reflection free room, are also shielded. For the shielded anechoic chambers, SE can as well be carried out. Since AC is a non-reflective free space environment, the destructive signals coming from the surrounding environment are blocked and the RF signals generated are absorbed by different foam absorbers and ferrite tile absorbers present inside the chamber. This ensures that measurements are not affected by interference from the surrounding as well as reflection from any emitting sources under test. Figure 2.8

shows a photograph of the rectangular anechoic chamber that uses pyramidal absorber as main RF absorbing material.

Free-space Method

The free-space method is a technique to characterize the electromagnetic properties complex electromagnetic medium. This is done by characterizing the reflection and transmission path through that medium. It is a method that can be easily applicable to inhomogeneous media [21, 23]. Figure 2.9 schematically illustrates the free-space set-up for material evaluation.

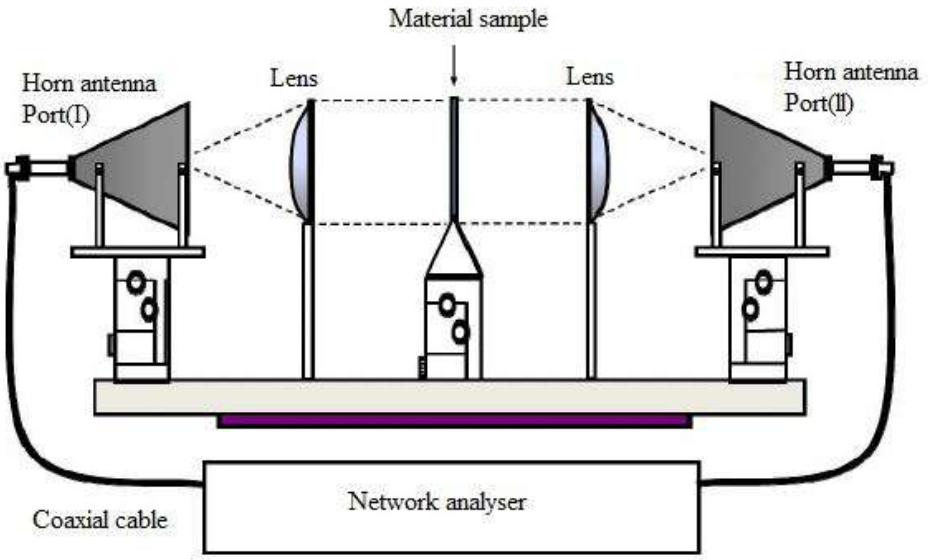

Figure 2.9: Schematic of the free-space measurement set-up.

It consists of two oppositely positioned horn antennas. Power generated by the network analyser is transferred through coaxial cable and emitted by one antenna and received by the second antenna on the opposite side of the medium to be characterized. In front of the antennas are convergent lenses that are positioned to both sides of the material sample under measurement. The lens on the left ensures that the transmitted power from horn antenna connected to port one, is converged and directed to through the material sample. the lens on the right side of the material sample converges the power that has passed through the sample and directs it to the receiving horn antenna connected to port two of the network analyser. The measurement is controlled by a software on a PC, which collects the measured power and stored in terms of S-parameters for post processing.

2.6 Reverberation Chambers

Reverberation chambers are the latest development in EM testing. They are used for performing radiated immunity, radiated emission and shielding effectiveness tests [9, 18].

They have been used for many years for conducting these tests. A reverberation chamber is a highly conductive shielded enclosure used for generating an electromagnetic environment for electromagnetic compatibility testing.

Figure 2.10: Reverberation chamber for shielding effectiveness measurement [24].

It is equipped with one or more stirrers/tuners that are used for mixing the field modes within the chamber, to ensure that the fields within are statistically homogeneous, a condition that is required for a well operating chamber. Figure 2.10 shows a photograph of a vehicle inside a reverberation chamber for EMC testing. The chamber is equipped with a Z folder and has dipole antennas for signal measurement. The stirrer ensure that the field modes are mixed to obtain a modal structure within the chamber.

2.6.1 Reverberation Chamber Modal Structure

Modal structure can be defined as the sum of a set of basic functions which is useful for visualizing variations in fields as a function of location. Modal structures are excited within the chamber that results in the desired electromagnetic environment. These modal structures created within the chamber are established by means of stirrers/tuners positioned within the chamber, by effectively changing the boundary conditions and creating a complex field structure.

The structure of the reverberation chamber also influences the complexity of the field generated in the chamber. A more complex physical structure results to a more complex field with complex modal structures in the chamber, hence a better environment for measurements in a reverberation chamber. For this reason, definite shapes such as cubes

and shapes with multiple dimensions are discouraged if a complex measurement environment is desired. The objective of the reverberation chamber is to obtain a field which is constant on average, which has many polarization directions, and which is statistically uniform. This can be achieved by varying the boundary conditions of the whole chamber, by means of stirring.

A well-stirred reverberation chamber provides an electromagnetic test environment which is statistically isotropic, randomly polarized and uniform according to the requirement by standards that govern the measurements in a reverberation chamber [25]. A reverberation chamber EME is said to be isotropic if its the same in any direction inside the working volume. A randomly polarized EME is achieved when the phase relationship between polarized components are random while a uniform EME is achieved when the average field is the same at any location within the usable volume of the reverberation chamber.

2.6.2 Resonant Modes in a Reverberation Chamber

Since a reverberation chamber is a rectangular cavity equipped with stirrers, its dimensions satisfy the equation 2.14. When RF energy of a certain magnitude is introduced into an RC, and by means of stirrers, this energy is stirred thus striking the chamber surfaces randomly and at different angles. This effectively changes the boundary conditions, resulting in a complex field structure. In this complex environment exists resonant modes and multipath reflections. The resonant modes occur at different resonant frequencies determined by the dimensions of the chamber according to equation 2.14.

$$f_{(m.n,p)} = \frac{c}{2\pi}\left(\sqrt{\left(\frac{m\pi}{a}\right)^2 + \left(\frac{n\pi}{b}\right)^2 + \left(\frac{p\pi}{d}\right)^2}\right) \tag{2.14}$$

where m, n and p are integers, a, b, d are chamber dimensions and c, the speed of light.

2.6.3 Stirrers

To obtain a uniform field within the chamber, the modes have to be mixed by means of a stirrer. For any stirring methods, many samples need to be collected to perform the statistical analysis. The statistical independence of these collected samples directly relate to the uncertainty of the statistical results. Therefore, an effective stirring mechanism is required to produce highly independent samples. If highly independent samples are not achieved from the stirring, the collected samples will have a low correlation. For the samples to have a higher correlation, the environment within the chamber need to be a

Figure 2.11: Different stirrer designs as used in the two different chambers in this study. The shape and size of the stirrer used affect the measurement significantly.

complex one.

The structure within the chamber is considered complex and fit for electromagnetic compatibility tests when it is isotropic, randomly polarized and statistically uniform. When this complex test environment is achieved, then the equipment under test or enclosure under test is exposed to radiation from all angles and polarizations hence no need to move it during measurement.

The measurement time always depends on the tuner settling time. The tuner should occupy a reasonable space within the chamber of about 25-30 percent. The longer the time it takes for the tuner to settle the longer the measurement time.

2.6.4 Stirring Mechanism

There are several stirring mechanisms that can be used to achieve this uniformity, including, mechanical stirring, frequency stirring, polarization stirring, time stiring, source stirring and hybrid stirring [7, 26].

The most commonly used in reverberation chamber measurements is mechanical stirring and frequency stirring.

Mechanical Stirring

Mechanical stirring is achieved when the tuner or stirrer plates within the chamber are rotated. The rotation may be continuous or stepwise [7, 27].

While in mode-stirring, the stirrer continuously rotates at a set rate; in mode tuning, the stirrers are incrementally stepped through a complete rotation with a set dwell time applied at each step. In either case, one complete stirrer rotation will result in a complex test environment that is desired. The mode tuning technique has been used in this work, in which case, the maximum electromagnetic field level in the chamber is measured while

tuners are settled at specific angles as set by the controlling software.

Frequency Stirring

Frequency stirring is achieved when the frequency of a stimulus signal into the chamber is changed. By changing the frequency, reflections from the walls and stirrers also occur at different frequency and phases resulting into a changing standing wave. The change in standing waves within the chamber will thus result into independent samples. By averaging over a frequency window of a chosen bandwidth, a stirring effect is obtained. To obtain the measured data, the stirrer is held static and the average transferred power is computed over frequency [28].

Besides the use of stirrers, as earlier stated, the structure of the reverberation chamber also influences the complexity of the field generated in the chamber. A more complex structure of a reverberation chamber gives a complex modal structure when properly stirred and thus a better environment for reverberation chamber measurements.

2.6.5 Lowest Usable Frequency (LUF)

Besides the numerous capabilities of a reverberation chamber, it has a few limitations. Measurements and characterization of materials at very low frequencies may sometimes be inaccurate. This is because the performance of a RC is defined by its lowest usable frequency (LUF).

LUF is the frequency at which the chamber attains the right uniformity and validity for use in measurements. This frequency is determined by the size of the chamber and can be estimated by calculating the frequency at which the chamber has at least 60 modes. In [7], the number of independent modes is a function of frequency and is given by equation 2.15.

$$N = \frac{8\pi}{3} abd \frac{f^3}{c^3} - a + b + d \times \frac{f}{c} + \frac{1}{2} \tag{2.15}$$

where N is the number of modes, a, b and d are the chamber dimension and c is the speed of light.

A bigger chamber has a much lower LUF compared to a smaller chamber. The number of modes excited defines how well the environment within the chamber is suited for measurements. At the LUF and frequencies closer to this, the number of modes excited are less, hence not sufficient to generate a uniform field. Therefore, this thesis also investigates how increasing the number of stirrer positions can improve the chamber uniformity at

these frequencies.

2.7 Reverberation Chamber Standards

Since its inception many years ago, several standards have been put in place to define the shielding effectiveness measurements in a reverberation chamber. Some of the standards are:

- MIL-STD (Military standards) - which describes the attenuation measurements for enclosures and electromagnetic shielding for the purpose of testing electronic devices. It describes these tests for a frequency of 100 kHz to 10 GHz.

- IEEE – 299 standards - Institute of Electrical and Electronics Engineers standards, in the application of the IEEE Std 299-1997 "Standard Method for Measuring the Effectiveness of Electromagnetic Shielding Enclosures, described and applied in [29].

- IEC 6400 standards (International Electro technical Commission). Section four describes the shielding measurement in a reverberation chamber [7, 25].

These standards have been revised regularly for the purpose of improving the measurement in terms of efficiency, convenience, cost and time. In this project, the IEC 61000-4-21 standard is observed and referred to. In the IEC 61000-4 the methods of measurements and procedures for reverberation chamber measurements are outlined. IEC 61000-4-21 outlines the requirement for the uniformity of a chamber, that would ascertain how well it is for carrying out measurements. The nested reverberation chamber measurement technique is further outlined in IEC 61000-4-12.

2.7.1 Advantages of Reverberation Chambers

The following are some of the advantages of using a reverberation chamber over the other methods of measuring shielding effectiveness.

- Better predictability of uncertainty associated with the tests.
- Better field uniformity.
- Repeatability.
- Ability to generate higher field levels and a screen environment with no ambient signals.

- It is possible to achieve high field strengths at relatively low input power levels than conventional anechoic chambers.
- A random field is generated in the chamber thus, the DUT/EUT is illuminated with equal energy from all directions, orientations and polarizations. Therefore, there is no need for turning the DUT/EUT. This ensures a thorough performance of the immunity tests.
- The reverberation chamber also measures total radiated power making it possible to disregard the need for the determination of maximum emissions, which is difficult at higher frequencies.
- Using reverberation chambers is cheaper compared to other testing facilities such as anechoic chambers. The construction cost is low and once constructed, the maintenance cost is very small. No absorbers are required.

Types of tests

- Radiated immunity tests.
- Immunity tests.
- Shielding effectiveness measurements.

2.7.2 RC Applications

Among many other applications of a reverberation chamber, below are a few that are important for this research.

- Shielding effectiveness measurements
- Simulation of a radio environment
- Measuring antenna efficiency- this is done using the scattering parameters

Chapter 3

MEASUREMENT TECHNIQUE

There are several factors that contribute to EMI problems as highlighted in chapter two of the thesis. In order to find a solution to a specific EMI problem, it is necessary to understand how all components that form the intended measurement set-up work together to achieve that goal. This chapter will focus on measurement technique, and basic measurement set-up, upon which measurements are made.

A number of techniques have been developed and introduced for the determination of shielding effectiveness of materials as discussed under the literature review in chapter two. These different methods have their advantages and disadvantages. This chapter provides the detailed steps and processes used in the determination of the shielding effectiveness of different materials, a nested reverberation chamber technique, which forms the core of this study.

3.1 Introduction

A measurement method is often chosen based on the type of measurement that needs to be done. In making the choice of the measurement method to be used, several factors are taken into consideration. For shielding effectiveness measurement in reverberation chamber, either frequency or time domain is used. Through a Fourier transform, one can easily convert the results of one measurement from one form to another. The measurement set-up for these two are slightly different as shall be seen later on in this thesis.

Time domain measurements are always computed over time, thus amplitudes are plotted against time. For instance, voltage is always plotted against time, for a time domain analysis of an electronic signal. Shielding effectiveness as defined in chapter two is the ratio of the incident power on a shield to the received power after the shield. It is expressed by equation 2.9.

In this work, SE measurement for a frequency range of 300 kHz to 8 GHz is presented. The range of measurement frequency is limited to the operation bandwidth of the measuring instrument. The measurement technique used, is the nested reverberation chamber [15, 30]. Measurements are done in adherence to the guidelines given in the IEC 61000-4-21 standards [7]. While efforts shall be put to conduct the same measurements in time

domain for measurement speed-up and for more accurate shielding measurement [9], these measurements, in the scope of this work, are carried out in frequency domain.

3.2 Nested Reverberation Chamber Approach

The nested reverberation chamber technique is a technique in which a smaller reverberation chamber is used within a larger reverberation chamber to perform measurements [15,30]. The smaller chamber is placed in the working volume of the larger chamber. The smaller chamber has an aperture through which rf energy enters or exits the nested chamber. The aperture properties can thus be evaluated and shielding effectiveness of any material placed on the aperture can be investigated. In [7], the nested reverberation chamber technique for shielding effectiveness determination is outlined in Annex G, "Shielding Effectiveness Measurements of Gaskets and Materials". Therefore, shielding effectiveness of a material that is placed in the aperture can be determined.

Measurements are done in a reverberation chamber according to the set-up given in figure 3.1. A smaller RC with an aperture where material samples can be held during measurement, is placed within a larger RC. Both the chambers are stirred throughout the measurement time to achieve the required uniformity as laid out in the IEC standards.

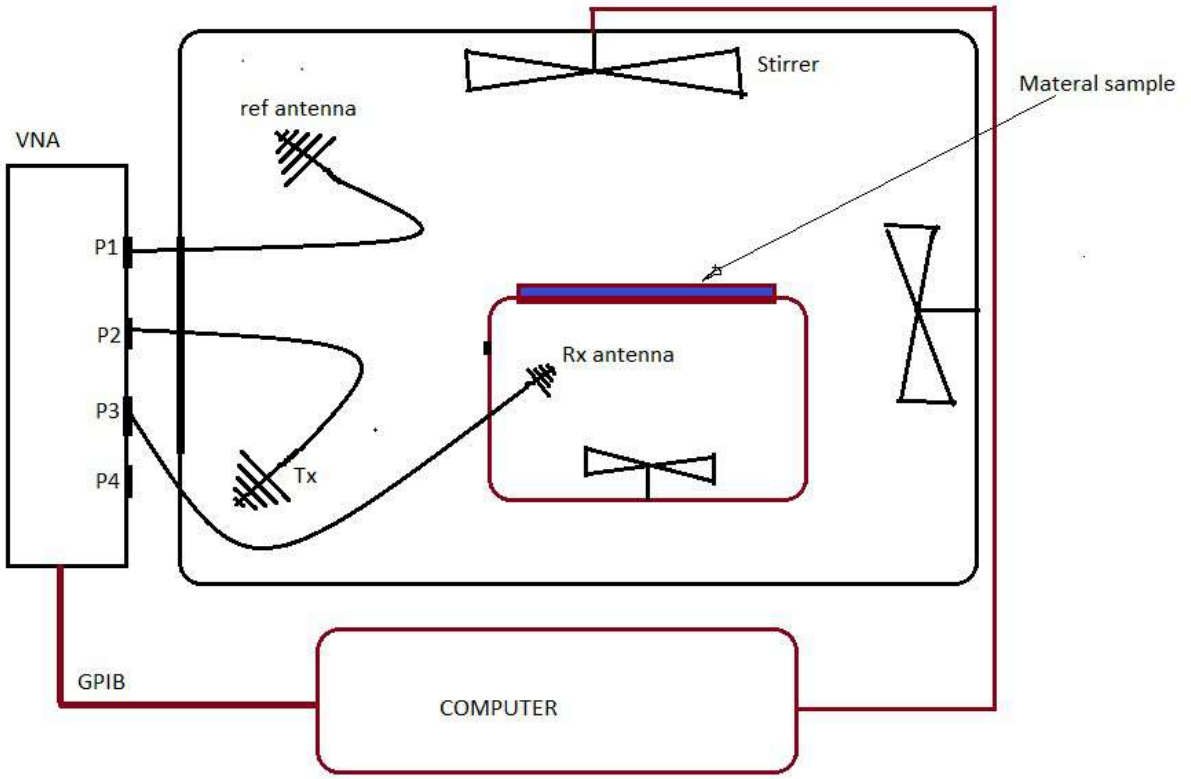

Figure 3.1: Measurement set-up for shielding effectiveness measurement.

Since the lowest usable frequency of a chamber is determined by its size, the nested

chamber size thus determine the lowest frequency of interest. However, as discussed earlier, like any other reverberation chamber, the nested chamber should not be a cube to avoid degenerate modes.

The equipment used in the set-up include the following:

- Main reverberation chamber
- Nested reverberation chamber
- Vector network analyser
- Antennas
- Computer

These are discussed in more details in the following section.

3.2.1 Main Reverberation Chamber

Two RCs are used in this study, one at Stellenbosch University and one at the SKA offices in Pinelands, Cape Town. For the rest of the study, these chambers will be referred to as RC1 and RC2 respectively.

Reverberation Chamber 1 (RC1)
This is the chamber at Stellenbosch University. The chamber is made of aluminium and measures 3.72m by 2.75m by 2.45m. Figure 3.2 shows the photograph of the chamber taken when loaded with the nested chamber and the antennas. The chamber has two stirrers aligned vertically and horizontally. These two stirrers are operated in mode tuned, through a MATLAB program during measurements. According to equation 2.15 and using MATLAB, the LUF of the chamber is computed to be approximately 205 MHz (gives 61 modes).

Reverberation Chamber 2 (RC2)
This is the reverberation chamber at SKA offices in Cape Town. It has a slightly larger volume than the first reverberation chamber, hence a lower usable frequency. It measures 5m by 3.8m by 2.78m, thus according to equation 2.15, its LUF is 150 MHz (gives 61 modes). It is equipped with one large Z fold stirrer placed horizontally and operated remotely in a mode stirred operation. Its photograph when loaded with the nested chamber and the antennas is shown in figure 3.3.

Figure 3.2: The reverberation chamber as used in the majority of work in this thesis. This is set up as per the nested chamber method

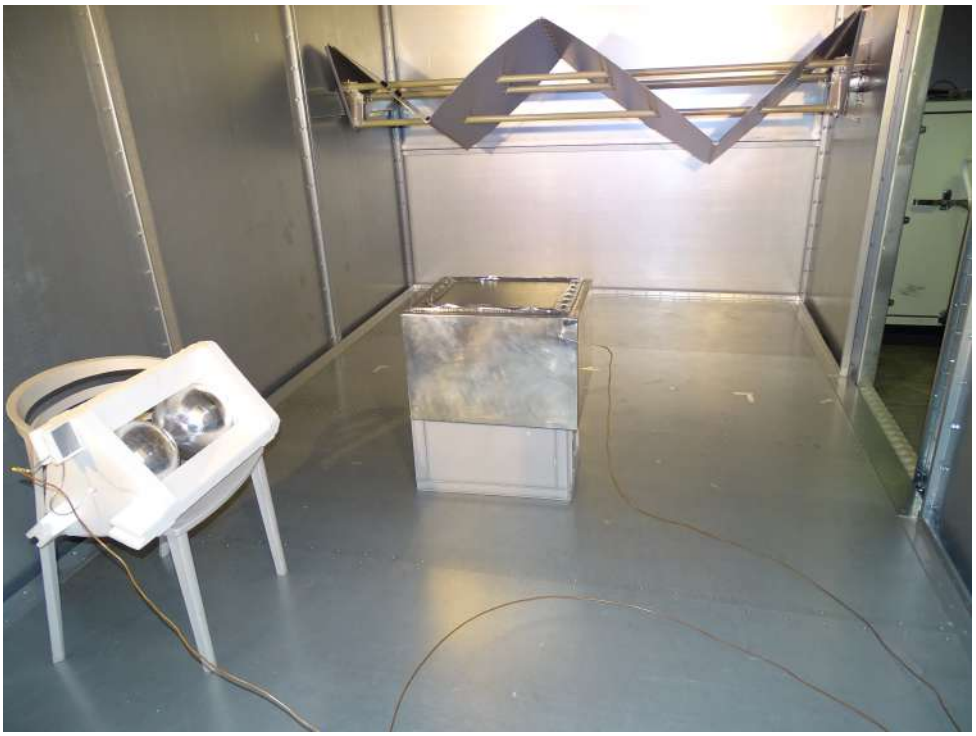

Figure 3.3: Photograph of the nested chamber measurement set-up in RC2

Stirrers

The stirrers in the chambers are large metallic reflectors that are used to change the boundary conditions of the fields within the reverberation chambers for statistical field uniformity. Their shape and size have an effect on the LUF of the main chamber. The two chambers have different stirrer designs hence efficiencies. RC1 has two stirrers placed

vertically and horizontally. They are square plates placed alternately on a cylindrical carbon-fibre rod.

RC2 on the other hand is equipped with one big Z fold stirrer placed horizontal towards one end of the reverberation chamber, figure 3.3. In both cases, the stirrers are rotated and controlled in mode tuned and mode stirred remotely through Matlab programs.

Mode Tuned

RC1 has its stirrers operated in mode-tuned. This is where the stirrer is made to move equal number of stepped angles for a defined position for one whole revolution. After every step movement, the stirrers settle and measurements are taken. The stirrers are moved in steps of 5 degrees resulting in 72 stirrer position for one complete stirrer revolution. The sweep time for the entire measurement, according to equation 3.1, is calculated as 25 minutes, for one complete revolution.

$$\mathrm{ST} = (\mathrm{DT}) \times (\mathrm{SP}) \tag{3.1}$$

Where ST is sweep time in seconds, DT is total dwell time per stirrer position in seconds and SP is the number of stirrer positions per revolution.

The sweep time obtained is 25 minutes. In the Matlab program, the dwell time is defined. The stirrers settles and the vector network analyser collects data in two seconds, a time defined in the program.

Mode Stirred

In this case, the stirrers rotate continuously throughout the measurement. The measurements are taken during the process. The speed of the stirrer is defined at 40 revolutions per minute. The measurement time is thus defined by the setting on the VNA machine instead.

The averaging in the vector network analyser (VNA) is set at average for 72 measurements. This averaging is done to improve the accuracy of the data as well as the dynamic range of the measurements although it slows down the measurements.

Smoothing is done during processing to reduce roughness in the frequency plots. This is done by averaging multiple frequency points and using the result at one frequency, by the help of a Matlab program.

3.2.2 Nested Chamber

The nested chamber is constructed of mild steel and it measures 60 cm by 50cm by 40cm. On the upper face measuring 60cm by 50cm is an aperture that measures 52cm by 42cm. It has 28 threaded holes that are used to hold a material sample by means of bolts and screws. These are fastened carefully to ensure that there is no breakage.

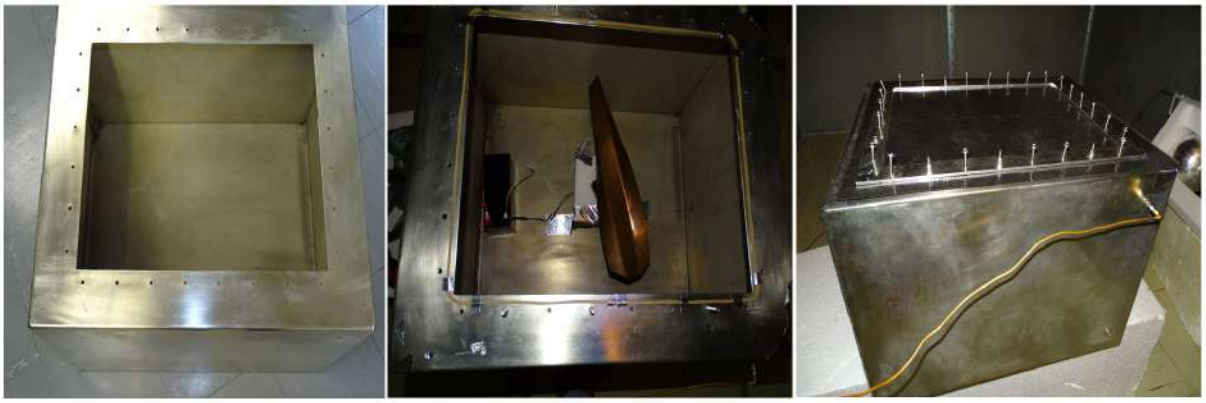

Figure 3.4: The nested chamber.

The nested chamber has a stirrer that is made from copper plates and that has a separate control unit, controlled independently using a micro-controller. This stirrer cannot be controlled remotely and is thus set to run on a mode stirred operation when measurements commence. The nested chamber also has loop antennas as shown in figure 3.4. A loop antenna is a single coil of wire which produces a voltage at its terminals proportional to the frequency. This voltage is a factor of the area of the loop, the field strength and the measurement frequency, as given in equation 3.1. These loop antennas are used to monitor the fields within the small chamber.

$$V = 2\pi f \mu_0 A H \tag{3.2}$$

where;
A, is the area of the loop (square meter)
f, is the measurement frequency (Hz)
H, is the magnetic field (A/m)

These antennas are placed according to the orientation of the box to configure and measure the fields in the x, y and z directions and/or orientations, as is shown by figure 3.5.

The loop antenna are of low impedance and does not match the impedance of other equipment that form the measurement set-up. Calibration of the whole set-up is done to

ensure that everything is matched and that any errors that may be associated to mismatch is eliminated. The field strength is monitored by three of the four loop antennas oriented in the x, y and z directions. The average of the measurements from these three loops is used in the evaluation of the SE of the material on the aperture.

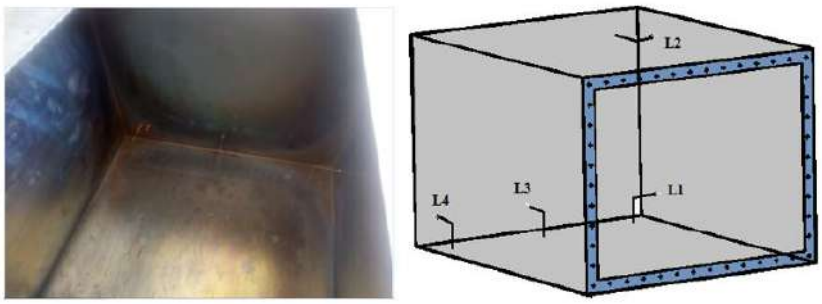

Figure 3.5: Loop antennas for nested reverberation chamber field strength monitoring.

Radio Frequency (RF) Gasket

On the surface of the aperture is mounted an RF gasket, figure 3.6, on which materials are placed. This is to ensure that there is good contact between the material sample under test and the nested chamber.

Figure 3.6: RF gasket.

The RF gasket is rated 80 dB, a value much higher than the expected shielding value of the materials under test, hence, it does not have an effect on the shielding value of the material sample under test

Vector Network Analyser

A vector network analyser (VNA) is an instrument that is used in measuring the electrical parameter of an electrical network. Two different VNAs are used in this study, a two port network analyser, ShockLine™ 2-Port performance VNA shown in figure 3.7,

and a four port network analyser, the ZVB-8, figure 3.10. The two instruments have measurement bandwidths of 20GHz and 8 GHz respectively. They take measurements in terms of scattering parameters (S-parameters), with both the magnitude and phase of a signal injected into the reverberation chamber recorded. The ZVB-8 was mainly used for characterization of the main reverberation chamber. For the shielding measurement of the materials the Shockline VNA was used for the two chambers, RC1 and RC2.

For any two-port network, four S-parameters can be measured at any particular time. Since only two ports are used, four S-parameters are measured; S_{11}, S_{12}, S_{21} and S_{22}. A signal generator is needed as an input for the chamber. The VNA however has an inbuilt signal generator, thus power levels are set accordingly.

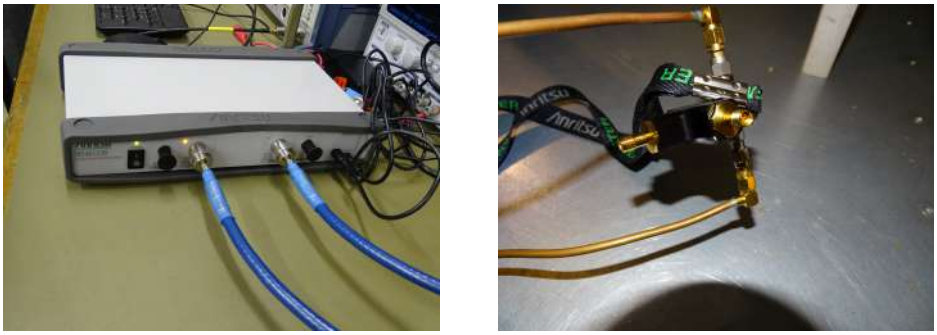

Figure 3.7: ShockLine™ 2-Port Performance VNA MS46522B with measurement frequency bandwidth upto 20 GHz, with the calibration kit.

In the figures 3.7 and 3.10, the calibration kit for the VNA is shown. The calibration kit contains four parts, a short, open, load and a through. These are used to characterise the reflected signals at the two ports up to the antenna ports , the losses as a result of loading the different ports as well as the transmission losses between the two ports up to the antenna ports. The S-parameters are computed in dB magnitude format and plots made of the same thereof.

3.3 Scattering Parameters

S-parameters are a way to describe an electrical network, its behaviour and response to signals input to it. It can describe any type of electrical network based on size as well as complexity. An electrical network is an interconnection of different electrical components that work together to achieve a particular functionality. An electrical network has either one port or multiple ports. Therefore, the size of such networks depends on the number of ports that the network has.

In measurement, the function of a vector network analyser is to determine the S-parameters. Any S-parameter has both the phase and magnitude information of the quantity being measured. Therefore, S-parameters are basically complex numbers. The phase and mag-

nitude information can be separated through processing.

Whenever a wave is incident on a port of a network, part of it is transmitted while part of it is reflected. S-parameters describe the relationship between these waves; incident, reflected and transmitted waves.

A network may have any number of ports, and the S-parameter used to describe it is a matrix consisting of elements equal to the square of the number of ports. Therefore, the S-matrix for an n-port network contains n^2 coefficients (S-parameters), each one representing a possible input-output path.

The S-matrix for any network with any number of ports is a square matrix, thus the number of rows equals the number of columns. This means that for a two-port network, the number of elements of the S-matrix is 4, for a three-port network, the number of elements is 9, with three rows and three columns etc.

Elements of the S-parameter are described using subscripts "ij", where "j" is the input port and "i" is the output port. S-parameters have both magnitude and phase information. Equation 3.3 shows the matrix algebraic representation of 2-port network. Some S-parameters matrices are symmetrical, meaning there is symmetry along the leading diagonals of those matrices. For example, in the case of a symmetrical 2-port network, $S_{21} = S_{12}$ and interchanging the input and output ports does not change the transmission properties. A transmission line is an example of a symmetrical 2-port network. Sometimes the gain (or loss) is more important than the phase shift thus phase information may be ignored.

Figure 3.8: Two port electrical network

$$\begin{bmatrix} b_1 \\ b_2 \end{bmatrix} = \begin{bmatrix} S_{11} & S_{12} \\ S_{21} & S_{22} \end{bmatrix} \begin{bmatrix} a_1 \\ b_2 \end{bmatrix} \tag{3.3}$$

S_{11} refers to the reflection at port 1 for an input at port 1. Referring to figure 3.8, S_{11} is the ratio of the two waves b_1/a_1 when $a_2 = 0$.

S_{21} refers to output at port 2 for the signal input at port 1 and is given by the ratio b_2/a_1

when $a_2 = 0$.

S_{12} refers to the output at port 1 for an input at port 2 and is given by the ratio b_1/a_2 when $a_1 = 0$.

S_{22} refers to output at port 2 for an input at port 2. It is given by the ratio b_2/a_2 when $a_1 = 0$.

Both the phase and magnitude of any incident wave changes when reflected or transmitted through a network. Therefore, the transmitted and reflected waves have different amplitudes and phase to the incident wave. However the frequency information remain the same.

Elements along the leading diagonal of an S-matrix refer to reflections occurring at one port. Other elements describe the transmission between different port. Taking equation 3.3 as an example, $S_{11}\&S_{22}$ describe reflections at ports 1 and 2 respectively. S_{12}, S_{21} on the other hand describe transmission from port 1 to 2 and from port 2 to 1 respectively. They are referred to as transmission coefficient when terminated in matched loads.

The characteristics and parameters of any given network affect and influence the different S-parameter output. These would include characteristic impedance of the source, the load connected to the output of the network, the frequency, etc. A change in any of these parameters results in a change in the S-parameters.

3.4 Antennas

To take measurements of the signals in a chamber, there should be a means of injecting these signals into the chamber as well as another coupling means for the received energies. The instrumentation used for that purpose is an antenna. An antenna is that part of a radio transmitting or receiving system which is designed to provide the required coupling between a transmitter or a receiver and the medium in which the radio wave propagates.As defined in the IEC standards [7], it's a means of radiating or receiving radio waves.

Measurements are made of either electric (E) field or magnetic (H) field components. Since our measurements are made in the far field as seen in chapter 2, the two fields are equivalent and related by the impedance of free space, equation 3.4.

$$Z = \frac{E}{H} = 120\pi = 377\ \Omega \tag{3.4}$$

A transmit antenna is required to couple the field to a measuring receive antenna. The electric field strength is specified in terms of volts per meter at a given distance from the

transmitter (transmitting antenna). These fields as collected by the antennas, converted and displayed in terms of S-parameters by the measuring receiver, the VNA. The internal impedance of the VNA is 50 ohm. The calibration of the set-up up to the antenna input is thus carried out at an impedance of 50 ohm.

3.5 Fundamental Antenna Parameters

There are several parameters that are fundamental to the operation of an antenna. Some of the parameters that very well describe an antenna are, antenna efficiency, antenna gain, operation bandwidth, radiation pattern and directivity. As much as all these parameters are required to fully characterize an antenna, not all are required for measurements in a reverberation chamber. The antenna gain is 1 in reverberation chamber. Shielding effectiveness measurement being a relative measurement, have most of these parameter cancel out during post processing.

Within the scope of this study, two different types of antennas were used. These two antennas were different in three major aspects, directivity, efficiency and operation bandwidth. These aspects are discussed further.

Directivity

For a radiating antenna, the direction of the power radiated is dependent on the structure of the antenna. Therefore, there are two main categories of antennas that are used in this study.

Directional Antennas

These antennas only radiate or receive power towards or from a certain direction. This may be defined by the orientation of the antenna during measurement. The directional antennas used in this study are wideband LPDA antennas. They consisted of an array of dipole elements and displayed stable impedance and pattern over the measurement bandwidth. They have a frequency coverage of 400 MHz to 6 GHz and were mainly used over the entire bandwidth, during the calibration of the chamber, since their efficiencies were predetermined from a previous study.

Omni-directional Antennas

These were broadband antennas made and described in [31], and were used to measure the field strength within the chamber during material characterization. These antennas, shown in figure 3.9 a, do not have a dominated direction for radiated or received power. Therefore, the orientation does not matter. They are highly efficient and have a frequency coverage of 200 MHz up to 40 GHz. In the reverberation chamber measurements, however, the directivity of the antenna does not matter. This is because once power is injected into the chamber, it is mixed and stirred by means of the stirrers. Thus at any

Figure 3.9: (a) Biconical antenna (b) Log Periodic Dipole Array (LPDA) antenna

point, the receiving antenna will see the same average, maxima and minima energies from whichever direction it is facing. Even though the directivity of the antenna does not play an important role in the measurements taken in a reverberation chamber, the antenna efficiency does.

Antenna Efficiency

The dielectric material of the antenna has a big influence on the efficiency of that antenna. The efficiency takes into consideration the dielectric losses through the dielectric material and the reflective losses at the input terminal of the antenna. Total efficiency of an antenna is a factor of both the reflection and radiation performance. Reflection efficiency is directly related to the S_{11} parameter, Γ, and is indicated by e_{ref}, as is defined mathematically in equations 3.5 and 3.6.

$$e_{ref} = (1 - |\Gamma|^2) \tag{3.5}$$

$$e_{ref} = (1 - < |S_{11}|^2 >) \tag{3.6}$$

where <> is the average taken for all the stirrer positions and | | is the magnitude of the measured S-parameters.

The radiation efficiency on the other hand, considers the conduction efficiency and dielectric performance of the material used for constructing the antenna. It is often determined through measurements, mainly in anechoic chambers. However, reverberation chambers can also be used. Radiation efficiency is determined by the ratio of the radiated power, P_{rad} to the input power at the terminals of the antenna, P_{in}:

$$e_{rad} = \frac{P_{in}}{P_{rad}} \tag{3.7}$$

Total efficiency is thus the product of the radiation efficiency and the reflection efficiency and is expressed mathematically by equation 3.8. Most commercial antennas have efficiencies of between 0.5 - 0.6. This is majorly due to the low dielectric constant of materials used.

$$e_{tot} = e_{ref} e_{rad} \tag{3.8}$$

3.6 Description of Measurement

Measurements done in a reverberation chamber are subject to errors due to losses in the cables as well as coupling and reflection between antenna ports. These errors need to be factored into the final measurement of the SE of the materials under test.

In order to factor the errors, a calibration of all equipment and the whole system is done. All the subsystems of the measurement set-up; the VNA, main reverberation chamber and the nested reverberation chamber, are characterised. The characterization values and factors are then applied to the SE measurements to eliminate any errors and reflect the true shielding quantity of the material under test.

Vector Network Analyser Calibration
The responses measured by a VNA are usually corrupted by systematic errors including:

- directivity and crosstalk errors associated with signal leakage
- source and load impedance mismatches associated with reflections
- frequency response errors associated with the measurement receivers

Multi-term error models capture these effects in the form of error terms in a signal flow graph. The most common error model uses six terms to account for errors in the forward direction and six additional terms to account for the error terms when the input and output port are reversed. The process of determining the coefficients of the individual error terms is referred to as calibration [32].

Both VNAs used in this study are calibrated before any measurement, up to the antenna input ports, using the respective calibration kits. The calibration ensures that any losses that may occur through the cables or within the network analyser itself are already factored out from the measurements obtained by the instrument. The calibration is done using a calibration toolbox containing a short, an open, a load and a through. These are connected to the end of the transmit cables through SMA connectors.

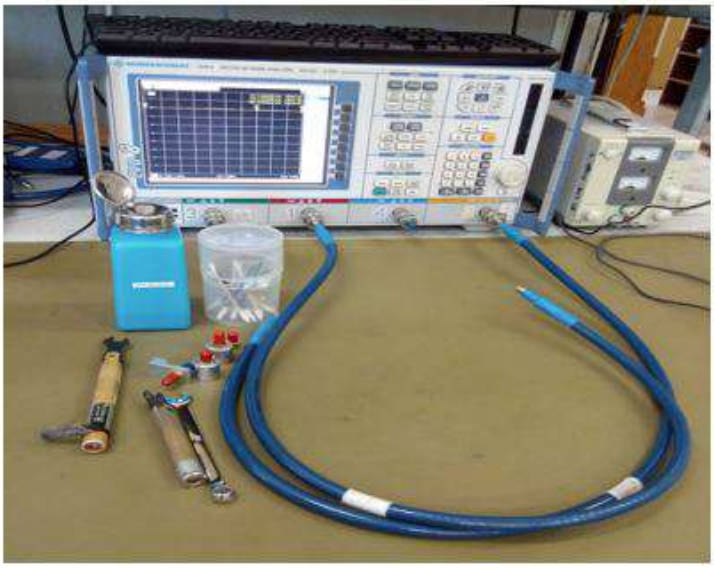

Figure 3.10: The ZVB 8 is internally matched to 50 ohms.

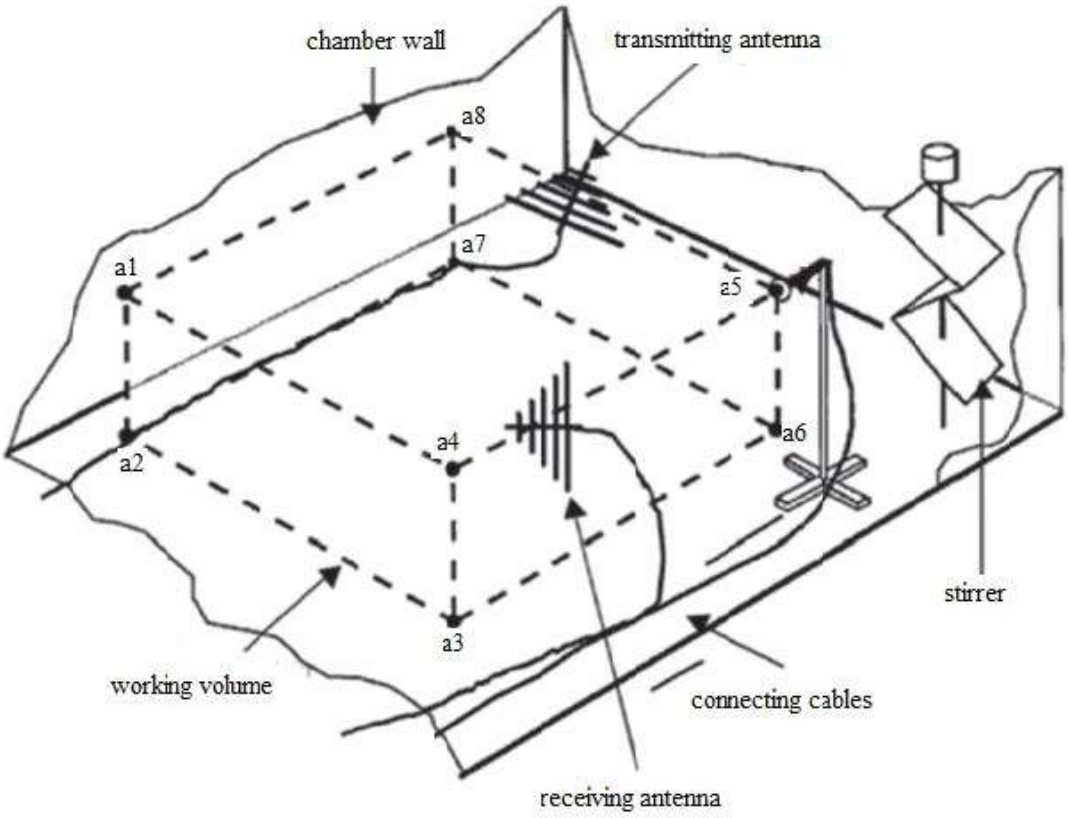

Figure 3.11: Calibration schematic of a reverberation chamber, according to IEC standards, with antenna location points indicated by the points a1-a8

Reverberation Chamber Characterization

Characterization of the reverberation chamber is done to ascertain its uniformity according to the IEC standards. In ascertaining the chamber uniformity, the transfer function of the RC is characterized. This requires the measurement and averaging of the power transfer

between the two antennas used for characterization, for all the 8 corner positions of the working volume of the chamber as identified in figure 3.11, (a1 through to a8), over a sufficient number of samples.

Calibration Set-up

The calibration data was collected over the entire operating frequency range of the measurement instrument, ZVB-8, that is 300 kHz to 6 GHz. The S-parameter data were sampled for 631 frequency points, spaced linearly over the measurement frequency bandwidth.

The VNA, ZVB-8 was set to a resolution bandwidth of 10 Hz, a setting that was kept for the rest of the shielding effectiveness measurements. Two identical LPDA antennas with predetermined efficiencies from previous study were used for the characterization of the chamber. Even though the measurements standards assume the efficiency of the LPDA antennas to be 0.75 , this was found not to be the case as presented in figure 3.12 [27].

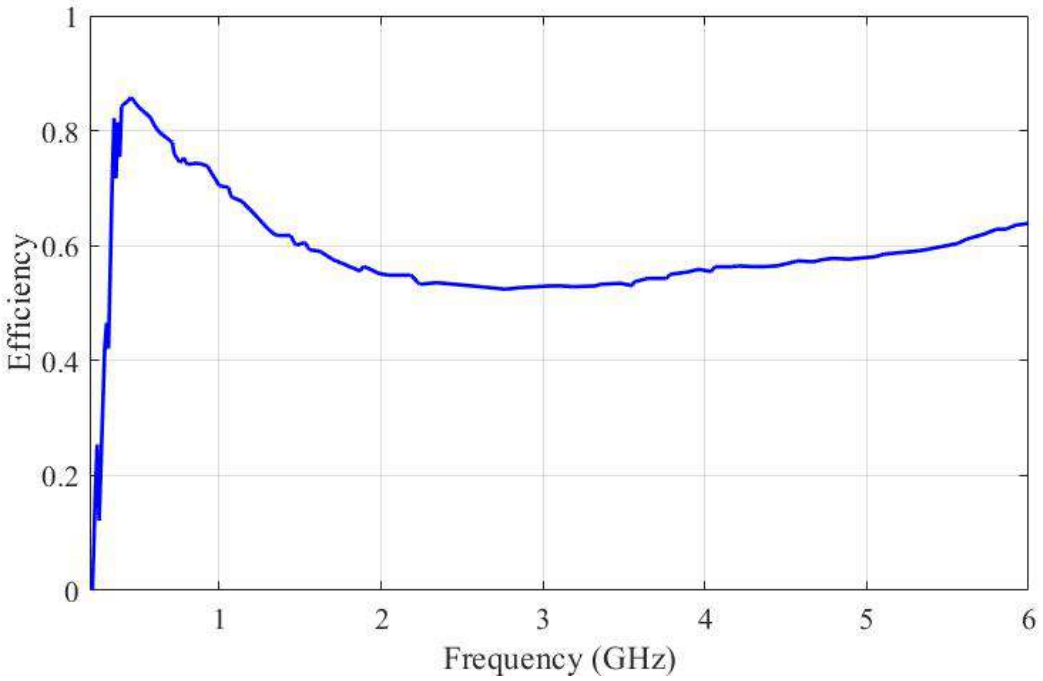

Figure 3.12: LPDA efficiency measured over a frequency up to 6 GHz [27].

3.6.1 Reverberation Chamber Transfer Function

The core concept of using a reverberation chamber is to characterise the transfer function (TF) of the chamber, that is, the ratio of the transmitted power to the received power, as given in equations 3.9 and 3.10.

$$\text{Transfer function} = \frac{\text{Received power}}{\text{Transmitted power}} \tag{3.9}$$

$$TF = \frac{P_R}{P_T} \tag{3.10}$$

Measurements are carried out using the VNA and recorded in terms of S-parameters. Expressing equation 3.10 in terms of S-parameters, we have the TF expressed as shown in equation 3.11.

$$TF =< |S_{21}|^2 > \tag{3.11}$$

where $|S_{21}|^2$ is the magnitude power transferred between receive and transmit antennas used, and <> is the average taken for all the stirrer positions. Equation 3.11 assumes that the two antennas are well matched. In case of mismatch, there occur reflections at the point of connection of the antenna port to the cable. The effect of this match is thus corrected both for the transmit ad receive antennas as given in as in equation 3.12.

$$TF_{corrected} = \frac{< |S_{21}|^2 >}{(1- < |S_{11}|^2 >)(1- < |S_{22}|^2 >)} \tag{3.12}$$

where, the numerator term represents the measured power transferred between the two antennas while the denominator terms represent the reflection coefficient of transmit and receive antennas. For an injected energy in a reverberation chamber, the stirrers are used to mix the energy to attain uniformity. However, during stirring, not all the energy interact with the stirrer. Therefore, the measured S-parameters is a combination of both stirred and unstirred components, where the unstirred part is the component that does not interact with the stirrers and thus couples directly to the receive antenna through line of sight. These compositions of the S-parameters are related as given in equations 3.13-3.16.

$$Sxy = Sxy_s + Sxy_{us} \tag{3.13}$$

$$Sxy_s = Sxy - \langle Sxy \rangle \tag{3.14}$$

$$S_{11s} = S_{11} - \langle S_{11} \rangle \tag{3.15}$$

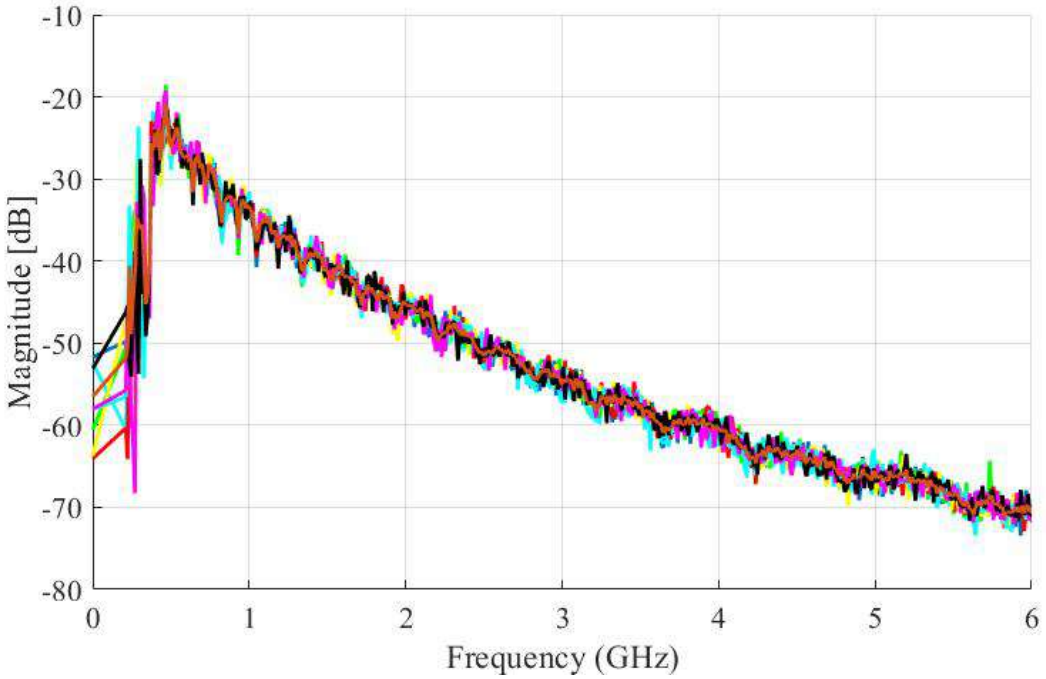

Figure 3.13: Reverberation chamber transfer function as measured using two different sets of antennas.

$$S_{21s} = S_{21} - \langle S_{21} \rangle \tag{3.16}$$

where x and y = 1,2, and the subscript s and us are the stirred and unstirred components of the measured S-parameters respectively.

3.7 Chamber Uniformity

The chamber transfer function is applied to the uniformity equation according to equation 3.17. The uniformity of the chamber was evaluated according to equation 3.18 and normalised as given in equation 3.19 and compared to the required standard deviation as described in [7] and result shown in figure 3.14. These eight corner positions in figure 3.11 define a zone within the chamber which is overmoded and that conforms to the standard test requirements, and are set at least $\lambda/4$ from the walls and stirrers. To achieve uniformity, the chamber is stirred according to the standard requirements. The stirring was done at steps of five degrees, for one complete revolution and measurement recorded and saved for a singular antenna position. This is then done for all the eight positions. The field uniformity is specified as a standard deviation, σ, from the normalized mean value of the normalized maximum values obtained at each of the eight locations during one rotation of the stirrer. The standard deviation is calculated using data from each antenna position and for all stirrer positions and frequency points. For a complete testing

process, the standard deviation is expressed relative to the mean value and converted to dB as given by equation 3.19.

$$\sigma = \sqrt{\frac{\sum (E_i - < E >)2}{n-1}} \tag{3.17}$$

$$\sigma_i = \sqrt{\frac{\sum_{n=1}^{n=8} (E_{ij} - < E_i >)_8}{8-1}} \tag{3.18}$$

$$\sigma(dB) = 20log10\frac{\sigma + < E_{xyz} >}{< E_{xyz} >} \tag{3.19}$$

where $E_{i,j}$ is the normalized maximum E-field in the i-direction (i = x, y, z) at the location j (with j = 1,2 ..8), and $< E_i >_8$ is the arithmetic mean of the normalized maximum field Ei for all eight locations for all vectors (Exyz).

A chamber is said to have attained the minimum requirements for operation when the number of modes is at least 60. Therefore, using equation 2.15, the minimum number of modes and thus independent samples occur at a frequency of 210 MHz. This matches our measurements in the chamber that indicate a LUF of 200 MHz as depicted in figure 3.14.

3.8 Key Reverberation Chamber Parameters

Reverberation chamber key parameters are the chamber characteristics that define how well the chamber is suited for measurements. Some of these characteristics define the frequency bandwidth of operation of the chamber, the behaviour of a signal when injected into the chamber and how much time it will take for the signal to fade away. This section describes parameters that define the effectiveness of a chamber.

3.8.1 Quality Factor

The quality factor, Q of a reverberation chamber defines and determines how well a chamber can store energy. When a signal is injected into a chamber through a transmit antenna, not all the signal is received by the receive antenna. This is majorly as a result of chamber wall losses which is a major contributor to chamber losses. Others include losses through apertures and losses due to loading. A higher Q value reverberation chamber stores energy well since there is a good reflection of field strength from the chamber wall

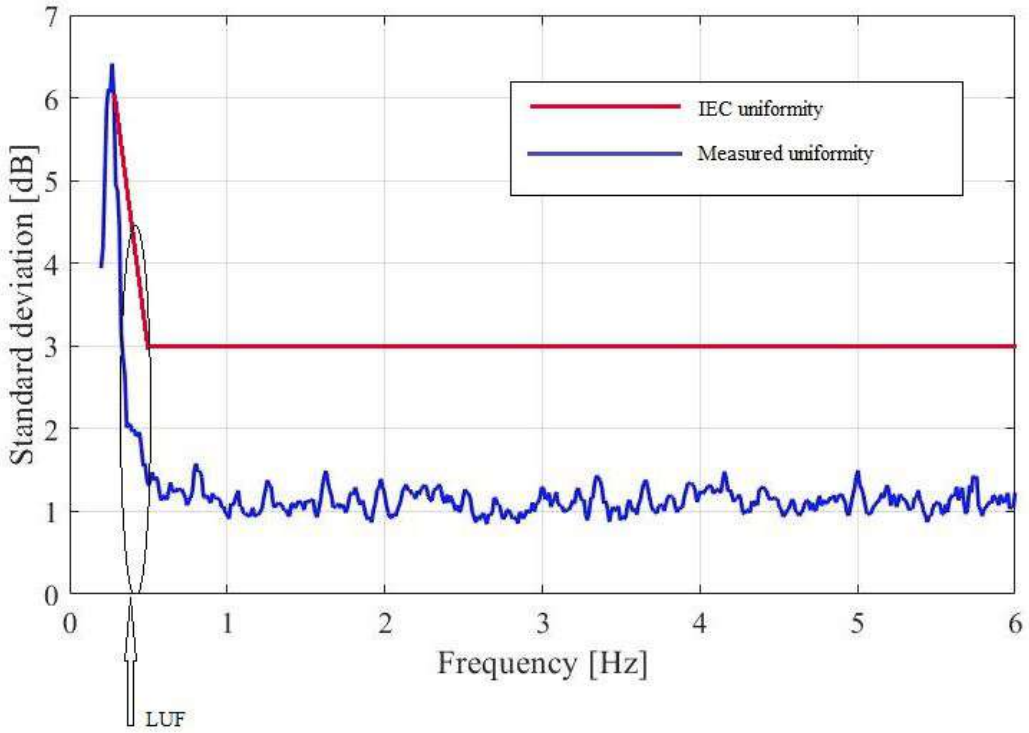

Figure 3.14: Normalised standard deviation for the Stellenbosch University reverberation chamber, in comparison to the required IEC 6100-4-21 standards requirement.

and thus less losses. A chamber with a lower Q factor on the other hand does not store energy well since losses in the chamber walls are dominant. Theoritically, the Q factor of a reverberation chamber is calculated according to equation 3.20 [33], which translates to equation 3.22 and 3.23 in measurement.

$$Q = \frac{3V}{2S}\sqrt{\frac{\omega_0 \mu_0 \sigma}{2\mu_r}} \tag{3.20}$$

$$Q = \frac{\omega U_s}{P_d} \tag{3.21}$$

$$Q = \frac{16\pi^2 V}{\eta_{tx}\eta_{rx}\lambda^3}\frac{P_{average}}{P_{input}} \tag{3.22}$$

$$Q = \frac{16\pi^2 V}{\eta_1 \eta_2 \lambda^3} < |S21|^2 > \tag{3.23}$$

where S is the surface area of the wall, V the volume of the chamber, σ, the conductivity of the material used, ω, the angular frequency, μ, the relative permeability of the material.

Loading the chamber significantly affects its Q factor, the effect being different depending on what materials and/or items are used for loading. A very high Q factor chamber is not ideal for measurements since the decay time for any signal injected into the chamber will take long to decay. This significantly increases measurement time. Therefore, when the Q factor of the chamber is very high, it is recommended that the chamber be loaded with a few absorbers to dump some energy. This keeps the Q factor low enough to agreeable levels. Figure 3.15 shows the effect on the Q factor when the chamber is loaded with the nested chamber set-up, antennas and some radio absorbing materials (RAM).

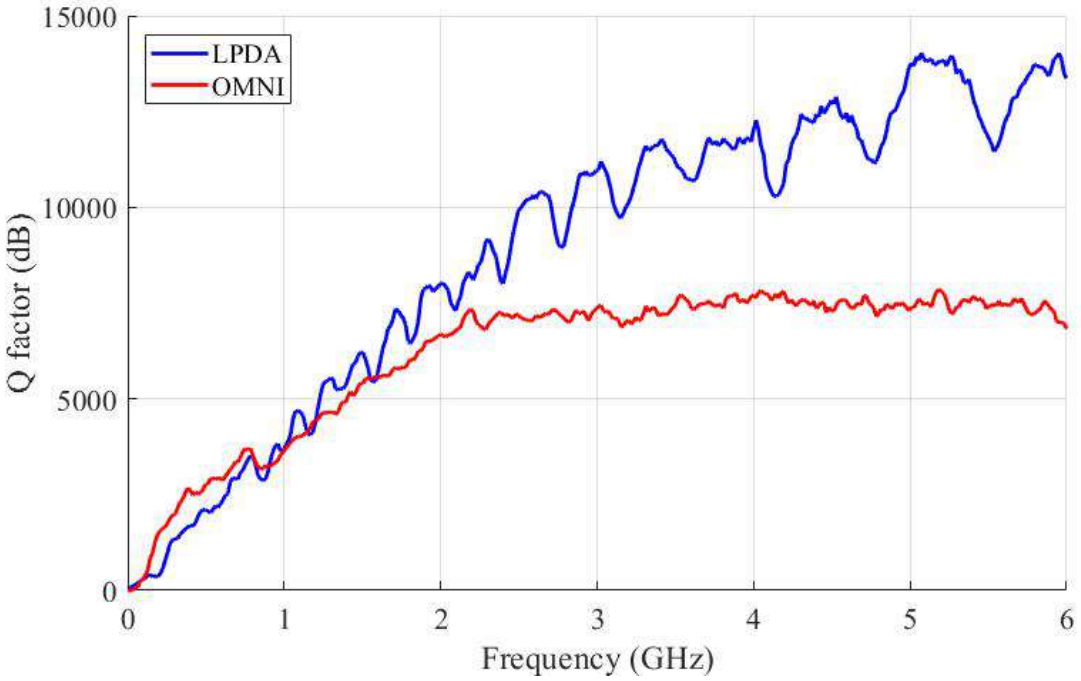

Figure 3.15: RC1 quality factor (red) loaded with the nested chamber set-up (using LPDA antennas) (blue) loaded chamber (using omni directional antennas), loading using the nested chamber and a few Radio Absorbing Materials (RAM).

3.8.2 Chamber Time Constant

The RCs time constant is based on the losses in the chamber and is thus related to the quality factor of the reverberation chamber. The two parameters are related according to equation 3.21.

$$Q = \omega\tau \tag{3.24}$$

Where Q is the chamber quality factor, ω is the angular frequency and τ the time constant. These two parameters are obtained from the VNA measurement as described below.

As the chamber is loaded with more materials, the fading time constant reduces. This is because, with more loading, more losses within the chamber is experienced. Time constant of the chamber will be investigated further in chapter four.

3.9 Nested Chamber Characterization

The small chamber is also characterised to factor out the effectiveness of the chamber when there is no sample placed on the aperture. Characterization measurements are performed within the small chamber, which is made of mild steel as described in section 3.2. The dimensions of the nested chamber are 60 cm by 50 cm by 40 cm (figure 3.3). Using the resonant frequency equations for resonant cavities, the LUF of the small chamber is 1 GHz. The chamber is excited with a loop antenna that is soldered in the chamber and connected to the ZVB-8 through SMA terminations. The characterization of the nested chamber is important towards getting the correction factor for the measured shielding effectiveness of the material samples under test. Unlike the main chamber, the characterization of this small chamber does not involve measurement at the 8 corners of the working volume, but rather the measurement and averaging of field magnitudes at the three locations of the loop antennas. This is later used to correct the shielding values that shall be measured using the set-up in figure 3.1.

3.10 Shielding Effectiveness Measurement

The transmit antenna in the main chamber is used to inject power into the main chamber. By means of the stirrers, this injected power is being mixed to obtain an average power level in the chamber. The receive antenna in the chamber is then used to measure the power level received. Similarly, the receiving antenna in the nested chamber also monitors the power levels that shall have passed through the material sample mounted on the aperture into the chamber. The stirrer in the nested chamber stirs the chamber in order to obtain average power levels in the nested chamber.

A couple of measurements are then taken with the materials placed in the aperture one at a time during different sets of measurements. The sample materials are each cut to fit the aperture of the nested reverberation chamber. These samples are made from different materials and include glazed glass samples, aluminium and mild steel among others. When measurements have been done, the correct shielding effectiveness result must be evaluated considering the losses associated with the characterization of both the bigger reverberation chamber and the nested reverberation chamber, that is, the calibration factor is considered in calculating the overall shielding effectiveness of the material sample. The shielding effectiveness SE of the material is thus given by the equation below:

$$SE(dB) = 10log_{10}\frac{P_{rx1}}{P_{rx2}} \tag{3.25}$$

Where P_{rx1} and P_{rx2} are power received by the receiving antennas in the main chamber and nested chamber respectively.

3.11 Electromagnetic Wave Absorbing Materials

The main objective of this thesis is to characterise different cost effective shielding materials that can be used in place of the current expensive shielding materials. For this purpose, therefore, there is a need for materials which absorb the electromagnetic radiations that are incident to them. There have been a variety of choices of such materials that were subjected to study in this work as is discussed in this section

- Alodine Aluminium
- Mild steel
- Microwave absorbing sheet
- Space blanket (Radiant barrier roof insulation)
- Single glazed laminated glass with different layers of laminated material

Mild Steel

Mild steel is a solid metal that is commonly used in industries and at home. Being a solid material with good shielding properties, it was chosen for testing for reference purposes. As most of the solid materials have good shield of approximately 50 dB and above. The mild steel is very important in the manufacturing of metal items. Almost 90 percent steel products of the world is made up of mild steel because it is the cheapest form of steel. It can be used in building and constructing strong metallic structures which will have good shielding.

Spunsulation 5 Roofing Radiant Barrier

Spunsulation 5 roofing radiant barrier is a double aluminium foil with reinforcing scrim and binder. It is manufactured from pigmented ultraviolet light-resistant, non-toxic flame, retarded, non-woven spun bond polypropylene membrane laminated by means of homogeneous based poly olefin film web to both sides of a layer of aluminium foil. The polypropylene photo polymer granules are mixed with the UV fire retardant master batch and extruded into fibres which are then laid onto a moving porous belt and transported

through a heated calendar to form the non-woven spun bond. This fabric is then transferred to the lamination line where it is laminated to the aluminium foil via a poly olefin based extruded film web. The same process is applied for the second aluminium foil. This material comes marked with the trade name, batch number, date, agreement identification logo and a certificate number as illustrated in figure 3.16a.

Spunsulation 5 Roofing Radiant Barrier is very reflective and thus reflects most heat that is incident to it. This material is effective in keeping the temperature of a room at lower levels, by reducing heat gain from the sun, especially when installed directly under the roof. It was thus important to investigate its effectiveness value and see how suitable, convenient and efficient it is to use on the buildings at the site, for the purpose of reducing and/or attenuating the amount of radiation coming from within the processor building.

Figure 3.16: (a) Spunsulation 5 roofing radiant barrier material (b) Silver ripstop material

Ripstop Fabric

This is a microwave shielding material which has a consistent high quality and is a very conductive, high shielding performance fabric. It is always coated for improved shielding performance. Depending on the material used for coating, the shielding performance may vary from one type to another. For instance, pure silver coated onto a strong nylon ripstop material can be used for making window drapes. Other common uses include static control, electric field shielding, microwave shielding, anti-static surface, RF shielding jacket, hat, garment liner, faraday enclosure or appliance cover, etc.

Glass Samples

Glass samples used were single coated energy efficiency glass from PG glass Africa. These are all single glazed laminated glass, shown in figure 3.17b. The lamination material is different from one glass to another and are 6.38 mm in thickness. The properties of the laminations also differ thus there is an expectation of demonstration of different values of shielding from one glass to another.

Microwave Absorbing Sheet

This is a low-cost microwave absorber sheet that is made of carbon material and coated

on both sides with a thin plastic for easier handling and better durability, as shown in figure 3.17a. It is a unique material that is suited for absorbing electromagnetic energy thus eliminating the reflection of these energies.

(a) Microwave absorbing sheet #259N, lessEMF **(b)** Single glazed coated glass samples, PG glass

Figure 3.17: Material samples

It is 1.22 m wide and is very light, with a weight of 0.034 kg/m^2. This makes it convenient for use as a liner for doors at the radio astronomy core site. It has a thickness of 0.64 mm and a carbon resistivity of 3 Ω/m^2. Due to the plastic laminations on both of its surfaces, it doesn't have surface conductivity. Therefore, during measurements, the plastic layer is carefully removed to ensure that the material forms good contact with the nested chamber.

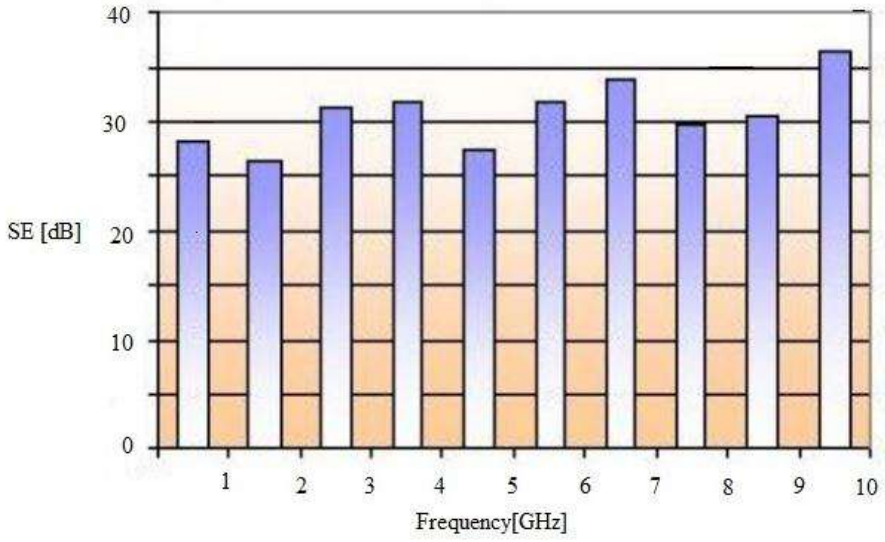

Figure 3.18: Shielding performance of Microwave absorbing sheet #259N [34]

It can be used to line walls, doors, make drapes or partitions, and its super light feature makes it more convenient for this purpose. When used in several layers, its effectiveness increases and can thus shield up to very high levels of electromagnetic energy. Besides being used as a surface layer material for shielding purposes, it could be used together

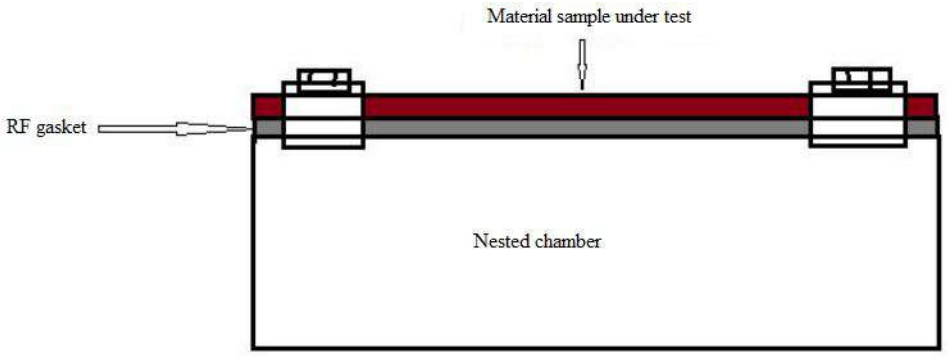

Figure 3.19: Configuration of the nested chamber set-up with the rf gasket for leakage prevention

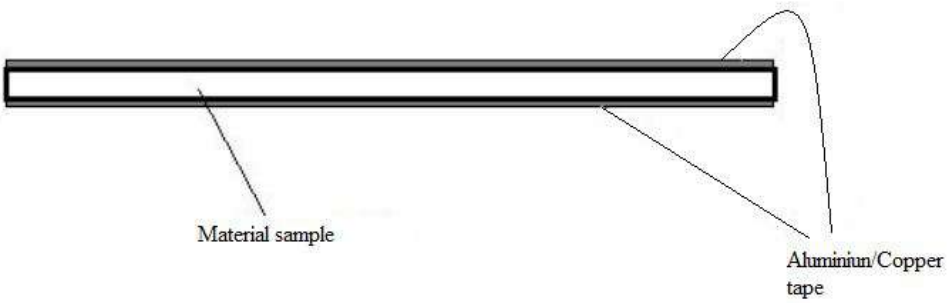

Figure 3.20: Material samples tapes using either aluminium or copper tape to ensure better conductivity between the nested chamber and the material under test

with other shielding materials to make even better shields. Just as there are double glazed glass with lamination in between, made of different materials of different shielding properties, a microwave absorbing sheet could be used as one of those laminations. Figure 3.18 shows the shielding performance of the microwave absorbing sheet over a frequency of up to 10 GHz.

3.11.1 Enclosure Seams

In any shielding enclosure, seams and slots limit the SE of the entire enclosure. Therefore, the slots must be well covered and closed, and the seams must have good contact with the enclosure. This ensures less RF leakage and hence better shielding. Contact between the seams and the enclosure is considered adequate when the contact area is conductive enough and the cross-section area of overlap is sufficient. To achieve this kind of contact better, RF gaskets are used. The use of gaskets to reinforce good electrical contact in shields is reffered to as gasketting.

The enclosure is constructed of mild steel, with an aperture on one side for sample holding. All other faces are well welded and tin plated. The aperture has holes where the material

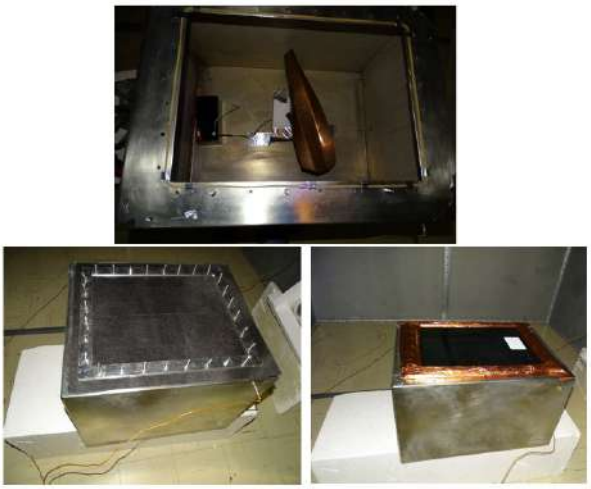

Figure 3.21: Photos of the nested chamber showing how the material samples are placed and secured for measurement.

sample is firmly held by means of bolts and screws. To ensure there is minimal leakage of RF energy into or out of the chamber, an RF gasket is used between the material sample and the box. After the sample is fixed onto the box, an aluminium tape or copper tape is used to further seal the contact edges to ensure no leakage happens. This is illustrated in figure 3.21. For some of the materials like glass samples, an aluminium tape is used to cover the edges of the sample for better contact. This again is illustrated in figures 3.17b and 3.20.

Due to the size of the nested chamber, according to the resonance frequency equation given in chapter two, the first resonance and hence the LUF is approximately 1 GHz.

3.12 Conclusion

Different components that form the entire measurement set-up are described. Each of these components influence the measurement and hence the entire results of any material measured. For instance, antenna efficiency and bandwidth are important parameters in SE measurements; the nested chamber and main chamber characterization are equally important.

Chapter 4

MEASUREMENTS, RESULTS AND DISCUSSION

4.1 Introduction

In this chapter, results are presented, analysed and discussed, for all SE of the materials and other measurements that pertain to it. Calibration results for chamber uniformity, the chamber transfer function, the chamber Q factor as well as the chamber time constant are shown. Also presented herein are the antenna efficiency measurements and plots.

The SE defined in equation 2.9 has been used to determine the SE of different material samples described in chapter 3 section 3.11 These measurements are carried out over a frequency range of 300 kHz to 6 GHz. The antenna efficiencies, being part of the equation for solving the shielding effectiveness, need be calculated.

4.2 Antenna Efficiency

In the measurement set-up, LPDA antennas and bi-conical antennas are used. The efficiency of the LPDA antenna is known while that of the bi-conical antenna is unknown. Measurements are first carried out to determine the efficiency of these antennas as they play a role in the equation for shielding effectiveness calculations.

Omni-directional Antenna (Bi-conical Antennas) Efficiency
The efficiency of these antennas is determined through measurements. This is done using two methods. The first method uses a reference antenna with predetermined efficiency and a second antenna whose efficiency is to be determined. In order to determine the efficiency of the unknown antenna the Q factor must first be obtained. The second method uses the knowledge of the power delay profile of the chamber to determine the efficiency of these antennas. These two methods are discussed in the following subsection.

4.2.1 Using a Reference Antenna

To determine the efficiency of an antenna using a reference antenna method, the efficiency of the reference antenna should be known. In this method therefore, the reverberation chamber was characterised using two identical LPDA antennas whose efficiencies were known. According to [7], the standard efficiency of the LPDA antennas is assumed to be 0.75. However, investigations done in [27], using Wheeler cap method, showed the efficiency to vary in a range of frequency from 0 to 6 GHz according to figure 4.1. Also shown are the electrical characteristics of these antennas in the chamber, in figure 4.2.

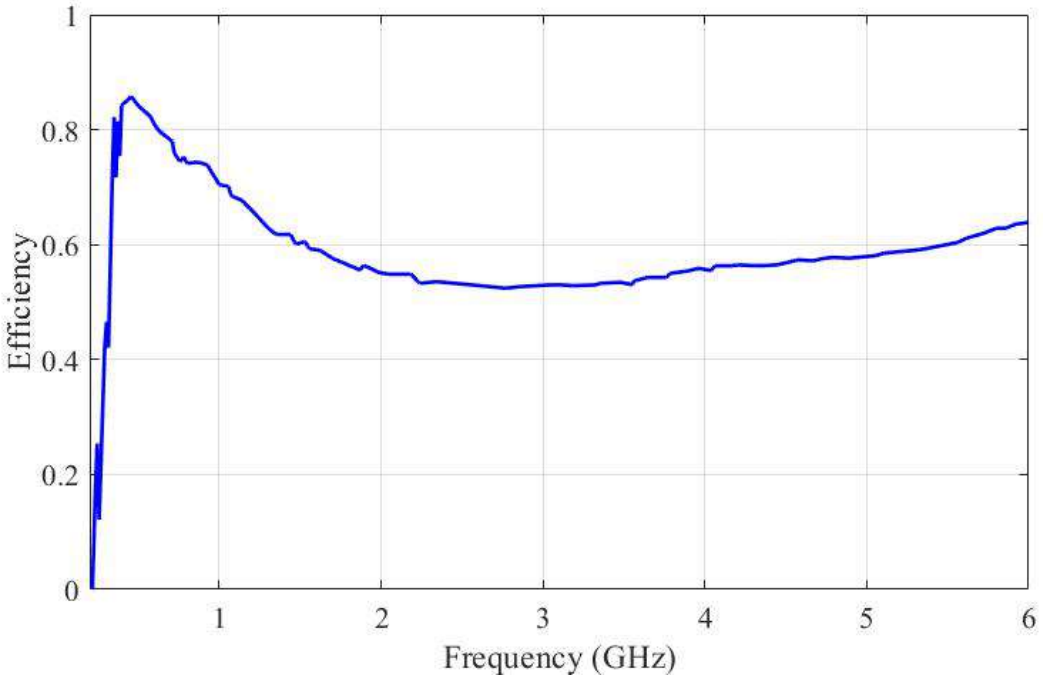

Figure 4.1: LPDA efficiency measured over a frequency up to 6 GHz using Wheeler cup method in [27].

LPDA antenna efficiency results obtained using Wheeler cup method in [27], is used in the reference antenna method, to determine the efficiency of the unknown bi-conical antennas. After characterising the reverberation chamber with the two LPDA antennas whose efficiencies were known, the Q factor of the chamber was calculated. As seen in chapter three, the Q factor of an RC is given by equations 4.1 and 4.2:

$$Q = \frac{16\pi^2 V}{\eta_1 \eta_2 \lambda^3} \frac{P_{average}}{P_{input}} \tag{4.1}$$

This in terms of S parameters is,

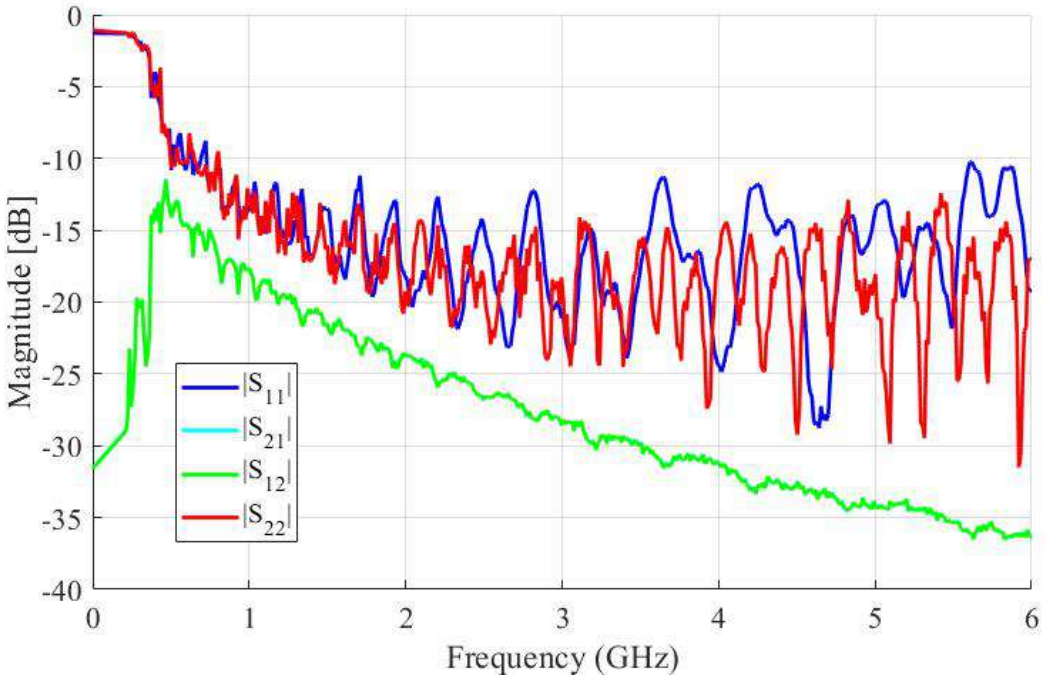

Figure 4.2: Reflection and transmission parameters using LPDA antenna.

$$Q = \frac{16\pi^2 V}{\eta_1 \eta_2 \lambda^3} < |S_{21}|^2 > \tag{4.2}$$

The quality factor measurement is not a relative measurement. Therefore, in order to accurately evaluate it, it's vital to use the part of energy within the reverberation chamber that interacts with the stirrers. When energy is injected into a reverberation chamber, there is part that interacts with the stirrers and the part that does not and thus couples directly to the antenna through direct line of sight. Considering the stirred part only, of the energy within the chamber, equation 4.2 becomes;

$$Q = \frac{16\pi^2 V}{\eta_1 \eta_2 \lambda^3} < |S_{21,s}|^2 > \tag{4.3}$$

where $S_{21,s}$ is computed as given in equations 3.13 and 3.14.

After determining Q factor of the chamber, a second set of calibration was done. In this case, one LPDA antenna was used as transmit antenna (reference antenna) and a bi-conical antenna with unknown efficiency used as receive antenna according to the set-up in figure 4.3. S-parameters are collected and recorded by the VNA and the Q factor previously obtained using the two identical LPDA antennas is then used in equation 4.3 to determine the efficiency of the unknown antenna.

Figures 4.5 and 4.6 below show the Q factor of the chamber using the two antennas and

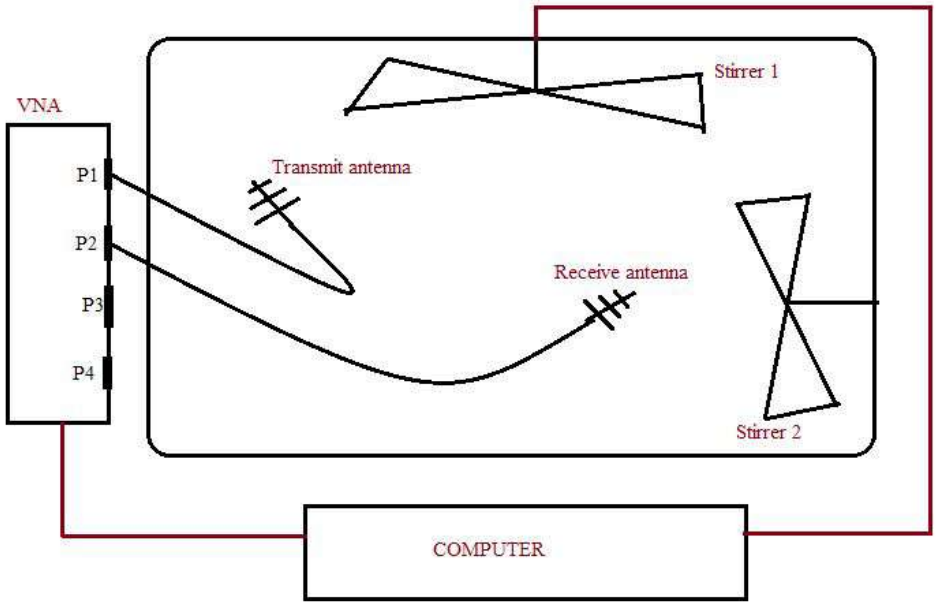

Figure 4.3: Measurement set-up for determining the efficiency of antenna from reference antenna, up to frequency of 6 GHz, as investigated and presented in [27].

the efficiency of the two bi-conical antennas respectively.

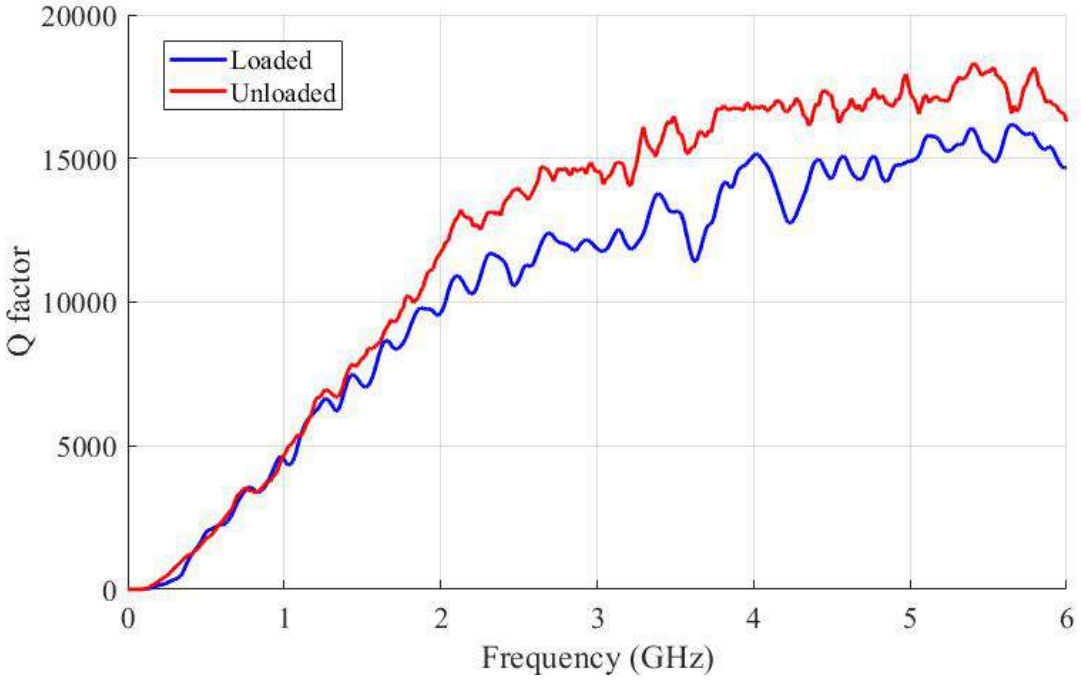

Figure 4.4: RC1 quality factor (red) unloaded chamber (using LPDA antennas) (blue) loaded chamber (using omni directional antennas).

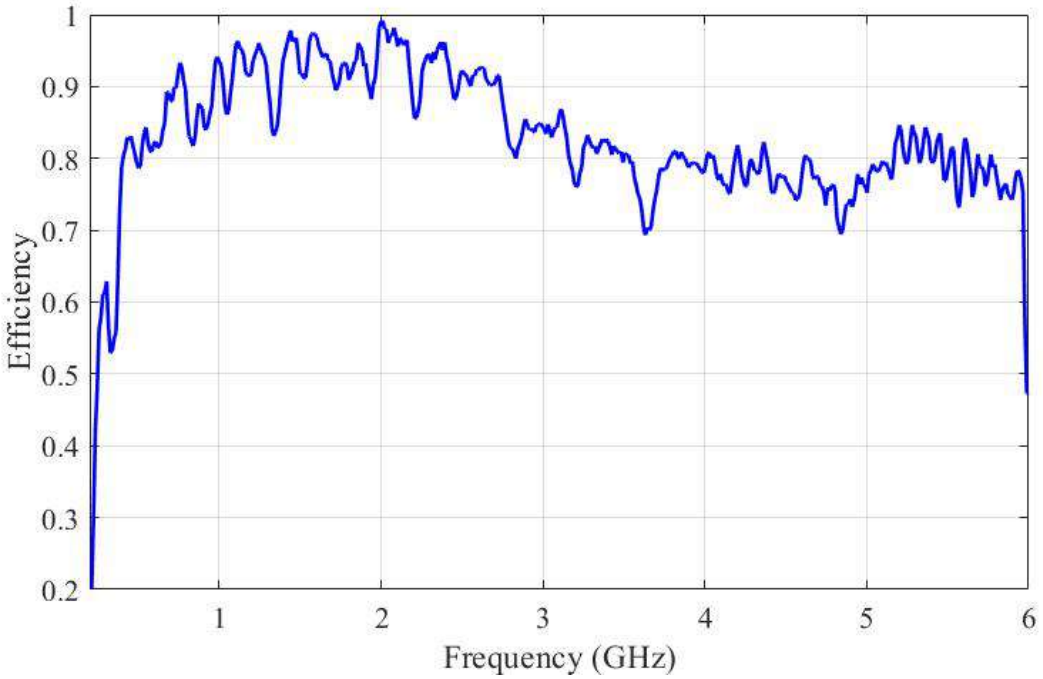

Figure 4.5: Bi-conical antenna efficiency as measured using the reference antenna method.

4.2.2 Power Delay Profile

The power delay profile (PDP) provides time delay information of any signal that is received through a multipath channel. In a reverberation chamber, there are independent samples created due to stirring. Therefore, the PDP gives the signal power of these independent samples received through a multipath channel as a function of time delay. In a PDP plot, the signal power of each multipath is plotted against their respective propagation delays and the slope of the linear part of these curves give the time constant of the chamber [29]. In this method, two antennas with unknown efficiencies are used to characterize the chamber. The efficiency of each antenna can then be determined when the chamber time constant is known.

The time constant of a reverberation chamber is a function of PDP, and it gives the information on how a signal when injected into a reverberation chamber, fades away. For an energy injected power into a reverberation chamber, the impulse response, h(t,n) is related to the measured S-parameters according to equation 4.4. Therefore, using the two bi-conical antennas, the S-parameters are measured and the impulse response calculated. As applied in converting time domain data to frequency domain data, the Fourier transform is also used to transform the frequency domain data to time domain data. Therefore, using the IFFT, the chamber impulse response can be obtained from the S-parameter data measured in the reverberation chamber according to equation 4.4. The PDP is then defined as the natural logarithm of the chamber impulse response as given

in equation 4.5.

$$h(t,n) = IFFT(S_{21}(f,n)) \tag{4.4}$$

$$PDP(t) = ln(< |h(t,n)|^2 >) \tag{4.5}$$

where h (t,n) is the impulse response of the chamber expressed by equation 4.7

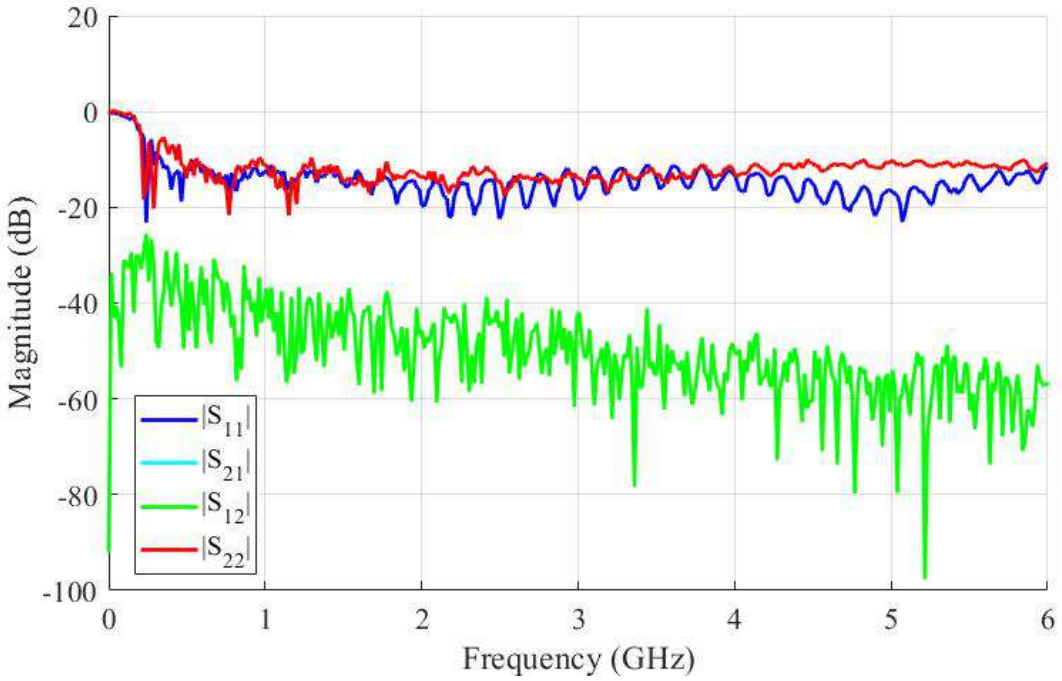

Figure 4.6: Reflection and transmission parameters for bi-conical antenna.

The determination of time constant of RC1 was done from frequency domain measurement, using the ZVB-8 VNA. In this work, measurements are done in frequency domain, and as is already known, using Fourier transform, the corresponding time domain data can be obtained. The converted time domain data has just enough information to obtain the time constant of the chamber. When the IFFT is done to obtain the time domain data, not all information about the original signals can be obtained. For example, the IFFT cannot be applied to get the accurate information of when the different frequency components are in the signal whose spectral content varies with time. The power delay profile obtained from the S-parameter data is the plotted against time as shown in figure 4.7. The inverse slope of the linear part of the PDP curve of a signal injected into a chamber gives the time constant of that chamber as illustrated in figure 4.7 and given in equation 4.6.

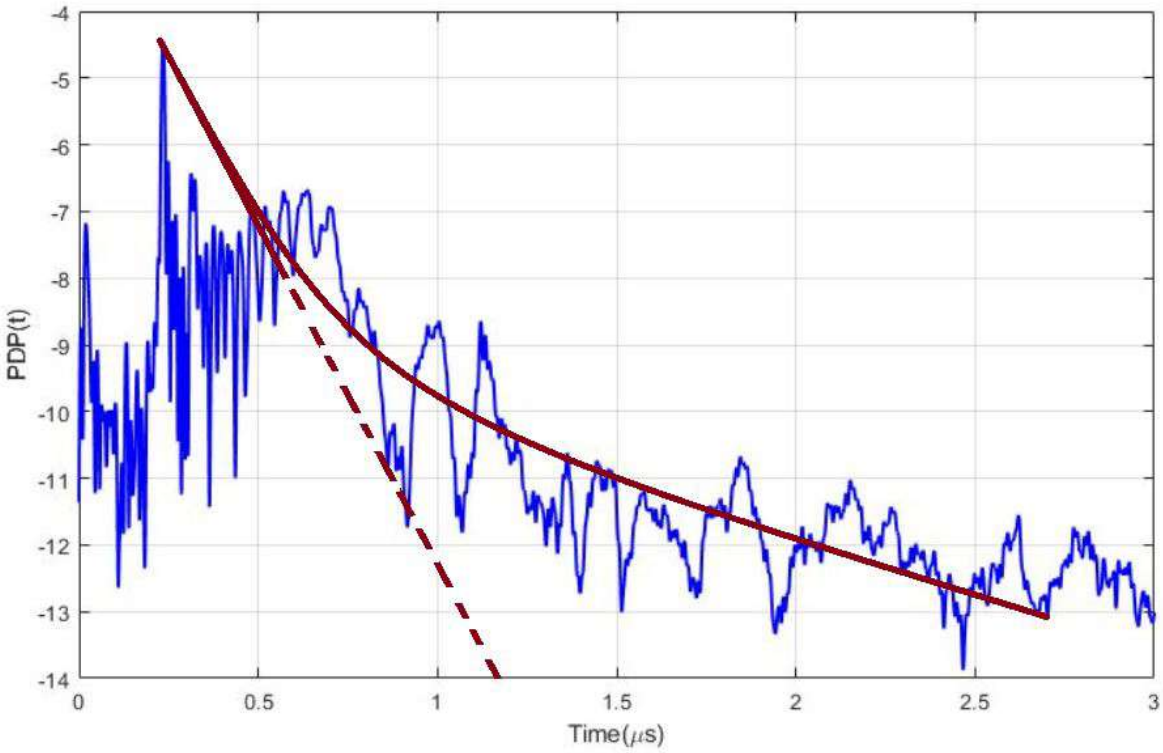

Figure 4.7: Power delay profile of RC1 using bi-conical antennas.

$$\tau = \frac{-1}{k} \tag{4.6}$$

where k is the slope of the linear part of the power delay profile curve.

Given the chamber time constant, the efficiency of the two antennas used in measurement can then be calculated according to equations 4.7 and 4.8. The information about the Q factor in this case does not need to be known.

$$\eta_1 = \frac{1}{(1 - | < S_{11} > |^2)} \sqrt{\frac{C_{RC}}{\omega e_b \tau} < |S_{11,s}|^2 >} \tag{4.7}$$

$$\eta_2 = \frac{1}{(1 - | < S_{22} > |^2)} \sqrt{\frac{C_{RC}}{\omega e_b \tau} < |S_{22,s}|^2 >} \tag{4.8}$$

where, e_b and C_{RC} are the chamber constant and backscatter constants respectively, and are defined according to equation 4.9 and 4.10

$$C_{RC} = \frac{16\pi^2 V}{\lambda.^3} \tag{4.9}$$

$$e_b = \sqrt{\frac{< |S_{11,s}|^2 >< |S_{22,s}|^2 >}{< |S_{21,s}|^2 >}} \tag{4.10}$$

The efficiency of the antennas is then given in figure 4.8.

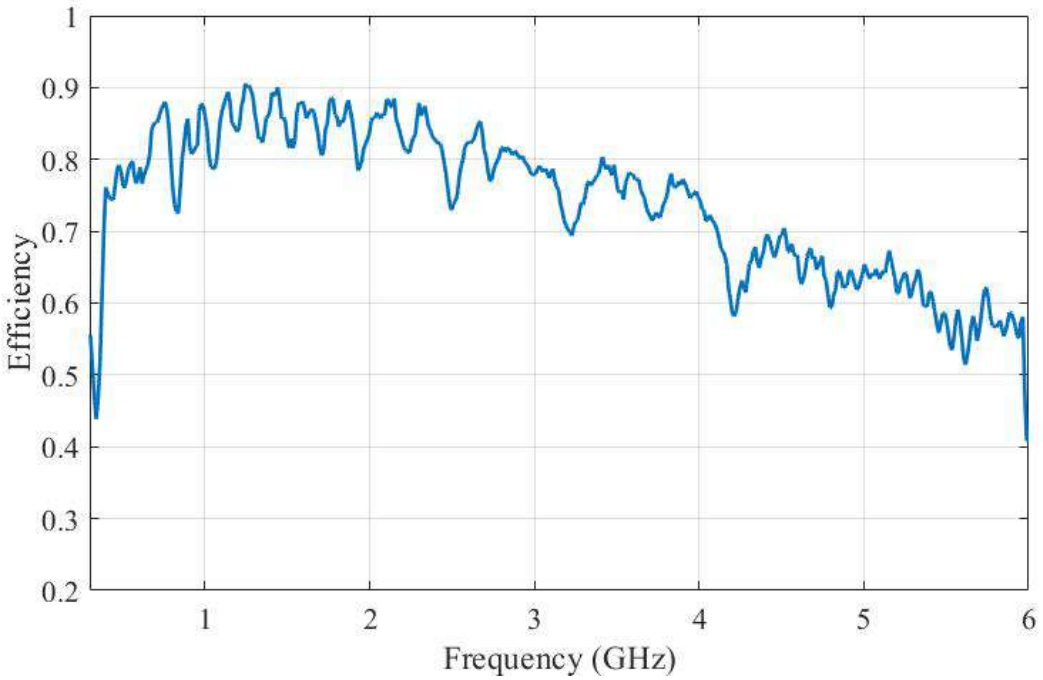

Figure 4.8: Bi-conical antenna efficiency as measured using the PDP method.

The variation in efficiency of these results using these two methods is owed to the fact that the second method was a close approximation of time domain data which was obtained from Inverse Fourier transformation of the measured frequency domain data using the frequency domain measurement instrument, the VNA.

The power delay profile could thus accurately be obtained through pure time domain measurements by introducing a pulse into the chamber and observing how long it takes for the signal to fade away.

4.3 Materials Shielding Effectiveness

Having determined the efficiencies of the antennas, measurement for quantifying the shielding effectiveness of the material samples are carried out in the two reverberation chambers, and analysed and processed using MATLAB. Equation 4.11 is used in the SE calculation, where the ratio of the energy measured in the nested chamber in the absence of a material on the aperture to the energy measured in the nested chamber in the presence of the material sample is taken.

$$SE(dB) = 10log_{10}\frac{P_{rx1}}{P_{rx2}} \tag{4.11}$$

In terms of S parameter, equation 4.11 becomes.

$$SE(dB) = 10log_{10}\frac{|S_{21open}|^2}{|S_{21closed}|^2} \tag{4.12}$$

The small chamber exhibits some amount of shielding. Therefore, in order to get the exact effectiveness of the material on the aperture, a correction factor associated with the losses in the small chamber must be taken into account. This correction factor is given according to equation 4.13 and is used for the rest of the measurements in correcting shielding values for the different materials

$$SE_{enclosure} = 10log_{10}\frac{P_{MC}}{P_{ONC}} \tag{4.13}$$

where P_{MC} is power received by the reference antenna in the main chamber and P_{ONC} is the power received by the receive antenna in the nested chamber, with no sample on the aparture.

With three antennas used for measurements, a pair for each set of measurement, the reference measurement associated with the nested chamber when no sample is present is calculated, and any correction for subsequent material shielding measurements done accordingly. The first antenna is the transmit antenna, the second is the reference antenna within the main RC and the third antenna is the receive antenna in the nested chamber. All measurements are recorded in terms of S-parameter and shielding effectiveness calculated according to equations 4.14 and 4.15.

$$SE(dB) = 10log_{10}\frac{<|S_{21open}|^2>\eta_1\eta_2}{<|S_{21closed}|^2>\eta_1\eta_3} \tag{4.14}$$

$$SE(dB) = 10log_{10}\frac{<|S_{21open}|^2>\eta_2}{<|S_{21closed}|^2>\eta_3} \tag{4.15}$$

Where η_1,η_2 and η_3 are the efficiencies of transmit antenna, reference antenna in the main chamber and receive antenna in the nested chamber respectively. The magnitudes of the S-parameter measurements are obtained for all the 631 frequency points and 72 stirrer positions. For a complete set of measurements, the stirrers are stepped at five degrees resulting in 72 stirrer positions. For each stirrer settling position, the VNA collects S-parameters for 631 frequencies. The square of the magnitude of the S-parameters are

proportional to power. Therefore, the average of these independent square magnitudes is taken over the entire measurement frequency bandwidth, as denoted by $\langle . \rangle$.

As seen in equation 4.15, the shielding effectiveness of the material is a relative measurement that is dependent on the energies within and outside the small chamber, and the efficiency of the receive antennas in the two chambers. From this relationship, apart from the measured S-parameters measured by the VNA, one needs to determine and know the efficiencies of the two antennas in order to correctly compute the effectiveness of the enclosure when open, for purposes of correction. The antennas' efficiency is discussed in section 4.2.

Figure 4.9: Photograph of the nested chamber with material place directly in contact with the nested chamber surface. No measures taken to minimize RF leakages.

If antennas used in the two measurements are identical and all equipment held at the same place during measurement, then the shielding effectiveness value of the box will just be the ratio of the S-parameter values, as the effect of antennas will cancel out.

4.3.1 Slots and Seams

Whenever there are openings in the nested chamber, RF energy leakage occurs into and out of it. Due to these leakages which occur as a result of the seams and slots, the SE results obtained may not reflect the true shielding value of the material on the aperture.

Initial measurements were made with no RF gasket in place. No extra measures were

taken to ensuring that leakages of RF energy were minimized as much as possible. Figure 4.9 shows the photograph of the nested chamber with mild steel on the aperture for this scenario.

Shielding measurement were done and SE evaluated. Results of four material samples are shown in figure 4.10.

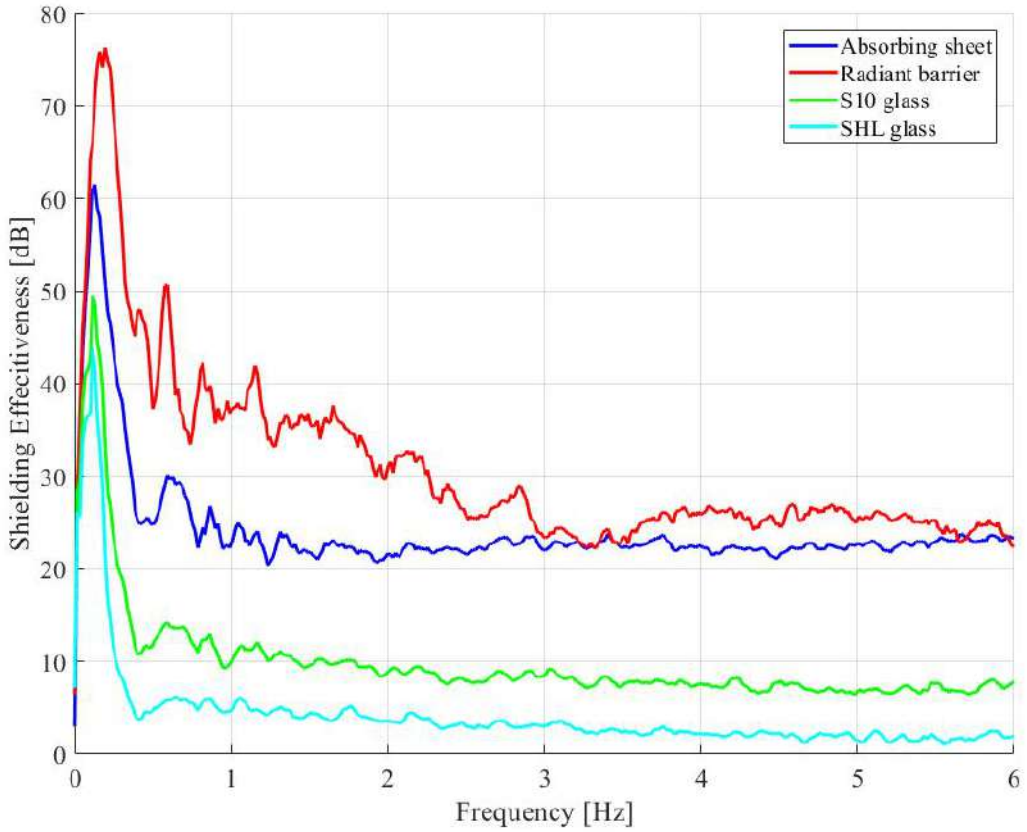

Figure 4.10: Shielding effectiveness results when no RF gasket was used for proper contact between material sample and nested chamber.

Test Fixture Modification

Similar to the first measurement, a second measurement was done with an RF gasket placed between the material sample and the nested chamber. This was to ensure that there was no interference between the environments within and outside the nested chamber, and that energy would be transferred only though the material sample under test. This modification and SE evaluation of the same showed an increase in the shielding effectiveness. The shielding value increased even further when copper tape was used to seal the edges of the contact of the material sample and the nested chamber. Figure 4.11 shows the set-up for FD measurement with the nested chamber sealed with a copper tape at the edges of the box where the material sample makes contact with the nested chamber.

Figure 4.11: Photograph of the nested chamber sealed with copper tape on the edges and over the bolts, to prevent RF energy leakage.

As shown in figure 4.12, there is a significant increase in the amount of shielding exhibited by each material in this case. Between 200 MHz to 3 GHz for instance, the shielding effectiveness of mild steel is 60 dB as compared to previous 40 dB, which is fairly close to the shielding effectiveness of solid metals of equivalent thickness. The glass samples also have shown SE values of about 20 dB as compared to slightly more than 10 dB when no extra measures are applied.

As is seen in figure 4.13, the shielding value increases a little more when copper tape is used.

4.3.2 Mild Steel Study

In [27], the shielding effectiveness of a whole enclosure made of mild steel was investigated. The results of this investigation compare closely to the shielding effectiveness of mild steel measured in this study, without using an RF gasket. In measurements in [27], the nested chamber was stirred using an independently controlled stirrer, in mode stirred operation. The stirrer system being controlled by an electronic board introduces interference in the box. This not being part of the energy transmitted, has a reduction effect in the evaluated shielding value of the enclosure. Thus, the results in this study show improvement in results from the first scenario.

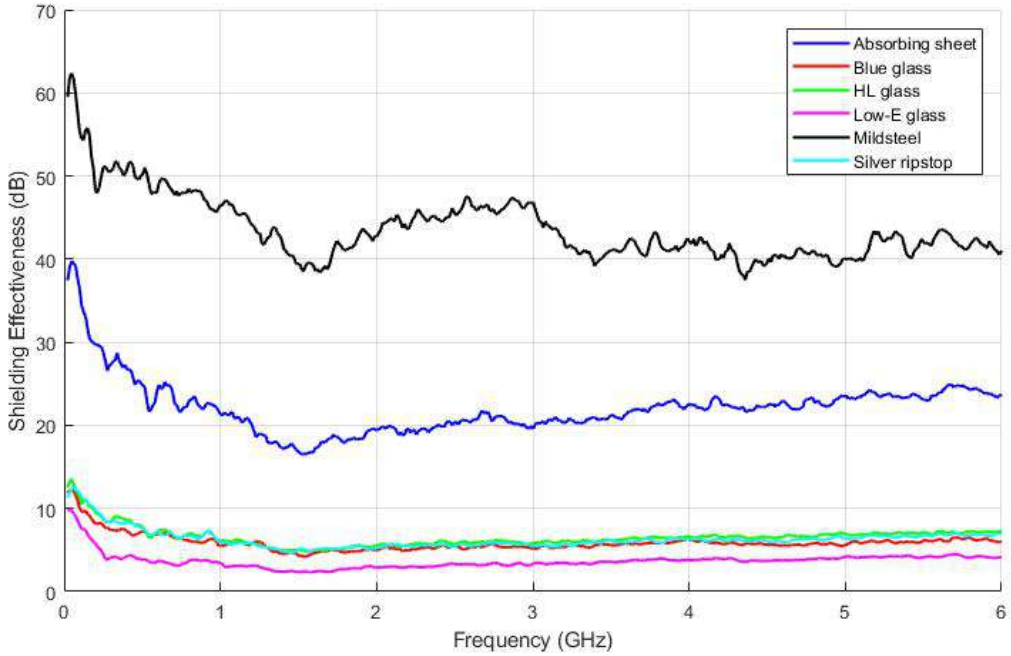

Figure 4.12: SE of materials as measured with RF gasket only present. No copper or aluminium tape used for extra shielding.

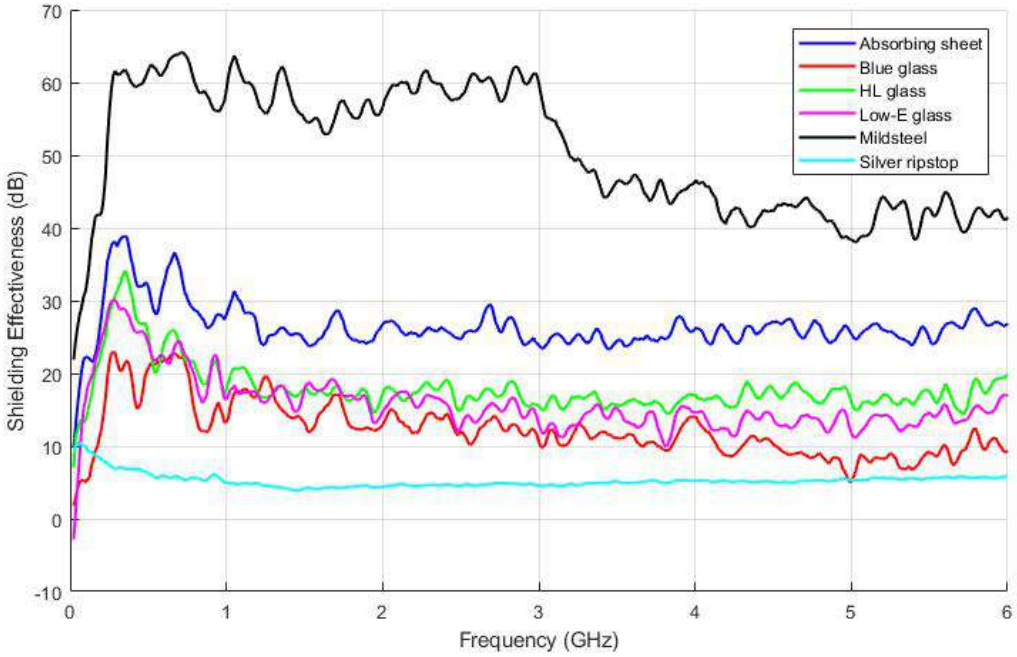

Figure 4.13: SE of materials as measured with RF gasket present and copper tape used for extra sealing.

The variations is not as uniform as would be expected, as seen in figure 4.14. This may be attributed to the fact that the former investigation was done for a complete enclosure with less seams and apertures. In this study however, the introduction of the aperture and

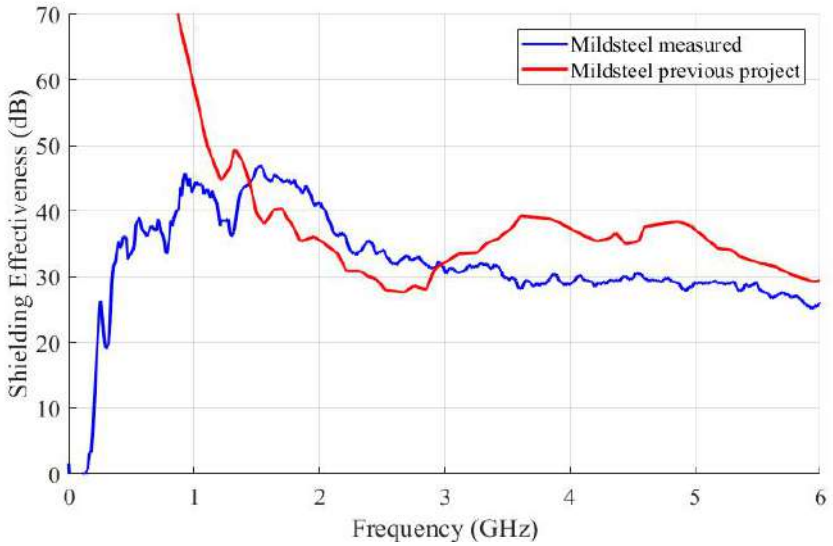

Figure 4.14: SE of mild steel, comparison by mild steel enclosure investigated in [27]

the threaded holes allow more energy to go into the small chamber thus a lower shielding effectiveness value.

Besides the introductions of more seams and apertures, the measurements dynamics are also a little different. This would include the types of antennas used, the settings on the VNA and the methodology used. In [9], the measurements were carried out in time domain and for a complete enclosure with less seams and smaller apertures.

4.3.3 Shielding Effectiveness of Alodine Aluminium

In RC1, the SE of alodine aluminium was calculated, first using a fitting bi-conical antenna within the chamber and second using the loop antennas within the chamber. The nested chamber is small in volume and is equipped with a small stirrer. Therefore, the bi-conical antennas used in the main chamber cannot be used despite their efficiency because of their size. As a result, it is requisite to use smaller antennas that would still allow a significant working volume and ensure that the LUF of the small chamber is reduced further. But since SE measurement is a relative measurement, the loop antennas efficiencies have no significant effect on the shielding values of the materials tested.

This is shown in figure 4.15, where plots are made of alodine aluminium when using a bi-conical antenna in the nested chamber and when using the loop antennas. the two plots compare very closely above 1.5 GHz with variation of around 8 dB at lower frequencies. This ascertains that the loop antennas, just as the bi-conical antennas are effective and suitable for the measurement.

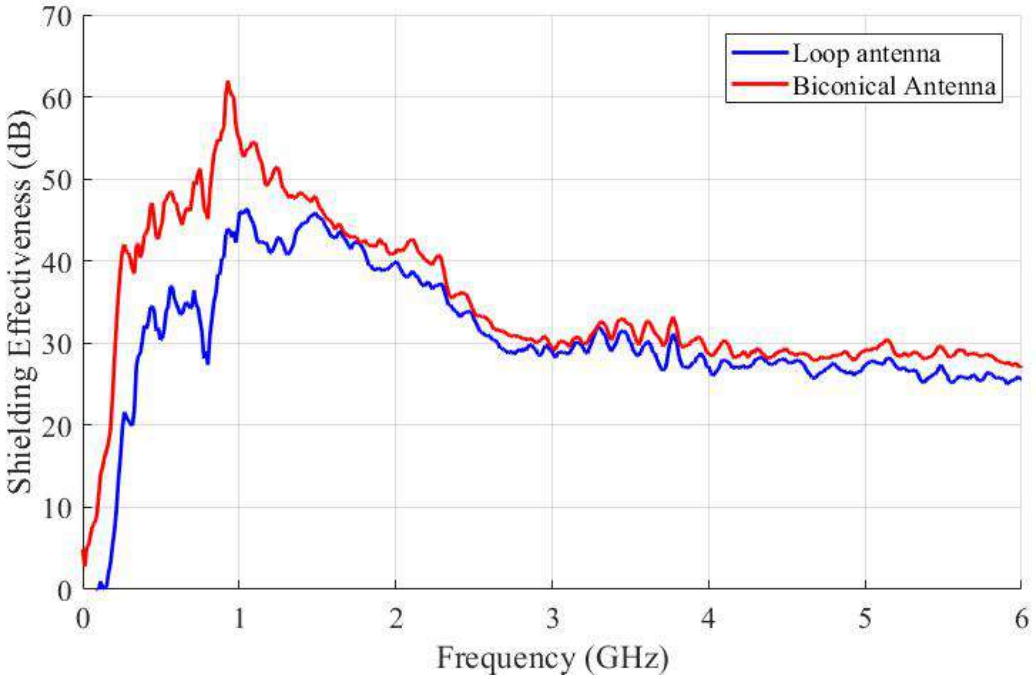

Figure 4.15: SE of mild steel sample, as measured using two different types of antennas as receive antenna inside the nested chamber. No copper tape used for extra shielding.

4.3.4 Other Materials

Shielding effectiveness results of all the other materials evaluated are presented in the figures 4.16-4.19. These materials were evaluated for measurements carried out in the two chambers, RC1 and RC2. These materials were also tested for the same scenarios; without the RF gasket, with the te RF gasket present and with copper tape used for extra shielding to ensure no leakages.

The results at lower frequencies up to 1 GHz are not so stable. These results do not accurately ascertain the effectiveness of the materials over those frequencies. Since the relative measurement for the shielding effectiveness is taken within and without the nested chamber, its LUF play a factor in determining from which frequency the results can be reliable. Due to its small volume, its LUF is very high, 1 GHz. The chamber therefore lacks uniformity a condition required for well operation of a resonant cavity as a reverberation chamber, at frequencies below 1 GHz.

This pattern is exhibited for the measurements carried out in the two main reverberation chambers, RC1 and RC2.

Both chambers were calibrated up to a frequency of 6 GHz and shielding results shown for the different materials in figures 4.16-4.19.

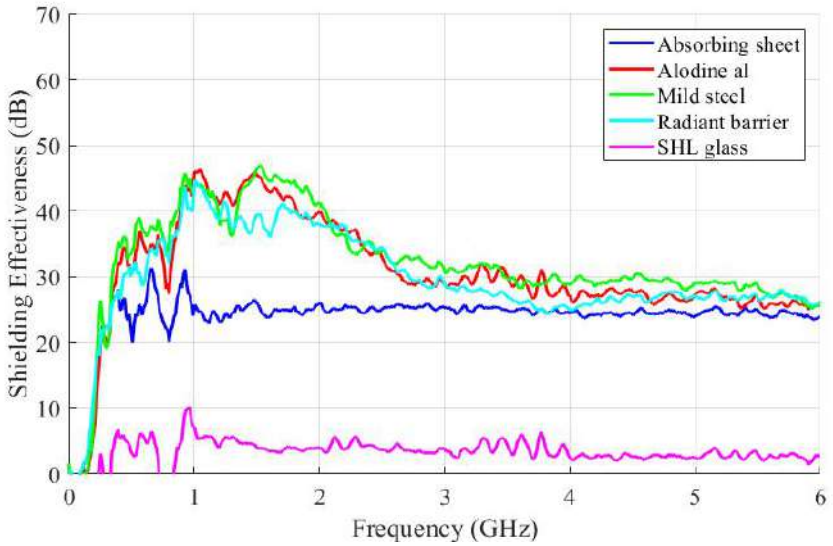

Figure 4.16: Material samples SE measured in RC2, RF gasket present and no copper tape used for RF energy leakage prevention.

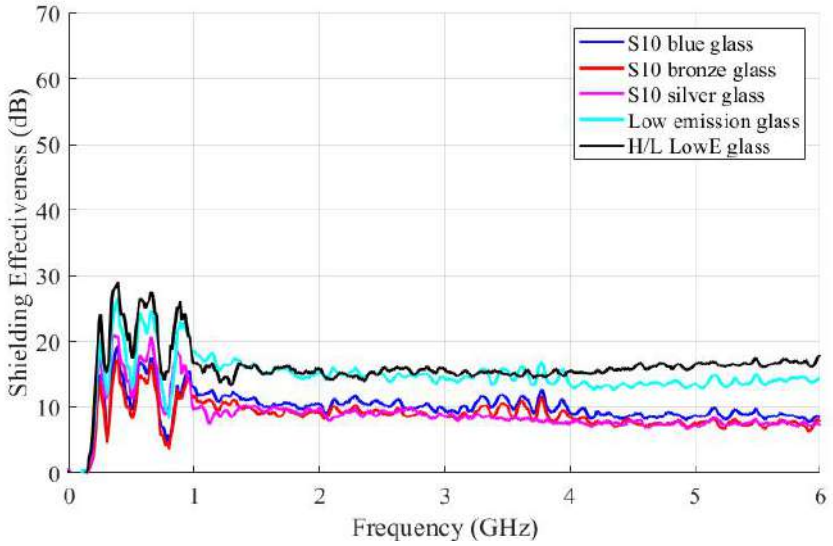

Figure 4.17: Glass samples SE measured in RC 2, RF gasket present and no aluminium tape used for RF energy leakage prevention.

4.4 Measurement Accuracy

The efficiency and accuracy of measurement depend greatly on the efficiency of the instruments that are deployed for the same. From the results shown in figures 4.16 - 4.19, it is evident that the shielding effectiveness of the materials measured only vary well between frequencies of 1 GHz and 3 GHz. At the lower ends, frequencies of up to 1 GHz, the results are unstable. This is attributed to the very high usable frequencies of the nested chamber. The size of the nested chamber dictates the LUF of the chamber, and according to equation 2.15, this value is 1 GHz. Beyond 3 GHz, however, the results show a flat sim-

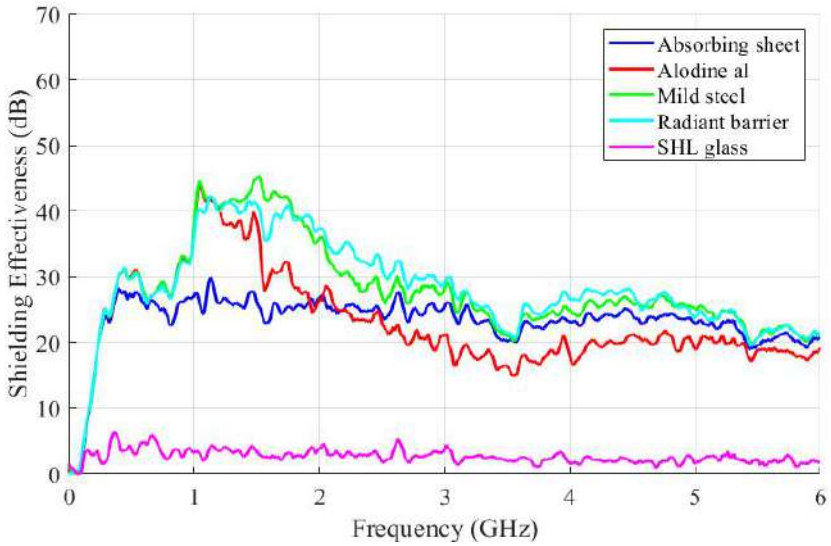

Figure 4.18: Material SE as measured in RC1, RF gasket present and no aluminium tape used for RF energy leakage prevention.

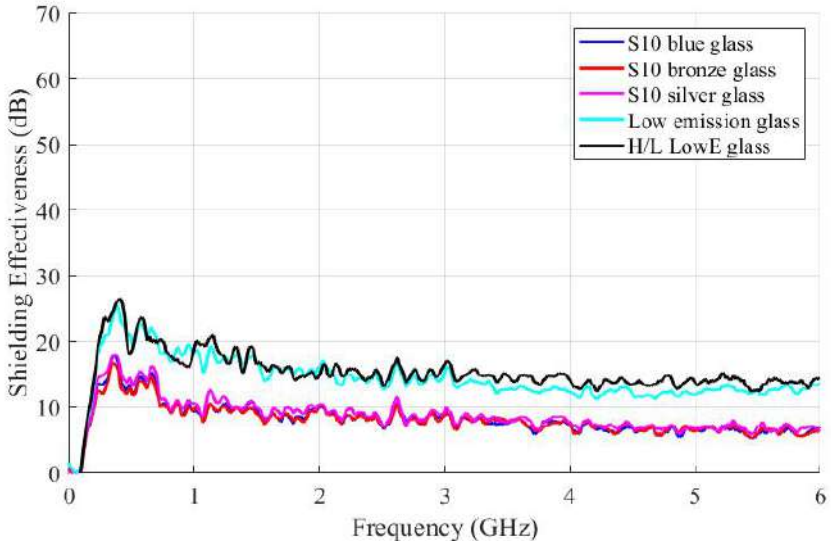

Figure 4.19: Glass samples SE measured in RC1, RF gasket present and no aluminium tape used for RF energy leakage prevention.

ilar trend. Beyond this point of the measurement bandwidth, the instruments have gone past the available dynamic range, hence untrusted results. The VNA used has a dynamic range of approximately 30 dB thus measurements using a more sensitive equipment are done.

Dynamic range limitation

The noise flow of the ZVB-8 VNA is at 100 dB and the measured power transfer between the transmit and receive antenna for an empty chamber varies from 70 dB to 30 dB at 6 GHz, as illustrated in figure 4.20 for transfer function. Thus;

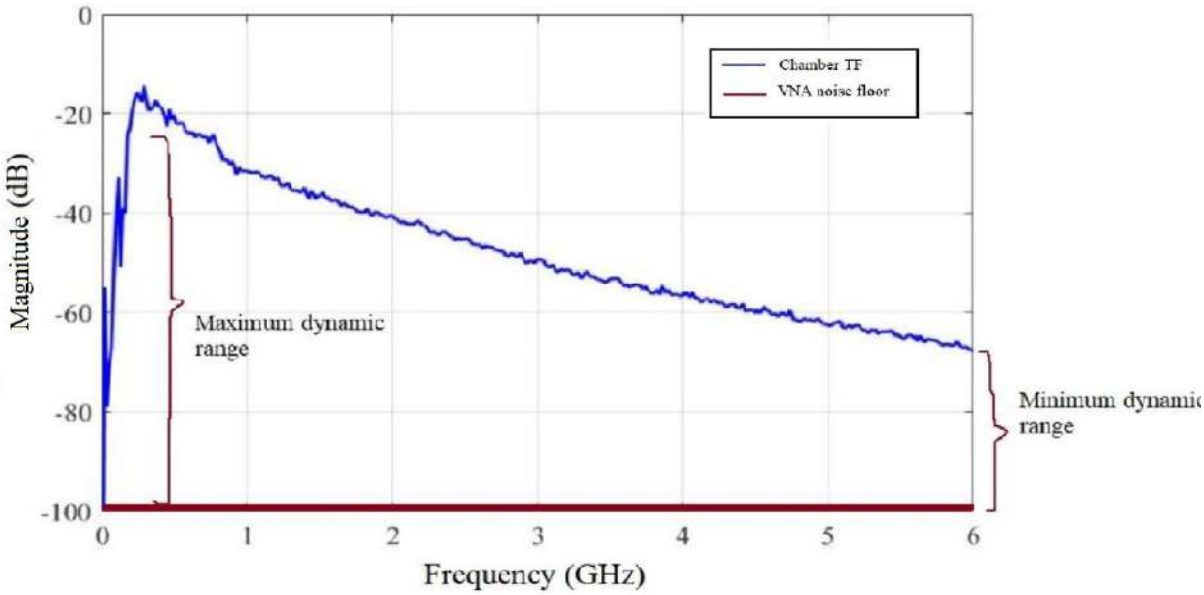

Figure 4.20: Dynamic range of the VNA, ZVB-8.

From the transfer function profile, the dynamic range of the VNA reduces as the frequency increases. Thus, better characterization is achieved for the lower frequencies while for the higher frequencies, measurement of materials with slightly higher shielding values are likely to go into the noise floor of the instrument.

4.5 Validation of Results

In order to validate results for a particular work done, there should be a basis or a foundation upon which the results are compared. The validation could be through other methods of measurements for the specific quality under investigation, it could be through simulations, other measurement techniques, previously obtained data from other sources or through the manufacturer data on the same. In this study, even though measurements have been done in two different chambers, most have been done using the same measurement technique and methodology, that is, frequency domain. For validation purposes therefore, the obtained data and hence results are compared to results from previous measurements as well as manufacturers' data. Comparisons of the investigated material samples are presented in this section.

4.5.1 Energy Saving Glass Study

In [35], different types of glass panels and window panes are investigated. Table 4.1 describes the materials.

Single panes, standard types	
Specimen name	**Construction**
Cool Lite SS132	Coated Solar Control Sprandel Glass
Panibel G fas T	Hard Coated Low Emission Glass
Planitherm Ultra ll	Soft Coated Glass 1 Silver Layer
Cool Lite SKN165	Soft Coated Glass 2 Silver Layers

Table 4.1: Measurement samples of single glazed window panes.

The results are shown in figure 4.21. These are single-glazed glass panels with single layer lamination. The glass panels are thus considered to have close properties with those whose shielding effectiveness is being investigated in this study. The comparison of these results show close agreement.

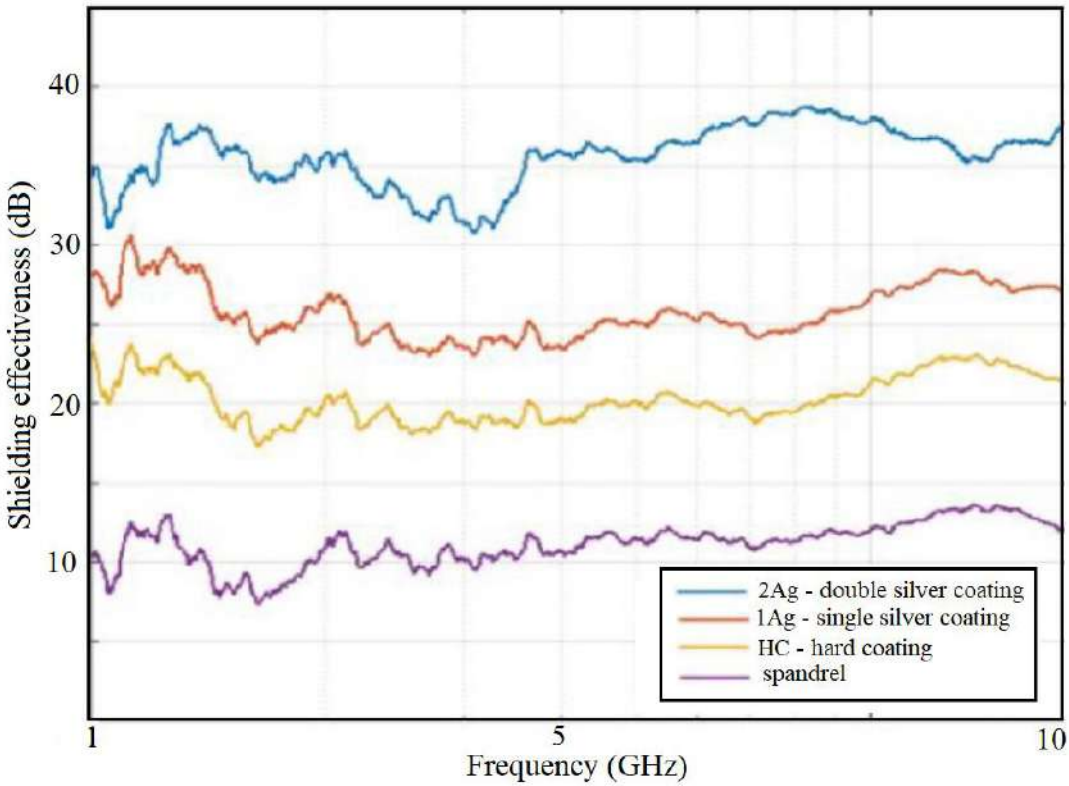

Figure 4.21: SE single glazed window panes [35].

The S10 glass sample in figure 4.16 exhibit the same shielding as the Spandrel glass, and the hard coated low emission glass also exhibits a shielding value close to the low emission glass in our study.

4.5.2 Microwave Absorbing Sheet Data

The absorbing sheet demonstrated a fair amount of shielding, approximately 30 dB.

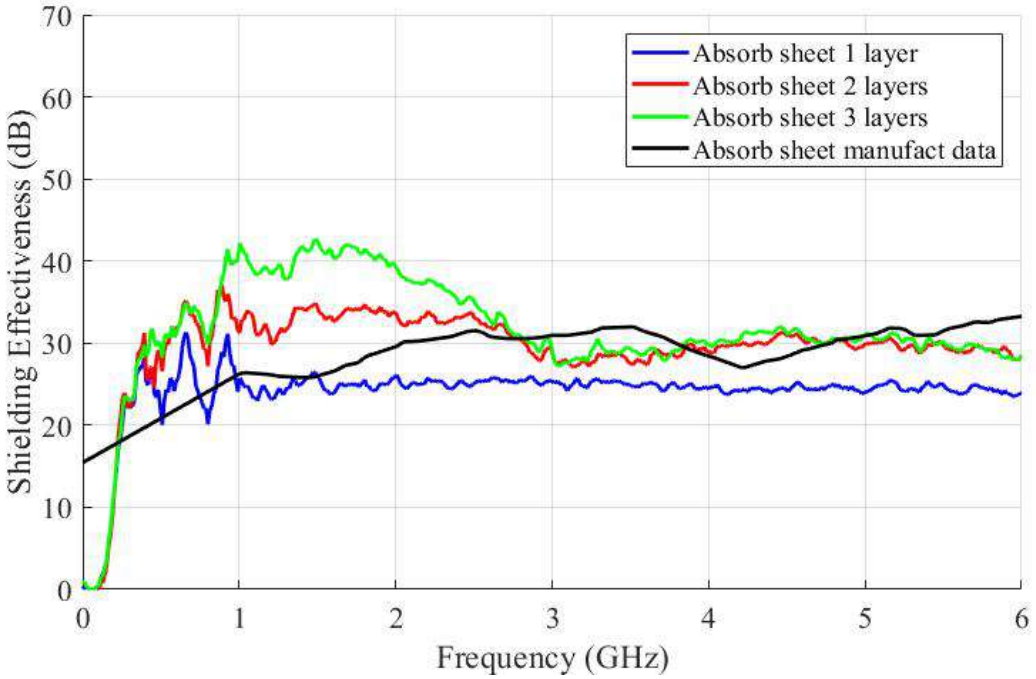

Figure 4.22: SE of different layers of microwave absorbing sheet.

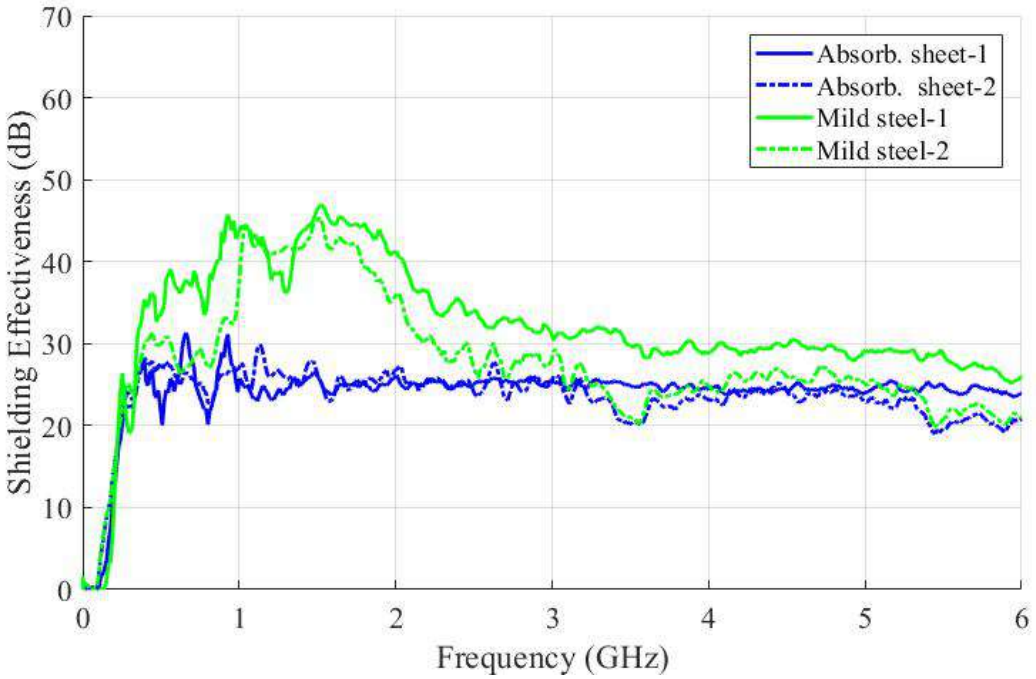

Figure 4.23: SE of mild steel and absorbing sheet as measured in RC1 and RC2, with no aluminium tape used for RF energy leakage prevention.

This compares favourably to the manufacturer's shielding value of a single layer absorbing sheet [34]. It is, however, worth noting that as the layers of the sheet are increased, the shielding value increases significantly. Figure 4.22 shows shielding effectiveness results of the absorbing sheet materials for a single and multiple layers. The shielding value for

double and triple layer do not vary much at higher frequencies. This is due to lack of sufficient dynamic range at higher frequency, as shown by figure 4.20 hence measurements go into the noise floor of the measurement instrument, the VNA.

In figure 4.23, the results of shielding effectiveness of two of the materials, absorbing sheet and mild steel, as measured in the two chambers are compared. The graphs show that the shielding effectiveness of the different materials as measured in the two reverberation chambers relate closely. However, there are slight differences, within 3 dB that can be owed to the differences in the chamber parameters, instrumentation and stirrer operation mode.

4.6 Towards Time Domain Measurement

Measurement in time domain have advantages over those of frequency domain. It would be beneficial if the investigation of the shielding effectiveness of these materials were done in time domain as well. An initial step was taken in performing measurements in time domain using the VNA inbuilt setting. In the figure 4.24, a comparison of the result of such measurement for a radiant barrier material, compared to the frequency domain measurement are shown.

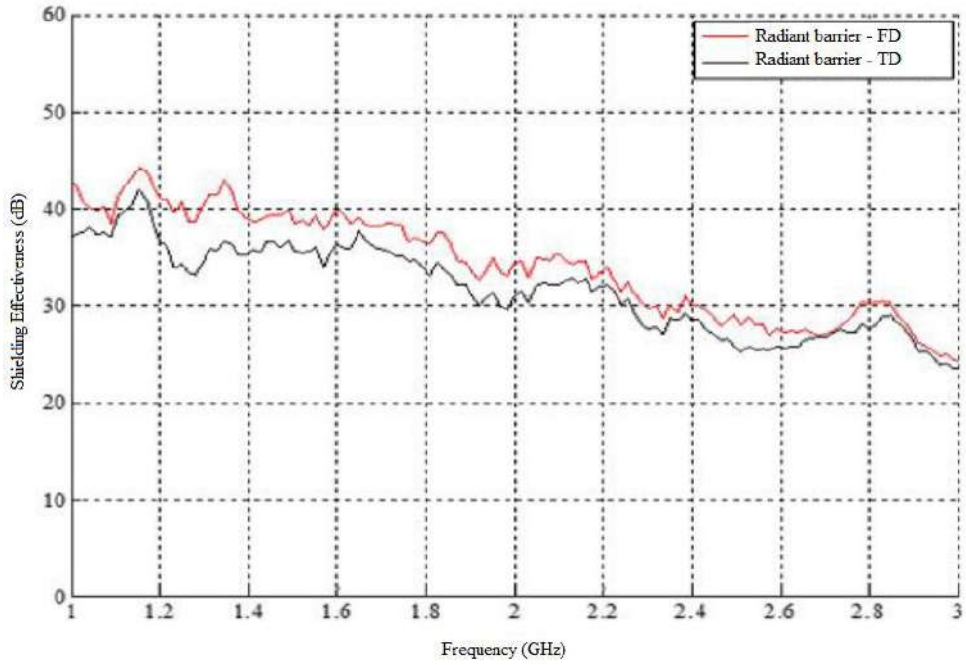

Figure 4.24: Comparison of SE of Radiant barrier material from the FD and TD measurements using a VNA.

Even though, this kind of measurement is not a pure time domain measurement, it ascertains the data extraction method using IFFT to obtain the frequency domain data which is used in the computation of the SE value.

4.7 Time Domain Measurements

Measurements in frequency domain are time consuming and limited to the dynamic range of the measurement instruments (VNA) used. For time speed up, further measurements are done in TD using a real-time transient analyser (RTA3) [36]. These measurements are carried out in RC2. Before measurements, the SKA reverberation chamber (RC2) was characterized to ascertain its uniformity. Figure 4.25 shows both the S_{11} and S_{21} for the empty chamber, for the bi-conical antennas used in characterization.

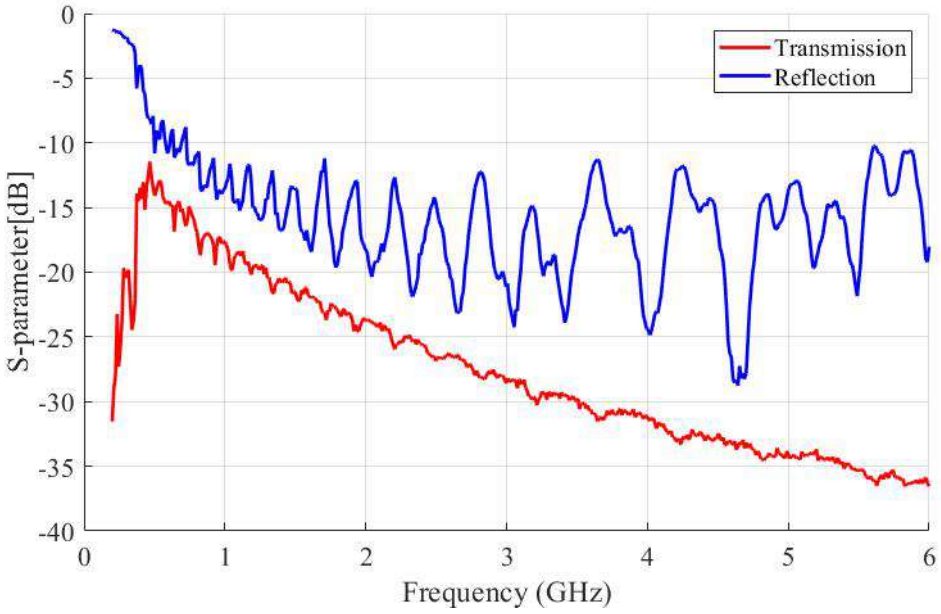

Figure 4.25: Magnitudes of the S-parameters as measured in RC2

4.7.1 Real-Time Transient Analyser 3 (RTA-3)

The RTA is a high dynamic range time domain receiver with a measurement bandwidth of up to 3 GHz. Figure 4.26 shows the schematic diagram of the instrument.

It has two main sections, analog and digital. The equipment is controlled through a computer running on UBUNTU operating system. Two signal ports are used during its operation, that is, the RF input port which is SMA connected to the output cable from the reverberation chamber, and an ethernet port that serves as the output of the RTA and through which data is transferred to the computer.

The RTA was developed with a group of university students in collaboration with the SKA (SARAO), and was used as a time domain receiving instrument, for time domain measurements, and for the RFI campaigns. It has a 900 MHz instantaneous bandwidth (BW) and high dynamic range of 80 dB. Besides its high dynamic range, it is highly

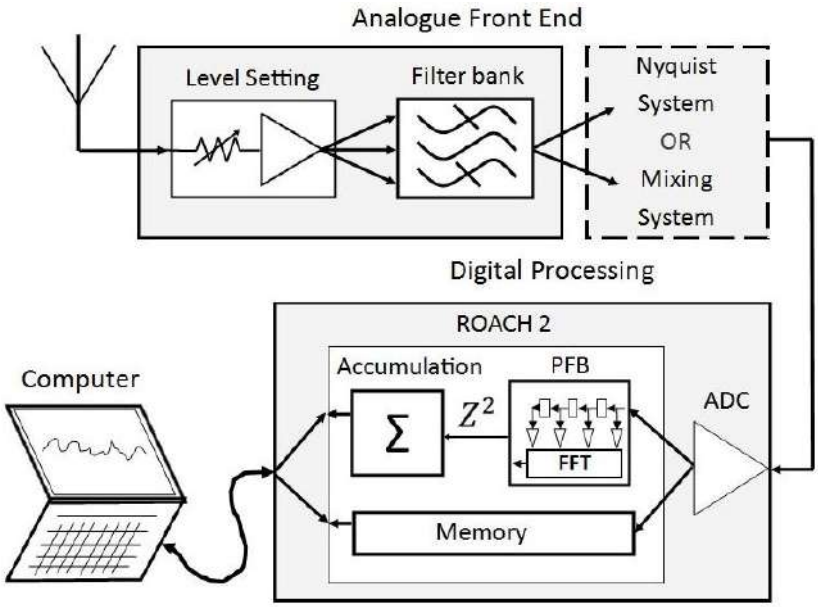

Figure 4.26: Schematic representation of RTA-3 [37]

sensitive and cost effective. It was initially developed purposely for SKA RFI site monitoring, but has since been used for university research and measurements. For the TD measurement, the set-up is as shown in figure 4.26.

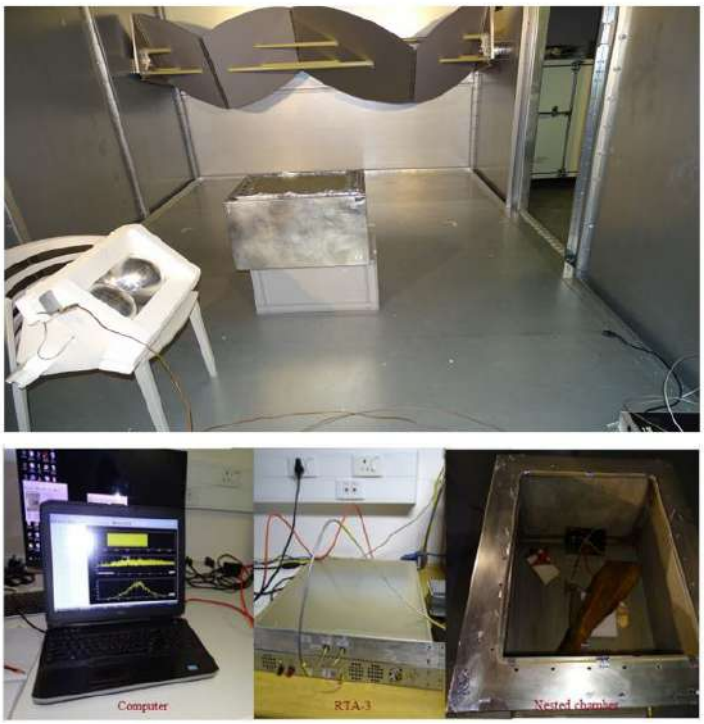

Figure 4.27: A photograph showing the arrangement of equipment used for TD measurement of material SE.

A bi-conical antenna was used as the receiving antenna whereas a comb generator was used as the TD transmitter in the nested chamber as depicted in figure 4.27. The photographic

representation of the set-up can be summarized in a block diagram according to figure 4.28.

Prior to taking measurements, the instrument is calibrated. With the calibration done, the calibration file is applied to the measurement according to the python program written on UBUNTU.

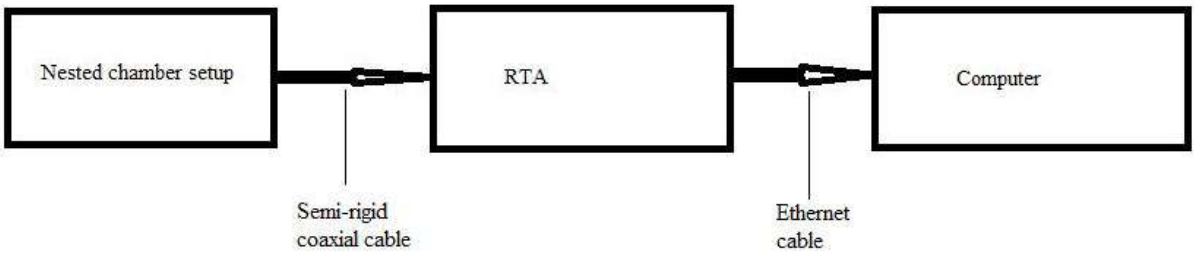

Figure 4.28: Block diagram for equipment arrangement for time domain measurement set-up

RTA has two modes of operation, frequency domain and time domain, either of which is activated with the commands $rfi-spectrum.py$ and $rfi-spectrum.py$ on the UBUNTU program, respectively. The frequency output is as a result of an inbuilt IFFT program that calculates the frequency response from the time domain data obtained from measurement. The data is saved as .h5 files that is later extracted using HDFView and processed using MATLAB.

Time Domain Measurements Procedure

The RTA measurements for SE evaluation was carried out in RC2 using the set-up shown in figure 4.27. The radiated RFI from the comb generator was received by the bi-conical antenna within the main RC and to the RTA.

This was then collected by the computer through the Ethernet cable, as shown both in figures 4.27 and 4.28. By using the triggering option of the RTA rfi-time.py function, transients were effectively captured, figures 4.30 and 4.31, even though initial measurements caused the device to produce ADC over-range warnings, causing the equipment to clip. For this reason, materials with higher shielding value needed additional attenuation for measurement to be possible. Otherwise, the equipment would just stay clipped, which is also dangerous and could easily damage the RTA. An additional attenuation of 20 dB was then added to the RF input port to acquire safe measurable signal levels.

These increases in attenuation at the input to the channel also ensured that most of dynamic range of the instrument was used.

The first set of measurement was taken with the comb generator in the nested chamber, the

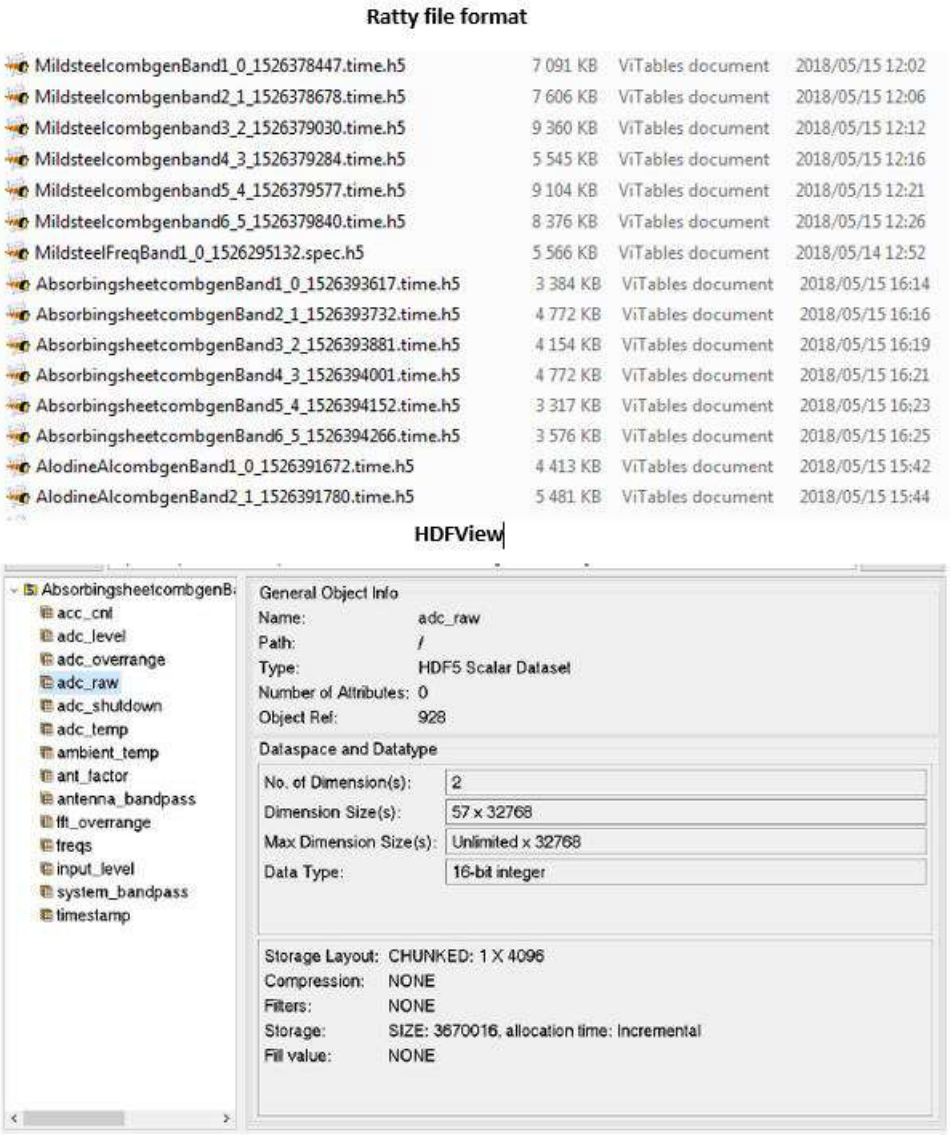

Figure 4.29: Screen capture showing the different fields measured and recorded by the RTA during any single measurement.

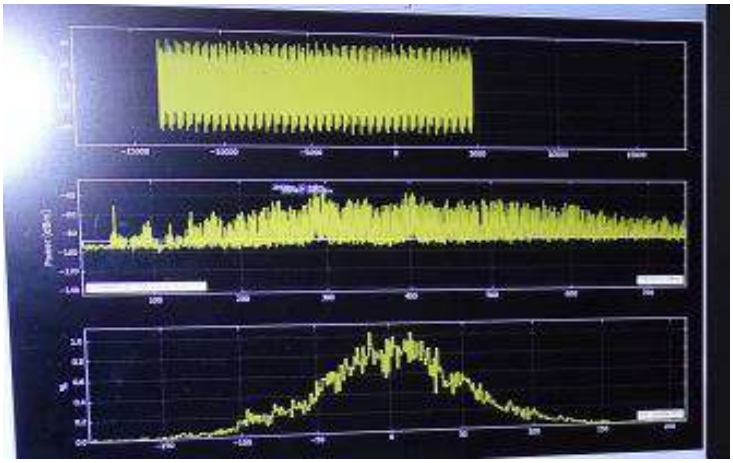

Figure 4.30: TD plot capture for a transient measurement using $rfi - time.py$.

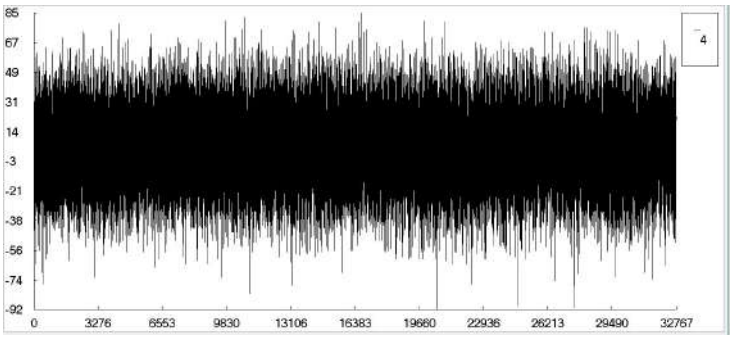

Figure 4.31: pulse capture for time domain measurement

aperture open and nested chamber stirred. This was the reference measurement against which all other SE measurements were calculated. With the material sample in place, the same measurement was repeated with at least 40 pulse captures per measurement per material sample.

Shielding effectiveness was calculated using the same equation as for frequency domain. Using a Matlab program, the IFFT of the time domain data of the averaged captures was calculated and the matrix applied to equation 4.15. The results were then plotted and compared to the frequency domain SE measurement of corresponding materials.

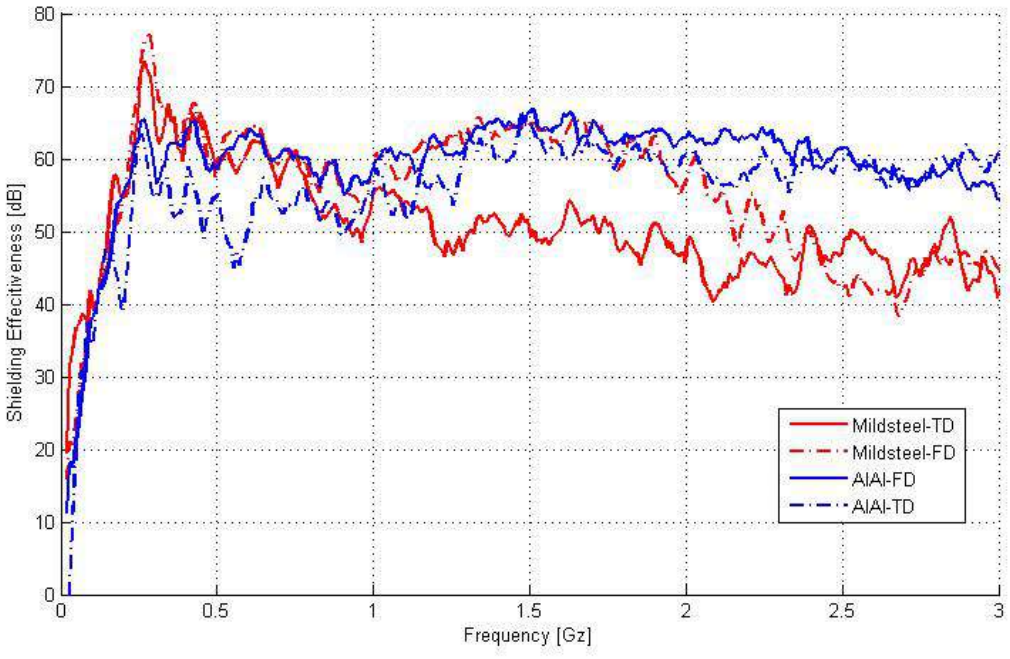

Figure 4.32: SE comparison for TD and FD measurements.

From figure 4.32, it can be seen that the SE of mild steel as measured in TD only agree with that measured in FD up to around 1.6 GHz. Due to the fact that the full bandwidth of operation of RTA is 3 GHz, measurement can only be obtained up to that frequency. In figure 4.28, however, no reliable measurement could be made past the 1.6 GHz due to

the fact that the comb generator had weak pulses that could only be well captured in the first two band spectra of the RTA. The rest of the four spectra had the measurement go into the noise floor and thus no clear SE ratio could be calculated.

4.7.2 Advantages of Time Domain Over Frequency Domain

Time domain measurements have the advantage of time speed-up over measurements in FD. In TD, the amount of time taken to estimate the time delay constant of a signal in a cavity or reverberation chamber is shorter since the antenna mismatch and the pre-reverberant energy are gated out while in the frequency domain approach the antenna effects are inseparable. This makes the time domain measurements independent of the antennas used. Therefore antenna efficiency investigation is not vital for these measurements. However, from TD measurement of RC time constant, one can easily calculate the quality factor of the chamber which would easily aid the calculation of antenna efficiency, if two identical antennas are used in chamber characterization.

For instance, the comb generator used generate signals at a frequency rate of 2 MHz. The signal however takes approximately 6 microseconds to fade or decay. With this knowledge, one can therefore calculate the quality factor of the chamber for every frequency, contrary to FD measurements where either time constant of the chamber or antenna efficiency has to be known beforehand or investigated separately.

4.7.3 Conclusions

This chapter summarized the results obtained from SE measurement of materials as done in the two chambers described in chapter three. These results were shown for frequency domain and verified in time domain. Validation of these results has also been presented from previous measurements and manufacturers' data.

Chapter 5

CONCLUSION AND RECOMMENDATIONS

5.1 Conclusion

In a world where efficiency is key in any processes and systems, it is vital that all aspects and factors that contribute to it are observed and addressed carefully. Besides the system operating well, it is important that the cost of materials as well as cost of processes of the operations are brought to a possible minimum while at the same time achieving the expected results.

Even though though SKA SA has worked to ensure that its processor building is well shielded, studies and material information reveal that current RF shielding materials used to achieve the amount of shielding required are quite expensive and could impact the cost towards additional buildings for SKA1-MID.

Shielding effectiveness of several alternative materials has been presented in this thesis. The results have been satisfactorily confirmed through measurements done in two reverberation chambers both in frequency and time domain. Microwave absorbing sheet and spurious roofing materials particularly demonstrated a good amount of shielding for frequencies up to 3 GHz. Their form and flexibility will be an added advantage in their use at SKA for shielding.

Besides the achieved SE results of material samples, the measurement technique used achieved a good level of repeatability and can thus be easily adapted for standard material characterization of shielding materials in a reverberation chamber. The outcome of the work has also shown that the reverberation chamber is well suited for shielding effectiveness measurement based on the validation of the results done using the previous measurements as well as using the manufacturers' data. These results were also verified by second set of measurements in a second reverberation chamber. However, the gasketing and contact of the sample materials are essential for accurate measurement.

5.2 Recommendations

The work in this thesis is partly carried out in frequency domain and partly in time domain. The frequency domain measuring instruments were of lower dynamic range hence did not provide reliable results for higher frequencies. It is thus recommended that the instruments used for future measurements should be of better dynamic range to ensure that the reverberation is utilised fully to properly characterize materials over a wider range of frequencies.

Although the measurements in a reverberation chamber are influenced by the lower usable frequency of the chamber, the nested chambers lower usable frequency plays an important role in the characterization of the materials using the technique. Even though the lower usable frequency of the main chamber was as low as 220 MHz, that of the nested chamber was close to 1 GHz. Therefore, for lower frequency measurements, the results could only be reliable from 1 GHz.

The performance of a chamber at lower frequencies could be improved by a better stirring mechanism. Since the nested chamber is small in volume, its lower usable frequency is large. However, with a better stirring mechanism or technique, the response of the chamber in this lower end of measurement frequency could be improved.

A frequency stirring mechanism is recommended instead of mechanical stirring used in the study. The stirrers occupy a considerable volume in the chamber thus reducing the working volume of the chamber, while at the same time introduce some amount of interference in the chamber since they are not controlled remotely. It is also recommended that a better signal generator be used for time domain measurements. This would ensure stronger pulses that would eventually allow the use of the entire operation bandwidth of TD receiver, RTA.

Besides the reverberation chamber measurement, free-space transmission technique with time-domain gating is also recommended for shielding evaluation. For this technique, characterization of materials for frequencies lower than 1GHz is possible. This measurement technique would ensure that measurement of SE of material samples is done easily without requiring any special environment, for the material sample under test, providing separation between transmitting and receiving antennas.

With additional telescope dishes and infrastructure being built for SKA-MID, SKA is quickly expanding. Additional smaller buildings will be constructed which will require shielding. Some of the materials that have been investigated are suitable for use for shielding at different levels. Radiant barrier material could be used bonded with the currently used roofing materials for added shielding benefit. Glass samples can also be

used for shielding windows especially when additional layers of coating are added for improved shielding. Absorbing sheet materials can be used as air filters given their form, while at the same time providing a good amount of shielding.

Appendix A

Appendix

A.1 Datasheet for Glass Samples

Glass samples used in the study are from PG glass. All of them were single glazed with different laminations. The figure A1 shows datasheet of glasses as obtained from PG glass.

A.2 Emission Reference Source (ERS)

This is a standard RF radiator with a known measured field strength. It is used for field generation for time domain measurements. It comes in various types, shapes and with different frequency coverage. The generated field is spaced at specific frequency and distance according to specification of each ERS. It has an inbuilt monopole radiator. ERS sources ensure measurement integrity and reduce measurement uncertainty [38].

Emission Reference Source (30 MHz - 1GHz)
This is a portable self contained RF comb generator that radiates RF energy in steps of 2 MHz over a frequency range of 30 MHz to 1 GHz.

It provides a known strength RF field with calibration data supplied for a distance of 3 m. Its output is a closely spaced harmonic series which permits frequencies across the spectrum to be checked over the full range required by EMC specifications.

It comes with calibration data thus, appropriate correction can be applied to the measurements, considerably reducing measurement uncertainty.

Specifications
Output : Narrow band 30 MHz - 1 GHz.
Level : Approximately 30 - 70 dBuV/M @ 3 m. Full calibration data supplied with the unit.
Supply : Rechargable internal batteries.
Discharge indication : Automatic indication if battery is low.
Antenna : Top loaded monopole.
Polarization : Vertical and horizontal.

SOLARSHIELD™ LOW E

Products			Visible Light		Solar Energy					Shading Co-efficient	U Value	Damage Weighted Transmittance
IGDB No.	SOLARSHIELD™ Low E	Range	Transmission	Reflection	Total Elimination	Reflectance	Absorption	Direct Transmission	SHGC	Ratio	(W/m²).K	Tdw-ISO
16032	Silver	S10	9	39	81	35	58	7	0.19	0.21	3.7	7%
16044		S20	24	27	71	23	60	17	0.29	0.33	3.7	18%
16002		S30	34	17	63	17	57	26	0.37	0.43	3.7	25%
16021	Aquamarine	S10	8	27	81	28	66	6	0.19	0.22	3.7	6%
16033		S20	19	19	72	19	67	15	0.28	0.32	3.7	15%
16046		S30	28	14	66	13	65	22	0.34	0.40	3.7	21%
16023	Blue	S10	8	31	81	32	61	7	0.19	0.22	3.7	7%
16035		S20	18	21	73	22	64	14	0.27	0.31	3.7	15%
16001		S30	29	14	65	14	63	22	0.35	0.40	3.7	23%
16025	Bronze	S10	8	15	78	17	76	7	0.22	0.25	3.7	6%
16037		S20	16	11	72	13	74	13	0.28	0.32	3.7	11%
16048		S30	19	9	69	10	74	16	0.31	0.35	3.7	13%
16027	Grey	S10	5	14	80	20	75	5	0.20	0.23	3.7	4%
16039		S20	13	9	73	12	76	12	0.27	0.31	3.7	10%
16050		S30	18	8	69	10	74	16	0.31	0.36	3.7	14%
16029	Regal Blue	S10	8	20	80	24	69	7	0.20	0.23	3.7	7%
16041		S20	15	14	73	17	70	13	0.27	0.31	3.7	13%
16052		S30	23	10	67	12	68	20	0.33	0.38	3.7	19%
16031	Serene Green	S10	9	33	80	17	78	5	0.20	0.23	3.7	6%
16043		S20	22	20	73	13	75	12	0.27	0.31	3.7	16%
16121		S30	33	17	64	16	60	24	0.36	0.42	3.7	23%

![h]

SOLARVUE™ LOW E

Products			Visible Light		Solar Energy					Shading Co-efficient	U Value	Damage Weighted Transmittance
IGDB No.	SOLARVUE™ Low E	Range	Transmission	Reflection	Total Elimination	Reflectance	Absorption	Direct Transmission	SHGC	Ratio	W/m².K	Tdw-ISO
16003	Neutral	HL	43	14	57	12	56	32	0.43	0.49	3.7	31%
16098		XHL	54	10	49	9	49	42	0.51	0.59	3.7	38%
16055	Aquamarine	HL	40	10	56	9	59	32	0.44	0.50	3.7	29%
16090		XHL	44	9	54	8	57	35	0.46	0.53	3.7	31%
16056	Blue	HL	30	8	60	9	64	27	0.40	0.46	3.7	24%
16092		XHL	46	9	51	9	53	38	0.49	0.56	3.7	36%
16058	Bronze	HL	26	8	64	8	69	23	0.36	0.42	3.7	18%
16094		XHL	32	6	58	6	65	29	0.42	0.48	3.7	21%
16104	Grey	HL	24	7	63	7	70	23	0.37	0.42	3.7	18%
16096		XHL	28	6	59	6	66	28	0.41	0.47	3.7	21%
16004	Regal Blue	HL	30	8	60	9	64	27	0.40	0.46	3.7	24%
16100		XHL	34	7	57	8	61	31	0.43	0.50	3.7	27%
16105	Serene Green	HL	40	10	64	7	72	21	0.36	0.41	3.7	28%
16102		XHL	46	9	60	7	66	27	0.40	0.46	3.7	32%

![h]

Figure A.1: PG glass datasheet. It shows the characteristics of different glass materials.

Emission Reference Source (10 MHz - 3.5 GHz) - model ERS - 2

This is a self contained RF comb generator with a broadband output coverage of 30 MHz to 3 GHz in steps of either 10MHz or 50MHz. It was majorly used for the TD measurement as its frequency coverage matches that of RTA 3.5. However pulses could not be captured for the entire working bandwidth of the comb generator once inside the small nested chamber. This was because the pulses were attenuated and could only be observed in the first two bands of the RTA.

Figure A.2: A photograph of a comb generator used for time domain measurements.

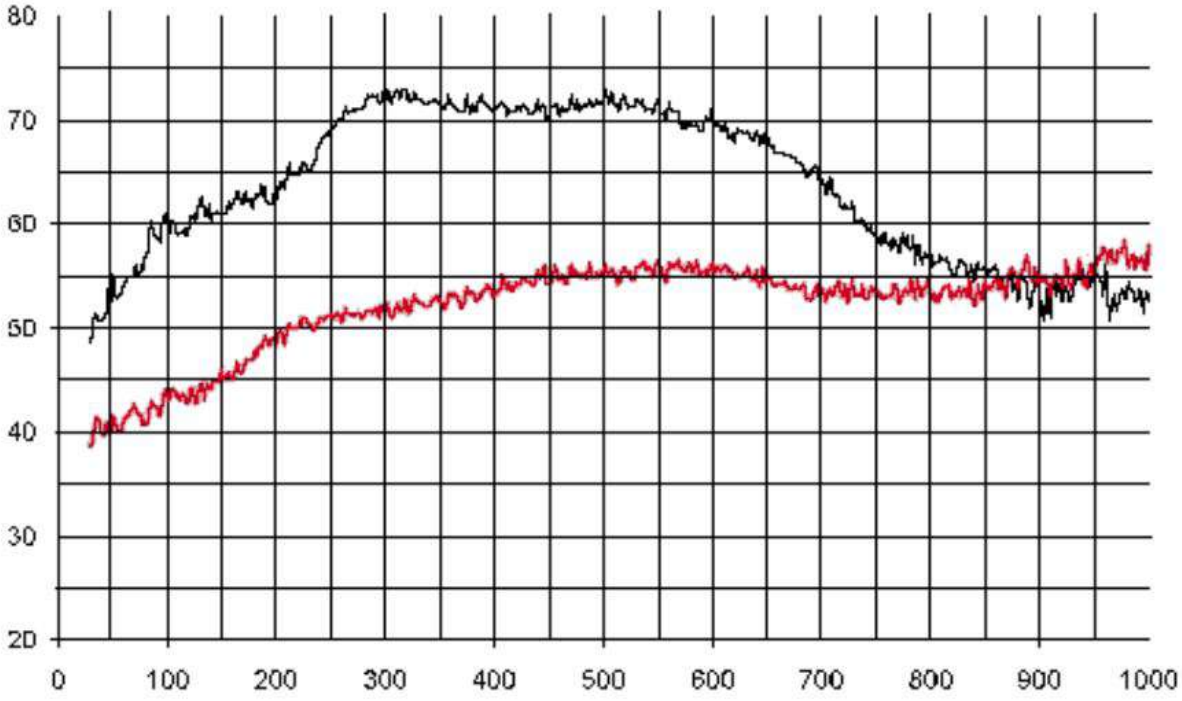

Figure A.3: A calibration plot showing harmonic peak values against a linear frequency axis, for both standard and low output versions.

Specification of Comb Generator ERS 10.5

Model : EMC 10.3 Frequency Range (MHZ) : 10 - 3500.

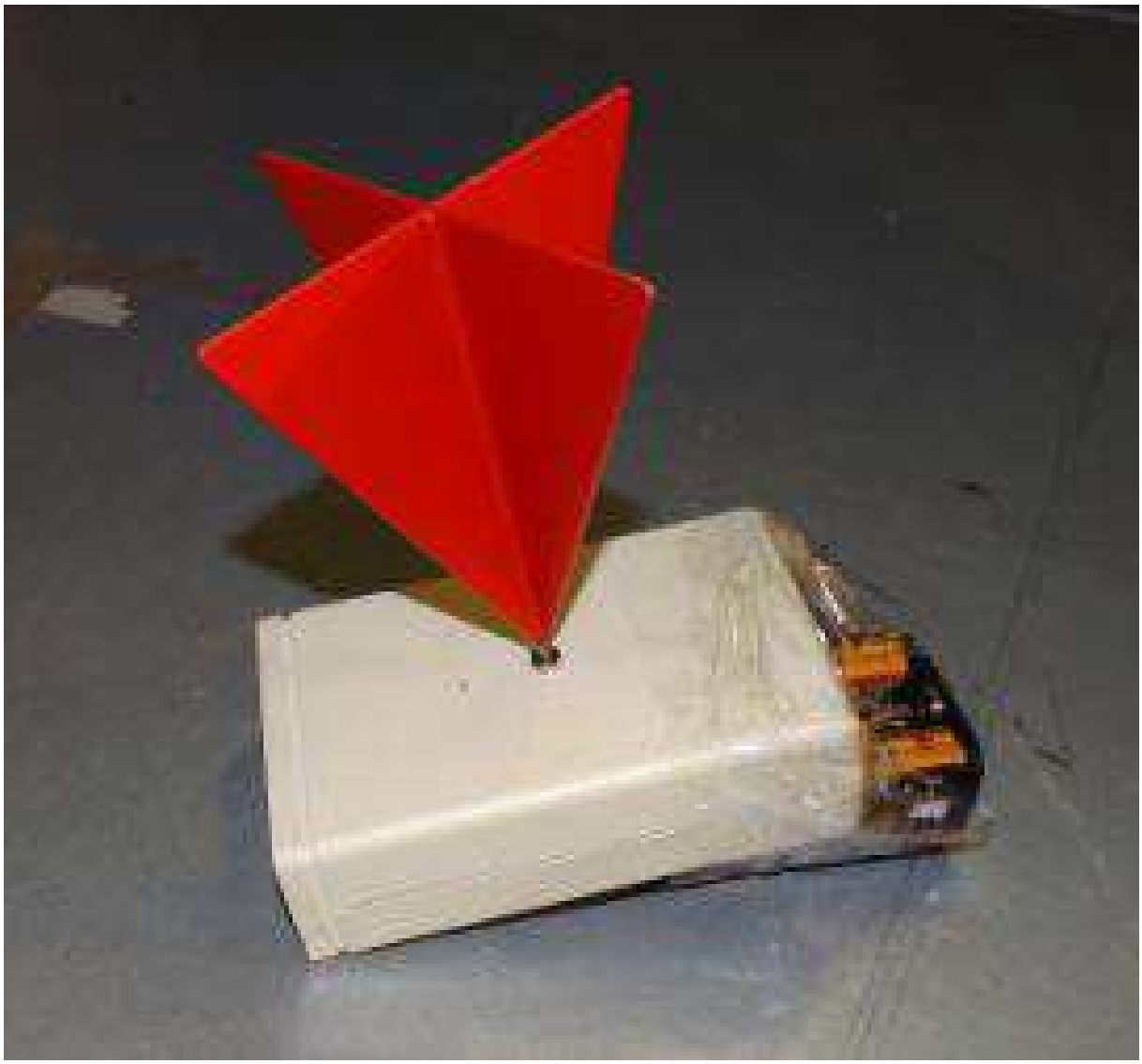

Figure A.4: A comb generator (ERS 10.5) shown with its remote control unit. The pair is used for time domain signal generator for SE measurement.

Harmonic Spacing : 10 MHZ - 50 MHz (Switchable).
Frequency Stability (ppm) : 100.
Radiant field polarization : Vertical
RF level at 3m (dBuV/m) : 40 -80.
Battery type : 6LR61 9v (PP3).
Battery life before charging : 8 hours.
Size with Antenna (mm) : 144 x 72 x 135.
Weight : 0.2 Kg.
Control : On/Off Harmonic switch, local and remote.

Due to its high output, it is ideal for use in test cells shielded enclosures measurements. Additionally, it has a remote control that allows switching between the operation frequen-

cies well outside the measurement area. The control connects to 10.3 G source via optic fibre. Figure A.5 shows the calibration plot of the ERS-2.

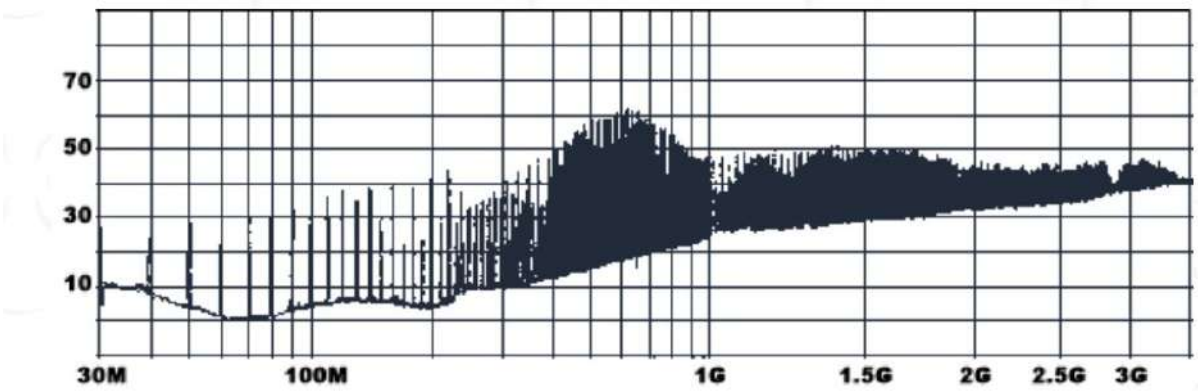

Figure A.5: Calibration plot for ERS 10.5.

Model	ERS	EMC 10.3
Frequency range (MHz)	30 - 1000	10 - 3500
Harmonic spacing	2 MHz	10MHz and 50MHz (switchable)
Frequency stability (ppm)	80	100
Radiated field polarization	vertical and horizontal	vertical
RF level at 3 m (dBuV/m)	50-70 30-50	40-80
Battery type	custom rechargable	6LR61 9V PP3
Battery life before charging	4hrs	8hrs
Size with antenna (mm)	120*64*188	144*72*135
Weight	1.5kg	0.2kg
control	on/off only	on/off harmonic switch, local and remote

Table A.1: Comparison of features of the two ERS used.

References

[1] H. Reader, P. van der Merwe, A. Otto, P. Wiid, J. Andriambeloson, P. Langat, and B. Kruizinga, "Emc techniques for a complex project: Karoo array telescope," in *Aerospace EMC, 2012 Proceedings ESA Workshop on*. IEEE, 2012, pp. 1–4.

[2] H. Pienaar, H. C. Reader, and D. B. Davidson, "Karoo array telescope berm shielding: Efficient computational modeling and multicopter measurement," *IEEE Transactions on Electromagnetic Compatibility*, vol. 59, no. 2, pp. 375–382, 2017.

[3] M. Senn, *South Africa SKA (Square Kilometer Array)*, (accessed February 3, 2017). [Online]. Available: http://www.ska.ac.za

[4] G. C. Southworth, "Early history of radio astronomy," *The Scientific Monthly*, vol. 82, no. 2, pp. 55–66, 1956.

[5] S. W. Ellingson, "Rfi mitigation and the ska," in *The Square Kilometre Array: An Engineering Perspective*. Springer, 2005, pp. 261–267.

[6] F. Silva, M. Fernandez, and P. J. Riu, "Electromagnetic interference and compatibility," *Wiley Encyclopedia of Biomedical Engineering*, 2006.

[7] E. Compatibility, "Part 4-21: Testing and measurement techniques—reverberation chamber test methods," *IEC Standard*, pp. 61 000–4, 2003.

[8] C. R. Paul, *Introduction to electromagnetic compatibility*. John Wiley & Sons, 2006, vol. 184.

[9] D. A. Hill, *Electromagnetic fields in cavities: deterministic and statistical theories*. John Wiley & Sons, 2009, vol. 35.

[10] T. Williams, *EMC for product designers*. Newnes, 2016.

[11] D. Bozec, M. Robinson, and C. Marshman, "Healthcare engineering and electromagnetic compatibility (emc)," *EBME Technical Article, available online: http://www.ebme. co. uk/arts/emc/, accessed date*, vol. 9, no. 5, p. 05, 2003.

[12] J. Norgard, "The electromagnetic spectrum," in *National Association of Broadcasters Engineering Handbook (Tenth Edition)*. Elsevier, 2007, pp. 3–10.

[13] Z. Haznadar and Ž. Štih, *Electromagnetic fields, waves and numerical methods*. IOS press, 2000.

[14] S. Schelkunoff, "The impedance concept and its application to problems of reflection, refraction, shielding and power absorption," *Bell System Technical Journal*, vol. 17, no. 1, pp. 17–48, 1938.

[15] W. J. Krzysztofik, R. Borowiec, and B. Bieda, "Some consideration on shielding effectiveness testing by means of the nested reverberation chambers." *Radioengineering*, vol. 20, no. 4, 2011.

[16] N. Xia, X. Yi, and W. Song, "Shielding effectiveness and coupling characteristic of metallic enclosures with apertures under emp," in *Power and Energy Engineering Conference, 2009. APPEEC 2009. Asia-Pacific.* IEEE, 2009, pp. 1–4.

[17] L. Golestani-Rad and J. Rashed-Mohassel, "The effects of apertures' shape and configuration on the shielding effectiveness of metallic enclosures," in *Microwave Conference Proceedings, 2005. APMC 2005. Asia-Pacific Conference Proceedings*, vol. 5. IEEE, 2005, pp. 4–pp.

[18] M. Bäckström, O. Lundén, and P.-S. Kildal, "Reverberation chambers for emc susceptibility and emission analyses," *Review of Radio Science 1999-2002*, pp. 429–452, 2002.

[19] Q. Xu and Y. Huang, *Anechoic and Reverberation Chambers: Theory, Design, and Measurements.* Wiley-IEEE Press, 2018.

[20] A. Manara, "Measurement of material shielding effectiveness using a dual tem cell and vector network analyzer," *IEEE transactions on electromagnetic compatibility*, vol. 38, no. 3, pp. 327–333, 1996.

[21] N. Dvurechenskaya, P. R. Bajurko, R. J. Zieliński, and Y. Yashchyshyn, "Measurements of shielding effectiveness of textile materials containing metal by the free-space transmission technique with data processing in the time domain," *Metrology and Measurement Systems*, vol. 20, no. 2, pp. 217–228, 2013.

[22] M. Badic and M.-J. Marinescu, "On the complete theory of coaxial tem cells," in *IEEE International Symposium on Electromagnetic Compatibility. Symposium Record (Cat. No. 00CH37016)*, vol. 2. IEEE, 2000, pp. 897–902.

[23] M. S. Sarto and A. Tamburrano, "Innovative test method for the shielding effectiveness measurement of conductive thin films in a wide frequency range," *IEEE Transactions on Electromagnetic Compatibility*, vol. 48, no. 2, pp. 331–341, 2006.

[24] L. R. Arnaut, "Mode-stirred reverberation chambers: A paradigm for spatio-temporal complexity in dynamic electromagnetic environments," *Wave Motion*, vol. 51, no. 4, pp. 673–684, 2014.

[25] I. E. Commission *et al.*, "Iec61000-4-21: Electromagnetic compatibility (emc)-part 4-21: Testing and measurement techniques-reverbera-tion chamber test methods," 2011.

[26] D. A. Hill, "Electronic mode stirring for reverberation chambers," *IEEE Transactions on Electromagnetic Compatibility*, vol. 36, no. 4, pp. 294–299, 1994.

[27] J. A. Andriambeloson, "Reverberation chamber time and frequency metrology for meerkat systems shielding evaluation," Ph.D. dissertation, Stellenbosch: Stellenbosch University, 2014.

[28] J. G. Kostas and B. Boverie, "Statistical model for a mode-stirred chamber," *IEEE transactions on electromagnetic compatibility*, vol. 33, no. 4, pp. 366–370, 1991.

[29] C. L. Holloway, H. A. Shah, R. J. Pirkl, W. F. Young, D. A. Hill, and J. Ladbury, "Reverberation chamber techniques for determining the radiation and total efficiency of antennas," *IEEE Transactions on Antennas and Propagation*, vol. 60, no. 4, pp. 1758–1770, 2012.

[30] C. L. Holloway, D. A. Hill, J. Ladbury, G. Koepke, and R. Garzia, "Shielding effectiveness measurements of materials using nested reverberation chambers," *IEEE Transactions on Electromagnetic Compatibility*, vol. 45, no. 2, pp. 350–356, 2003.

[31] M. De Beer, "Wideband direction finding of rfi for meerkat," Ph.D. dissertation, Stellenbosch: Stellenbosch University, 2017.

[32] A. Agilent, "1287-3 applying error correction to network analyzer measurements," *Agilent Technologies, USA*, 2002.

[33] D. A. Hill, M. T. Ma, A. R. Ondrejka, B. F. Riddle, M. L. Crawford, and R. T. Johnk, "Aperture excitation of electrically large, lossy cavities," *IEEE transactions on Electromagnetic Compatibility*, vol. 36, no. 3, pp. 169–178, 1994.

[34] L. E. Inc., *Laminated Microwave Absorbing Sheet)*, (accessed October, 2017). [Online]. Available: http://www.lessemf.com/259.pdf

[35] P. Ängskog, M. Bäckström, B. Vallhagen, and C. Samuelsson, "Shielding effectiveness of energy saving windows and hpm effects on coated window panes: Measurements conducted 2014–2016—results and lessons learned," in *Electromagnetic Compatibility-EMC EUROPE, 2016 International Symposium on.* IEEE, 2016, pp. 461–466.

[36] A. Botha, H. Reader, J. Manley, S. Malan, H. Kriel, P. van der Merwe, P. Meyer, P. van der Walt, W. Croukamp, and R. Anderson, "Dynamic rfi measurement systems on a roach-2 platform iceaa-ieee apwc-ems," in *Electromagnetics in Advanced Applications (ICEAA), 2013 International Conference on*. IEEE, 2013, pp. 502–505.

[37] A. Botha, "Development of a real-time transient analyser for the ska," Ph.D. dissertation, Stellenbosch: Stellenbosch University, 2014.

[38] R. Mayes., *Emission reference source)*, (accessed October, 2018). [Online]. Available: http://www.ramayes.com/emission_reference_source.htmf